SALT-SCALING DURABILITY OF FLY ASH CONCRETE

by

BRANDON STALLONE BORTZ

B.S., Kansas State University, 2008

A THESIS

submitted in partial fulfillment of the requirements for the degree

MASTER OF SCIENCE

Department of Civil Engineering
College of Engineering

KANSAS STATE UNIVERSITY
Manhattan, Kansas

2010

Approved by:

Major Professor
Dr. Kyle Riding

Copyright

Abstract

Fly ash is a by-product of coal-fired power plants. This material can be used as a partial cement substitute in portland cement concrete. Use of fly ash can improve concrete durability as well as utilize an industrial by-product that would otherwise be discarded in landfills. However, research on fly ash concrete has shown that in some cases, concrete with high volumes of fly ash can have deicer salt scaling problems. Salt-scaling is the flaking of a concrete surface that when severe enough may result in lower skid resistance and service life of the concrete.

In this study, concrete mixtures with six different fly ashes were tested in a laboratory using the ASTM C 672 standard. Curing compound, a wax-based coating sprayed on the fresh concrete surface to reduce evaporation, was used to compare the effects of curing on salt scaling of concrete containing high volumes of fly ash. Different variables measured were the type of fly ash, curing conditions, and total paste volume included in the mix.

Results showed that curing compounds will improve the salt-scaling resistance of concrete containing a fly ash that only marginally exhibits salt scaling. However, the salt-scaling performance of concrete that contains fly ash from a source that performs poorly in ASTM C 672 is not markedly improved by using a curing compound. Additionally, results showed that salt-scaling resistance of concrete containing fly ash performs better when the total paste volume is not increased by the addition of fly ash to the mixture.

The Kansas Outdoor Concrete Exposure Site (KOCE) at the Kansas State University Civil Infrastructure Systems Laboratory (CISL) was constructed to compare laboratory results to actual field conditions in the future. The site was developed based on experiences from the University of Texas-Austin outdoor exposure site and the CANMET exposure site in Ottawa, Canada. Alika silica reaction blocks were made to develop the procedure for future concrete durability testing at KOCE.

Table of Contents

List of Figures

List of Tables

Acknowledgements

I would like to thank Dr. Kyle Riding for allowing me the opportunity to work under him. The amount of knowledge I have gained is immeasurable. He has allowed me to work my way through most of the problems of this project on my own but has always made sure we were progressing in the right direction. I also want to thank the UTC for the tuition support and the Kansas State University Department of Civil Engineering for financial support over the past year and a half.

I have to give thanks to the rest of the Kansas State University civil engineering faculty and staff that have contributed to the success of this project. I want to specifically thank Dr. Mustaque Hossain and Mrs. Debi Wahl. Dr. Hossain has been a very large supporter of me and my goals of pursuing my master's and the long-term goal of a doctoral degree. Mrs. Wahl has been very patient with me about getting all my correct paperwork to her. I am grateful to her for being so understanding, especially on the freezer issues we had.

I sincerely thank Steven Hammerschmidt, Joey Holste, Rob Murphy, Luke McIntosh, Ryan Benteman, Lisa Beck, and Pat Sheedy. They were more than willing to help batch, move anything and everything, and do anything necessary throughout the process. Thank you Lori Bammerlin for providing much needed help throughout the duration of this project. She made the mundane task of moving "pucks" easier, was the first to give help when needed, and listened to me talk about how "cool" concrete was.

I have to thank all the companies for their donations to this project, especially Ash Grove Resources, Monarch Cement Company, MCM, Boral, Lafarge, Bayer Construction, W.R. Meadows, W.R. Grace, KDOT, C.B. Farms, and Konza Sand. Without their help, this project would not have gotten off the ground.

Thank you to my family, who has always supported me to do my best. Since the first day of kindergarten, Dad has told me, "Be good have fun. Do it right the first time, on time, every time." This has served me very well. Even though my sister and brother have chosen to go to other schools besides the great institution of Kansas State University, they have always been there for me.

Dedication

I dedicate this to everyone who has helped me throughout my life. You never know when you can influence somebody's life.

CHAPTER 1 - Introduction

1.1 Research Background

Today, the concrete industry has made sustainability a priority. Use of concrete has the ability of incorporating many industrial by-products that would ordinarily end up in the landfill. Fly ash, ground granulated blast furnace slag, and silica fume are examples of industrial by-products being used as supplementary cementitious materials (SCMs) in concrete. These materials are used as a partial replacement for portland cement, making a very viable and sustainable product. One major concern for this concrete, however, is de-icer salt-scaling durability when high volumes of SCMs are used.

Salt scaling occurs when concrete flatwork is subjected to de-icing chemicals and freezing and thawing cycles. Salt scaling can lead to a reduction in concrete service life performance. Researchers across the world have quantified many of the contributing factors leading to the reduction of salt-scaling durability. The mechanism for salt scaling is still highly debated. There is even debate on the proper method for testing salt-scaling durability. The American Society for Testing and Materials (ASTM) and the Ontario Ministry of Transportation (MTO) have both offered a similar test, but some critics say the tests are too severe and unnecessarily reject concrete mixtures that could otherwise have good durability as well as decrease the cost and environmental impact of concrete.

1.2 Problem Statement

Salt scaling has been a visible issue since the United States passed the Bare Roads Act requiring roads be cleared of snow and ice during the winter. Use of de-icing chemical has grown to maintain compliance with this act. In turn, the de-icing chemicals have lead to salt-scaling durability issues. Poor salt-scaling durability has been found in laboratory testing of concrete containing high volumes of SCMs, although many of these mixtures have performed well under field exposure. Thus, the interactions of SCMs in

concrete need to be studied more fully to determine ways to eliminate or minimize effects of salt scaling.

1.3 Research Objectives

The objectives of this research study are as follows:

1. To test the hypothesis that the lower fly ash specific gravity and consequent higher paste volume, used when the fly ash is replaced on an equal mass basis for portland cement, decreases salt-scaling durability;
2. To quantify the benefits of curing compounds on salt-scaling durability;
3. To develop an outdoor exposure site at the Kansas State University Civil Infrastructure Systems Laboratory (CISL) to correlate laboratory results with actual weathering results; and
4. To quantify the effects of using fly ash versus limestone sweetening in concrete on the alika silica reaction (ASR) expansion .

1.4 Scope of Research Program

The scope of this research study is limited to the nine fly ashes studied. Six fly ashes were used for laboratory and field testing, while three different fly ashes were used in outdoor testing only. Laboratory testing examined effects of paste volume when fly ash was used with and without a curing compound versus salt-scaling durability as measured using ASTM C 672. An outdoor exposure site was developed to investigate specimen size differences and the accompanying differences in finishing on salt scaling.

For laboratory testing, two concrete mixtures for each fly ash were developed. One mixture had a 40% substitution of fly ash by mass for portland cement. A second mixture was a 40% substitution of fly ash by mass substitution for portland cement, with the total cementitious materials and water content reduced to give a total paste volume equal to that of the control. The specimens were made and cured according to ASTM C 672, with the exception that half of the specimens were treated with a curing compound after finishing instead of curing with a plastic cover. After the first 24 hours of curing, all salt-scaling specimens were placed in the moist room at 23±1.7 ^{o}C (73.5±3 ^{o}F) and 100%

relative humidity. Specimens were ponded on the finished side with a calcium chloride solution and were subjected to 50 freeze-thaw cycles according to ASTM C 672. Every five cycles, the specimens were rated, photographed, and weighed.

While laboratory testing was being performed, the exposure site was built. After establishing the site elevation, two slabs were cast from each concrete mixture. One set started to receive a salt application last winter and will continue to have salt applications, while the other will serve as a control. A weather station was constructed to record the weather history of the exposure site. The site was developed to have the capacity for conducting different types of durability tests in the future.

CHAPTER 2 - Salt Scaling Literature Review

2.1 Salt Scaling

Salt scaling is defined as the "superficial damage caused by freezing a saline solution on the surface of a concrete body" (Valenza and Scherer 2007). Salt scaling is a process where small chips of mortar flake off of the surface leaving aggregates exposed as seen in Figure 2-1. Salt scaling alone may not destroy a concrete structure; however, it can accelerate the ingress of chlorides, and reduce the cover. This chloride ingress can lead to an accelerated deterioration of reinforcing steel, popouts of coarse aggregates, and can lessen skid resistance. Salt scaling, along with other types of deterioration, can lead to an aesthetically unappealing rough surface (Pigeon and Pleau 1995).

Figure 2-1 Severely Salt-Scaled Sidewalk

The microstructure of the concrete surface is the first defense against salt scaling. Three layers – different types of skins – have been described in the concrete surface. The cement skin, 0.1 mm (0.0039 in.) thick, is the top layer followed by the mortar skin, 5

mm (0.197 in.) thick, and finally the concrete skin, 30 mm thick (1.18 in.), is at the bottom of the three surface layers. These layers have higher cement paste content and higher porosity than the interior of the concrete. These differences in porosity and paste content are a result of gravity, vibration and compaction, and bleeding (Kreijer 1984). The microstructure can be very weak at the surface under some circumstances, such as over vibrating, trowelling too early, extensive plastic shrinkage, or excessive bleeding, leaving the surface susceptible to salt scaling (Jozwiak-Niedzwiedzka 2004).

2.2 Fly Ash

Fly ash is the fine residue trapped in chimneys after the combustion of pulverized coal. The ash is gathered by a collector system such as mechanical collectors, fabric filters, electrostatic precipitators, and wet scrubbers. Most commonly, the mechanical and electrostatic methods are used. The collection system delivers the ash to a silo. Fly ash can be interground into cements or added separately at the ready mixed concrete plant (Helmuth 1987).

Class F fly ash is produced from the burning of anthracite or bituminous coals and contains a low calcium oxide content (0-20%). Class C ashes are produced from lignite or sub-bituminous coals and contain high calcium oxide contents (generally 20-30%). However, fly ash has variable properties because it is not a manufactured product. It can vary by color, glass content, carbon content, particle shape and size distribution, and the presence of other minerals (Neville 1996).

2.3 Hydration Reaction

2.3.1 Hydration of Portland Cement Concrete

As the concrete‘s top-surface microstructure is a major factor in determining its resistance to salt scaling, the cement hydration and concrete microstructure development warrant further discussion. Hydration is the chemical change of concrete from a plastic stage to a solid one. This process begins as soon as water and cement come into contact. Several main phases in cement react during hydration. The following are the phases of

cement that contribute to strength gain, along with the notations used throughout the rest of this thesis: C=CaO, S=SiO_2, A= Al_2O_3, F= Fe_2O_3, H=H_2O, tricalcium silicate, alite, an impure form of C_3S; dicalcium silicate, belite, an impure form of C_2S; tri-calcium aluminateor C_3A; and tetracalcium aluminoferrite, C_4AF. Five stages of hydration as shown in Figure 2-2 are: dissolution, dormancy, hardening, cooling, and densification (FHWA 2006).

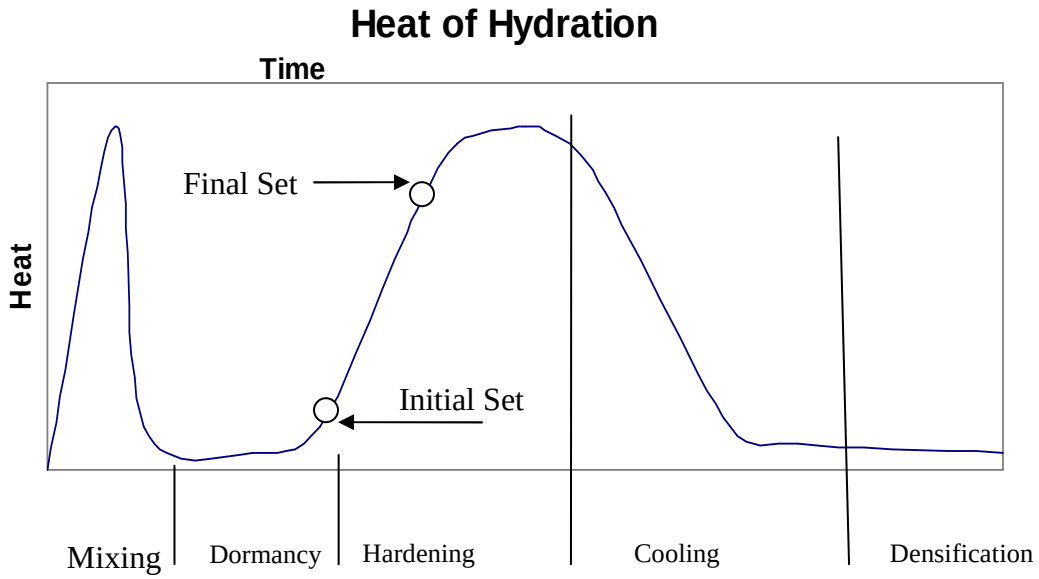

Figure 2-2 Heat of Hydration (after FHWA 2006)

2.3.1.1 Mixing /Dissolution

This stage starts as soon as water is introduced into the cement and aggregate mixture. The aluminate can generate significant heat and can cause flash set if not controlled correctly. The classical theory on the end of dissolution is that gypsum and aluminates react together to form monosulfoaluminate that coats the cement compounds. This coating will slow the aluminate reaction, in turn slowing the heat generation (FHWA 2006). Recent evidence has shown, however, that cement dissolution occurs at surface dislocations, which create surface pitting of the grains (Juilland et al. 2008).

2.3.1.2 Dormancy/ Dormant Period

As the aluminate reaction is slowed, reaction of the concrete goes into a dormant period. The concrete does not produce as much heat during this stage. The concrete is usually transported, placed, and finished during this period. The cement, especially the alite, and belite, continues to dissolve, and the water becomes saturated with calcium and hydroxyl ions (FHWA 2006). During the dormant period, the alite dissolution continues but at a reduced rate because of the high ion concentration in the solution. When the calcium concentration reaches the supersaturation limit, massive precipitation of hydration products occurs and the calcium concentration decreases, ending the dormant period (Juilland et al. 2008).

2.3.1.3 Hardening/Acceleration Period

Alite continues to dissolve at a faster rate because of decreased ionic concentrations forming calcium hydroxide (CH), calcium silicate hydrate (C-S-H), and it releases heat (Juilland et al. 2008). As hydration products precipitate, the mix begins to stiffen. Setting occurs when C-S-H forms bridges between solid cement particles to carry loads (FHWA 2006, Mindess et al. 2002).

2.3.1.4 Cooling/ Deceleration

The rate of reaction begins to slow down. This concept is not fully understood, although there are two principle theories: 1. the reaction becomes diffusion controlled; and 2. space is limited and growth and hydration is slowed (FHWA 2006).

2.3.1.5 Densification/ Steady State

In the final stage of hydration, reactions continue to slow and generate less heat. Densification of the hydration products continues to form a strong concrete mass, reducing the permeability. The reactions will continue as long as unreacted cement and water are both available (FHWA 2006).

2.3.2 Effects of Fly Ash on Concrete Hydration

Silica in fly ash reacts with CH in a pozzolanic reaction to form C-S-H gel xCH+yS+zH→ C-S-H (Neville 1996). Use of fly ash in concrete changes some concrete properties. Water demand of concrete with fly ash is lower than that of mixtures containing only portland cement, which allows for a lower water-cementitious material ratio (w/cm). Setting time may be delayed, especially by Class C fly ashes, although the effect is very dependent on the fly ash used. If the fly ash contains a low amount (~50%) of reactive silica, setting time may be longer (Neville 1996). Fly ash may reduce water demand by 5 to 15 percent, reduce long-term permeability, and reduce the rate of the heat of hydration (Neville 1996). The total amount of heat released from the use of fly ash can be higher when fly ashes with a high CaO content are used (Schindler and Folliard 2005).

Class C fly ash contains large amounts of calcium, some of which may be in the form of aluminate. This added aluminate can increase the rate of reaction and contribute to large variations in setting time (Roberts and Taylor 2007). Care should be taken to ensure that all materials are compatible at all possible concrete curing temperatures expected (FHWA 2006).

2.4 Contributing Factors

Even though salt scaling is not completely understood, it is believed to be affected by a combination of factors. Some of the more important factors are briefly discussed here.

2.4.1 Air-Void System

Air entrainment in concrete is known to protect the concrete paste system from damage. The American Concrete Institute (ACI) has set a prescriptive code requirement for total air content for concrete exposed to cycles of freezing and thawing. The ACI 318-08 (2008) requirements are reproduced in Table 2-1. Exposure Class F1 is concrete exposed to cycles of freezing and thawing, and that will also be occasionally exposed to moisture before freezing. Class F2 is assigned to concrete exposed to cycles of freezing

and thawing that is kept moist. Class F3 is assigned to concrete that will experience freezing and thawing and will be in contact with moisture and de-icing chemicals.

Table 2-1 Total Air Content for Concrete Exposed to Cycles of Freezing and Thawing (Reproduced from ACI 318-08)

Nominal maximum aggregate size, mm (in)	Air content, percent	
	Exposure Class F1	Exposure Classes F2 and F3
9.5 (3/8)	6	7.5
12.7 (1/2)	5.5	7
19.05 (3/4)	5	6
25.4 (1)	4.5	6
38.1 (1-1/2)	4.5	5.5
50.8 (2)	4	5
76.2 (3)	3.5	4.5

Spacing of air voids is known as the spacing factor. The spacing factor is an index of the maximum distance water, at any point in the cement paste, would have to travel to reach an air void (Neville 1996). The critical spacing factor is the threshold for which concrete with a higher spacing factor deteriorates rapidly when subjected to freeze-thaw cycles and de-icing chemicals (Pigeon and Pleau 1995). The critical spacing factor to prevent salt scaling is between 200-300 μm (0.00787 – 0.0118 in.) (Powers 1954, Pigeon and Pleau 1995, Valenza and Scherer 2007). It has also been shown that the mass loss is proportional to the spacing factor (Siebel 1989). Air entrainment, which reduces the spacing factor, improves salt-scaling resistance. Entraining air in concrete is usually accomplished by adding a chemical admixture known as an air-entraining admixture (AEA). The AEA helps stabilize spherical air bubbles in the concrete. The air-bubble spacing should be smaller than 200 μm (0.00787 in.), with most bubble sizes ranging between 10 μm (0.000394 in.) and 100 μm (0.00394 in.) to minimize the risk of salt scaling. However, adequate total air content does not necessarily correlate with an adequate spacing factor (Pigeon and Pleau 1995). As seen in Figure 2-3, both cross sections have a total air content of 6%; however, the majority of air bubbles in the top cross section are large, resulting in a bad spacing factor. The bottom cross section has many small air bubbles spaced out across the cross section, reducing the maximum distance that a freezing water particle would have to travel to reach an air void. This

makes it much more likely that water will not freeze in the concrete pores, causing damage.

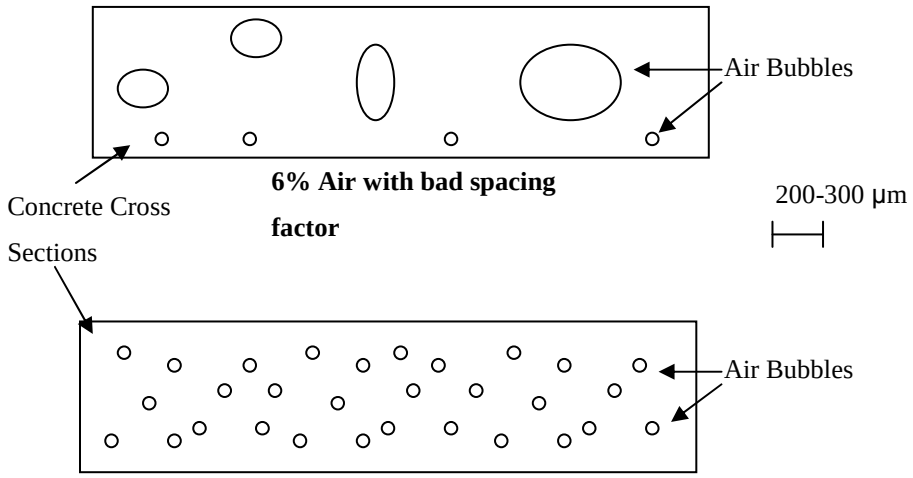

Figure 2-3 Examples of Spacing Factors

To determine the spacing factor of hardened concrete, two standardized methods are described in ASTM C 457-08 (2008), the linear-traverse method and the modified point-count method. The concrete sample is first polished to ensure a flat, even cross section with minimal damage to the air voids. The specimen is then placed under a stereoscopic microscope in a linear-traverse/point-count method device. For the traverse method, the sample is moved under the microscope and the summation of the distance of paste and air voids traversed are quantified. The summations are then used in formulas to determine different air void characteristics. The point-count method consists of moving the sample under the microscope a predetermined distance and recording the composition at each stop, in counts. These counts are then used to determine different air void characteristics.

Some issues are currently unresolved with the linear-traverse method. Discrepancies come from different preparation of specimens, operators, test methods, types of air voids counted, and magnification. Unsatisfactory surfaces can lead to higher spacing factors, and higher magnifications lead to smaller spacing factors, while only

measuring the entrained air voids reduces standard deviation of the spacing factor by 50%. Single-operator repeatability is, however, excellent when measurements are repeated along exactly the same lines of traverse (Sommer 1979).

2.4.2 Bleeding

Different densities of concrete constituent materials can cause some segregation of these materials. Some of the water in the mix can rise to the surface, which is referred to as bleeding (Neville 1996). Air entrainment reduces the amount of bleeding in fresh cement paste. Bleeding increases the w/cm ratio in the top layers of the concrete. Higher w/cm in the top layers reduces the strength of those layers (Pigeon and Pleau 1995, Neville 1996). This has been evidenced in experiments conducted by Afrani and Rogers (1994), in which testing was done on the molded bottom side of the specimens. In these experiments, no salt-scaling damage occurred, compared to severe scaling that occurred on the finished surface. Coarse aggregates and/or reinforcement can also trap bleed water as it tries to rise. This trapped water can create zones of weakness. These zones of weakness can make frost damage more likely to occur. Rising bleed water can carry a large amount of finer cement materials to the surface, making the surface more porous and weak (Neville 1996).

2.4.3 Temperature

Minimum temperature and duration at minimum temperature have been shown to affect the amount of scaling. No salt-scaling damage occurs when the minimum temperature is held above -10 ^{o}C (14 ^{o}F). The amount of damage is relative to the temperatures below -10 ^{o}C (14 ^{o}F), with the longer the duration at minimum temperature, the higher the amount of damage (Valenza and Scherer 2007). The freezing rate has been shown to have little to no effect on the salt scaling of concrete (Marchand et al. 1995).

2.4.4 Finishing and Curing

Salt scaling tends to occur more when the concrete is finished prematurely, before bleeding is complete. The finished surface denies the water a chance to escape, trapping it under the hardened surface layer. Trapped water leads the surface to have a higher

w/cm than the interior concrete, resulting in higher porosity and lower strength (Bleszynski et al. 2002).

Curing procedures have been shown to have a significant effect on salt scaling. Extended curing can help the concrete by increasing the degree of hydration of cement and strength at the surface (Pigeon and Pleau 1995, Valenza and Scherer 2007). A high curing temperature {>65 ^{o}C (149 ^{o}F)} has been shown to have a detrimental effect on salt-scaling resistance, probably because of increased porosity and lower long-term strength (Pigeon and Pleau 1995).

Curing compounds have shown reduction in the amount of scaling measured for some concrete specimens (Boyd and Hooten 2007). Curing compounds seal the surface layer during curing which reduces evaporation. This increases the degree of hydration of cement at the surface, which also increases strength gain in the concrete (Siddique et al. 2007).

2.4.5 Pessimum Concentration

The pessimum concentration is the salt concentration that causes the maximum amount of damage to a concrete surface during freeze-thaw cycles (Valenza and Scherer 2007). Approximately a 3%-by-weight solute has been found to be the pessimum concentration for concrete (Marchand et al. 1999). The pessimum concentration does not depend on the type of salt used (Valenza and Scherer 2005). Scaling did not occur when salt solution was not applied to the concrete surface (Valenza and Scherer 2006).

2.5 Test Methods

The following test methods are commonly used to determine the salt-scaling resistance of concrete. There has been evidence that some laboratory tests are much more severe than actual field conditions. The biggest difference is the formation of a porous, top concrete layer in laboratory specimens. The porous layer is thought to form because of the premature finishing of specimens before bleeding is completed (Marchand and Jolin 2005). A review of concrete salt-scaling test methods, including their advantages and problems is given in this section.

2.5.1 ASTM C 672: Scaling Resistance of Concrete Surfaces Exposed to De-icing Chemicals

ASTM C 672 (2003) is used to determine the resistance to scaling of a horizontal concrete surface exposed to freezing and thawing cycles in the presence of de-icing chemicals. The test is used to evaluate the effects of different variables such as mixture proportioning, surface treatment, curing, or other variables on salt scaling. Specimens must have a ponded surface area of at least 0.045 m^2 (72 $in.^2$), with a depth of at least 75 mm (3 in.). A 25-mm (1 in.)-wide and 20-mm (0.75 in.)-high dike is placed along the perimeter of the top surface of the specimen as seen in Figure 2-4. The dike can be of mortar if placed before curing or some other material if placed after curing.

Unless the curing condition is the variable being tested, specimens are covered with a plastic sheet after molding. Molds are removed after 24 hours. Specimens are then placed in a moist storage room for 14 days and then stored in air at 23±2 ^oC (73.5±3.5 ^oF) and relative humidity of 45-55 % for 14 days. After curing, a 6-mm (0.25 in.) layer of calcium chloride solution is applied to the specimens. The solution is to contain 4 grams (0.14 oz.) of anhydrous calcium chloride per 100 ml (3.38 fl. oz.) of water.

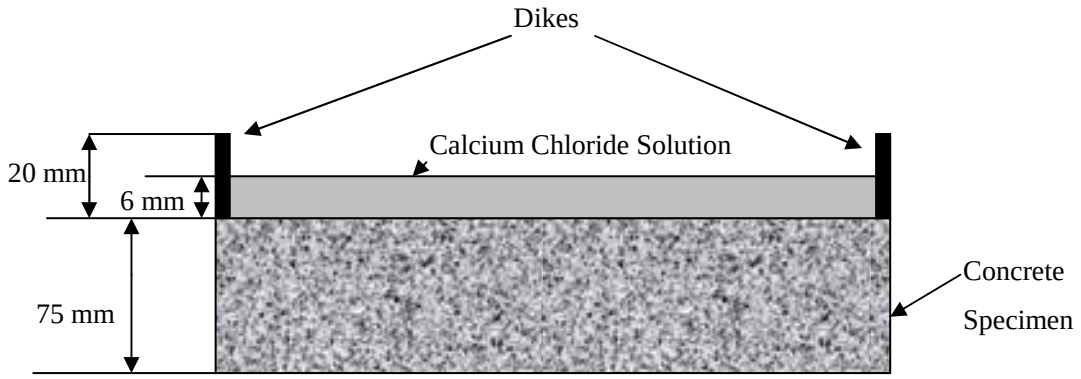

Figure 2-4 ASTM 672 Specimen (after Valenza and Scherer 2007)

The specimens are placed in a freezer at -18±3 ^{o}C (0±5 ^{o}F) for 16 to 18 hours. They are then removed from the freezer for six to eight hours and placed in laboratory air at 23±2 ^{o}C (73.5±3.5 ^{o}F) and relative humidity of 45-55 %. Solution is readded between cycles to maintain the proper depth. After five cycles, the solution is flushed off and a visual examination of the specimens is made. A rating of 0 through 5 is given after the visual examination as shown in Table 2-2. The test is finished after 50 freezing and thawing cycles.

Table 2-2 ASTM 672 Rating (Reproduced from ASTM 672 2003)

Rating	Condition
0	No scaling
1	Very slight scaling {3 mm (1/8 in.)} depth max (no coarse aggregate visible)
2	Slight to moderate scaling
3	Moderate scaling (some coarse aggregate visible)
4	Moderate to severe scaling
5	Severe scaling (coarse aggregate visible over entire surface)

Several possible shortcomings of the ASTM C 672 method have been identified. The rating scale is very subjective. The Portland Cement Association (PCA) has given examples of concrete samples at each of the different rating levels shown in Figure 2-5. Although subjective, the rating scale is good for a relative comparison of mixtures or qualifying mixtures to ensure no salt scaling. Critics of the test say the curing process of the laboratory sample does not reflect field curing and exposure conditions. This can be seen in experiments where cores from the field have been brought in and have performed better than the laboratory samples made from the same concrete batch (Boyd and Hooten 2007). The optional step of measuring the amount of mass loss has been suggested to be a more objective determination of amount of salt scaling (Valenza and Scherer 2007).

Figure 2-5 Salt-Scaling Rating (USACE 2010)

2.5.2 MTO LS-412 Scaling Resistance of Concrete Surfaces Exposed to De-icing Chemicals

The MTO LS-412 (1989) is very similar to ASTM 672, with a couple of small modifications. This test method uses specimens that are at least 300 x 300 x 75 mm (11.81 x 11.81 x 3 in.) in dimension or have a surface area of 0.09 m^2 (144 $in.^2$). This is twice the area required in ASTM 672. After each five cycles, specimens are washed off into a container, after which the washed-off material is oven dried. This gives the mass loss.

Measuring mass loss has taken out some of the subjectivity of the MTO LS-412 and the ASTM 672 test methods; however, repeatability of the test is questionable. Boyd and Hooton (2007) did a round-robin study at the Ontario Ministry of Transport (MTO) Laboratory and Lafarge's Belleville Laboratory to test specimens from six different mixtures. Boyd and Hooton also performed tests on two of the mixes. Differences in mass loss from each laboratory are summarized in Table 2-3. As seen in the table, there was a wide range of results. In the MTO standard, a mass loss greater than 0.8 kg/m^2

(0.164 lb/ft^2) after 50 cycles is considered to have poor salt-scaling resistance. Concrete mixtures 2 and 5 that were tested by the MTO passed this test, but failed when the tests were conducted by Lafarge.

Table 2-3 Differences in Scaling Test Results (Reproduced from Boyd and Hooton 2007)

	Average Cumulative Mass Loss (kg/m^2)		
Mix	MTO	Lafarge	Boyd and Hooton
1	1.6	2.02	1.44
2	0.5	1.24	
3	0.6	0.52	
4	1.4	1.55	1.4
5	0.36	1.24	
6	0.14	0.13	
1 kg/m^2 = 0.205 lb/ft^2			

2.5.3 Capillary Suction of De-icing Chemicals and Freeze-Thaw Tests (CDF)

The CDF test is used to determine the amount of scaling per unit surface area. Specimen slabs must have a total test area greater than 0.08m^2 (124 in.^{2}) and a height between 50 mm (1.97 in.) and 150 mm (5.91 in.). The concrete is placed into molds. The molds are removed after 24 hours and then placed in tap water at 20±2 ^{o}C (68±3.5 ^{o}F) up to the age of seven days. Specimens are then stored for 21 days at 20 ^{o}C (68 ^{o}F) and 65% relative humidity. Evaporation rate in the climate chamber must be 45±15 g/m^{2}hr (0.147±0.049 oz. /ft^{2}hr) for free water.

Next, specimens are sealed on their lateral surfaces between two and seven days before pre-saturation. Specimens are sealed with aluminum foil with a butyl rubber adhesive or sealed with a solvent-free epoxy resin. When aluminum foil is used to seal the specimens, there is to be an overlap of foil of at least 20 mm (0.787 in.). If resin is used, the bottoms and tops of the specimens must be kept clean of all resin.

Specimens are placed in a stainless steel test container. As seen in Figure 2-6, specimens sit on top of racks 10 mm (0.394 in.) above the bottom of the container. A sodium-chloride solution, 3% by weight, is then added to a level of 15 mm (0.591 in.). The top of the specimen remains dry in the sealed container. The containers are allowed

to sit for seven days at 20±2 °C (68±3.5 °F) to allow for capillary suction. The container is set inside a temperature-controlled chest with coolant as shown in Figure 2-6. Before undergoing freeze-thaw cycles, specimens are placed in an ultrasonic bath to remove any loosely adhering particles and dirt.

A 12-hour freeze-thaw cycle is applied to the concrete specimens. Starting at 20 °C (68 °F), the temperature is lowered in 4 hours to -20 °C (-4 °F) with a constant rate of -10 °C /h (50 °F/h). For 3 hours the specimens are kept at -20 °C (-4 °F) and then increased to 20 °C (68 °F) at a constant heating rate of 10 °C/h (50 °F/h) and kept constant for 1 hour at +20 °C (68 °F). At cycles 14 and 28, when the specimens are above 15 °C (59 °F), they are placed in an ultrasonic bath for three minutes to remove any loose particles. The concrete mass loss is then measured (Setzer et al. 1996, Setzer and Auberg 1995).

The following are the steps to the CDF Test:

1. Dry storage
2. Sealing of specimen
3. Presaturation of test liquid by capillary suction
4. Cleaning of test surface before starting the freeze-thaw cycles
5. Freeze-thaw cycles
6. Determination of surface scaling

The precision of the CDF test allows separation of several phenomena. Scaling can be separated into two parts – initial scaling and later, continuous scaling. Using the CDF test, it is possible to distinguish between chemical and physical influences (Setzer 1997).

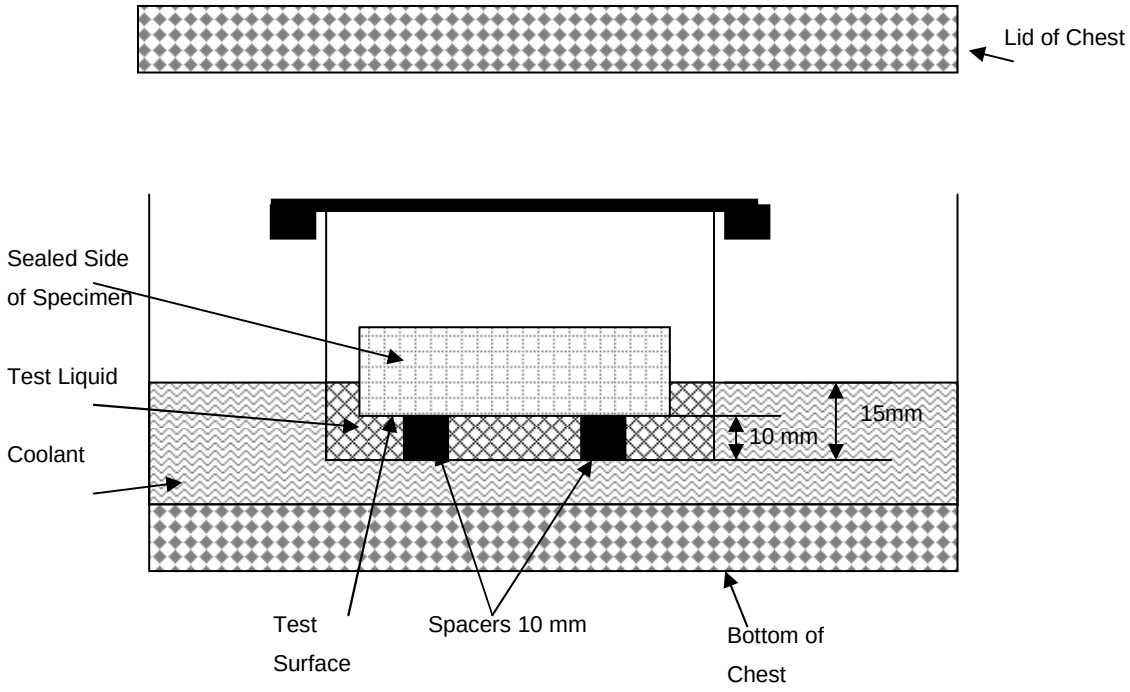

25.4 mm = 1 in.

Figure 2-6 CDF Test Container (after Setzer et al. 1996)

2.5.4 Swedish Standard SS 13 72 44 (Boras method)

The Boras method is similar to ASTM 672 with two modifications. Unidirectional freezing is desired, so approximately 20 mm (0.787 in.) of insulation is placed on sides and bottom of the sample as seen in Figure 2-7. To prevent evaporation of the solution, a plastic sheet is placed 20 mm (0.787 in.) above the solution. Samples are 50-mm (1.96 in) thick with a solution depth of 3 mm (0.118 in.). In the freezing cycle, the specimen is cooled to -17±2.5 ^{o}C (1.4±4.5 ^{o}F) over a period of 12 hours and then held at the minimum temperature for 4 hours. The specimen's temperature is then raised to 20±5 ^{o}C (68 ± 9 ^{o}F) over a period of 8 hours (SS 1372 44 1992).

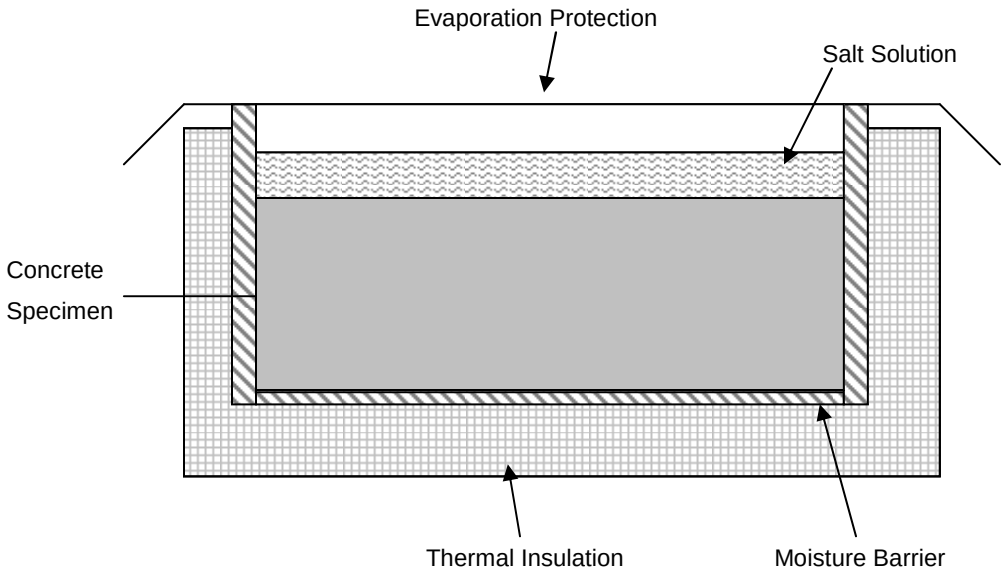

Figure 2-7 Boras Method Test Setup (after Pigeon and Pleau 1995)

Specimens are subject to at least 56 cycles. Solution is removed from the specimen every seven cycles. The specimen is lightly brushed to remove all loose materials, which are collected and dried to obtain a total mass loss. This test has two advantages over the ASTM C 672 method. Freezing progresses vertically from top to bottom – the same way freezing occurs in the field. The assessment is also quantitative instead of qualitative, as with the visual rating in the ASTM 672 (SS 1372 44 1992).

2.5.5 Laboratory Test Results Versus Field Performance

It is hard to represent true field conditions in a laboratory test. Natural conditions are varied, complex, and extremely difficult to reproduce. The deterioration process in the field may take years, while in the laboratory the process only takes weeks. To accelerate the process, tests usually amplify the severity of exposure conditions, and consequently, an amplification of damage (Pigeon and Pleau 1995).

Some tests, such as ASTM C 672, will only pass the most durable concretes while failing the rest. False-negative tests unnecessarily eliminate potentially durable concrete,

when it possible that the concrete in question could be highly functional in other situations (Pigeon and Pleau 1995).

Another concern about laboratory tests versus field performance is that placing of and finishing of small samples in molds do not represent placement of concrete in the field. For laboratory tests, the concrete is put into small molds. The surface can easily be overworked, creating a sample that is not representative of field placement. Marchand et al. (2005) did comparisons of molds and cores from a sidewalk from the same concrete loads. Nine batches of concrete, consisting of five different mixes, were used in construction of a sidewalk. Laboratory specimens were made by ASTM 672 standard, and subjected to the ASTM 672 test. Sixty days after placement, the sidewalk was cored. The cores were also subjected to the ASTM 672 test and the results can be seen in Table 2-4. As can be seen in the table, field cores performed better than the lab specimens, even though all specimens were made from the same batches of concrete.

Table 2-4 De-Icer, Salt-Scaling Test Results (Marchand et al. 2005)

Mix	Mass Loss of Lab Specimens (kg/m^2)	Mass Loss of Field Cores (kg/m^2)
1	0.64	0.03
2	0.45	0.03
3	1.91	0.16
4	1.07	0.03
5	4.28	0.23
6	2.56	0.52
7	1.43	0.32
8	1.68	0.31
9	2.19	0.09
$1\ kg/m^2 = 0.205\ lb/ft^2$		

Boyd and Hooton (2007) conducted a study in which they placed in-ground slabs along with two different sets of laboratory specimens. The first set was tested with the MTO LS-412 test, following the standard in which specimens were cured in the laboratory and testing began at the age of 28 days, while the second set of specimens were allowed to cure in field conditions for 127 days and then tested following the MTO LS-412 standard. The differences can be seen in Table 2-5, where the specimens that

were allowed to cure in field condition outperformed the specimens that were cured in the laboratory.

Table 2-5 Differences in Mass Loss for Two Curing Conditions (Boyd and Hooton 2007)

Mix	Average Mass Loss - Lab Cured (kg/m^2)	Average Mass Loss - Field Cured 127 Days (kg/m^2)
1	1.69	0.97
2	0.87	0.195
3	0.56	0.098
4	1.45	0.193
5	1.6	0.198
6	0.135	0.065
1 kg/m^2 = 0.205 lb/ft^2		

2.6 Salt Scaling in Concrete Containing Supplementary Cementing Materials (SCMs)

Use of SCMs has economical and environmental benefits, as most SCMs are waste from industrial processes. Addition of SCMs can increase long-term concrete strength (>28 days) (Valenza and Scherer 2007). SCMs, however, have produced mixed results in salt-scaling performance as will be explained later in this chapter. Chemical and physical properties of representative SCMs are shown in Table 2-6.

Table 2-6 Chemical Analyses of Cement and SCMs (Reproduced from FHWA 2006)

	Type I Cement	Class F Fly Ash	Class C Fly Ash	Blast Furnace Slag	Silica Fume
Silica ($Si0_2$) %	22	52	35	35	90
Alumina (Al_2O_3) %	8	23	18	12	0.4
Iron Oxide (Fe_2O_3) %	3.5	11	6	1	0.4
Calcium Oxide (CaO) %	65	5	21	40	1.6
Sulfate (SO_4) %	1	0.8	4.1	9	0.4
Sodium Oxide (Na_2O) %	0.2	1	5.8	0.3	0.5
Potassium Oxide (K_2O) %	1	2	0.7	0.4	2.2
Specific surface, kg/m^2 (lb/ft^2)	150-250 (31-51)	250-600 (51-123)		350-500 (72-102)	15000-20000 (3072-4096)
Particle size, μm (in.)	3-100 (0.000118-0.00394)	1-100 (0.000039-0.00394)			0.01-0.5 (0-0.00002)

2.6.1 Fly Ash

Concrete containing fly ash as a partial cement replacement has a lower strength gain rate than that of ordinary portland cement concrete; however, between one and two months, the strength of concrete containing fly ash may surpass that of concrete containing only portland cement (Neville 1996). Some fly ash can be detrimental to the development of the air-void system. These fly ashes contain unburned carbon that absorbs air-entraining agents. If carbon content is highly variable, air content may also be highly variable (Pigeon and Pleau 1995, Neville 1996).

Resistance of concrete to salt scaling appears to be influenced considerably by the fly ash utilized, quantity used, construction conditions, and curing (Bilodeau et al. 1994). Several studies have shown that fly ash diminished resistance to scaling in standardized

laboratory tests. As the mass of fly ash substituted for portland cement increases, bleeding also increases, which may contribute to a weaker surface (Valenza and Scherer 2007).

Marchand et al. (1997) concluded in testing that the amount of fly ash substituted for cement correlated directly with the mass loss. The findings are summarized in Figure 2-8. Concrete with no fly ash (0% FA) outperformed those with 20% and 40% fly ash, with the 40% sample having the highest mass loss.

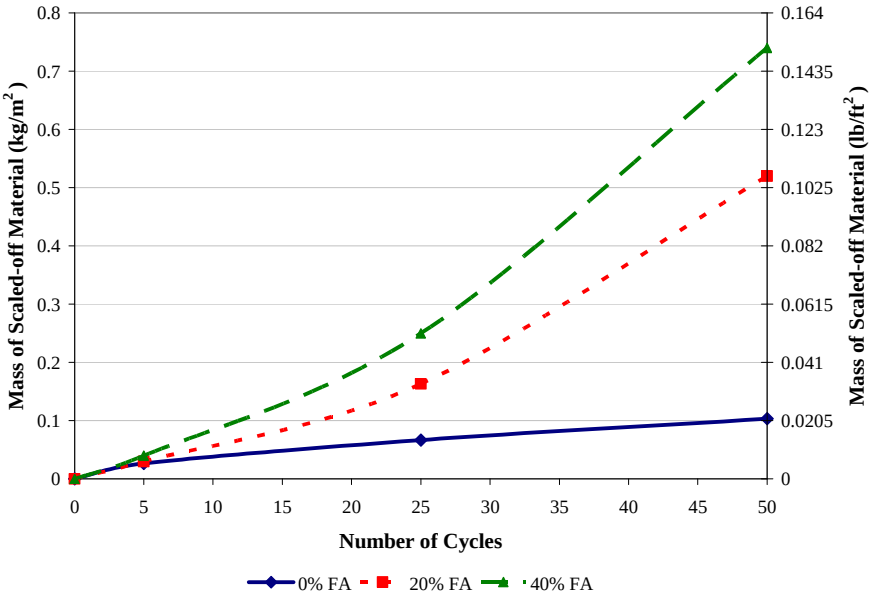

Figure 2-8 Amount of Fly Ash Comparison (Reproduced from Marchand et al. 1997)

Bilodeau et al. (1994) conducted salt-scaling tests on concrete specimens containing fly ash with different specific gravities from different sources around the United States. The cement was replaced at a rate of approximately 58% by mass. The specimens underwent the ASTM C 672 tests. Results of mass loss versus specific gravity at 50 cycles and 100 cycles can be seen in Figure 2-9. Results conclude that the higher the specific gravity, the higher the salt-scaling resistance.

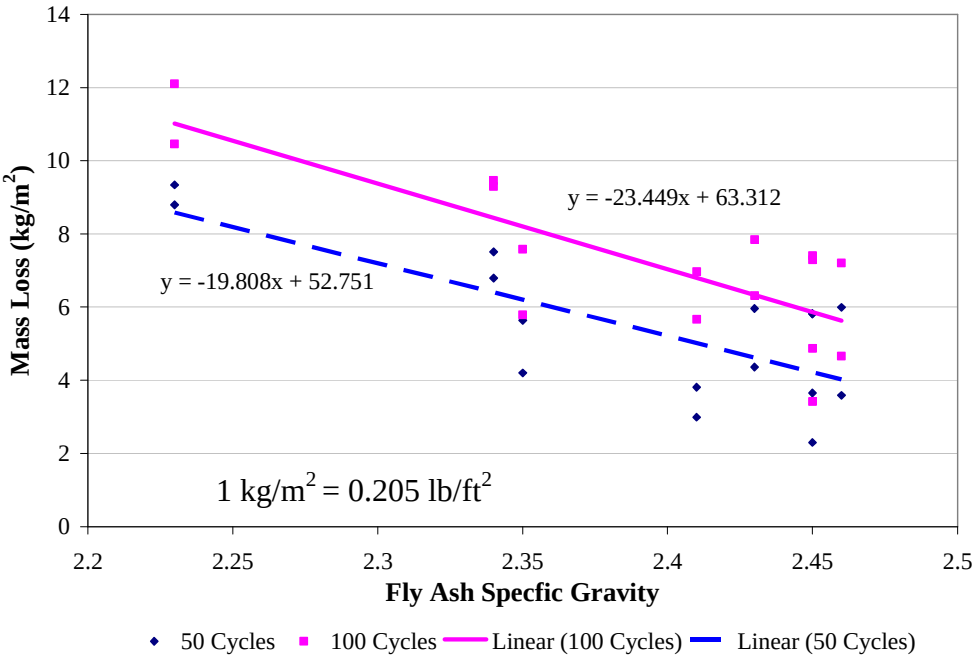

Figure 2-9 Salt Scaling by Specific Gravity (Bilodeau et al. 1994)

2.6.2 Silica Fume

Silica fume is a by-product of the metallurgical process used in the production of silicon metal and ferrosilicon alloys. It is composed of very fine spherical particles ranging in size from 0.01 to 0.5 μm (0-0.00002 in.) of usually greater than 90% amorphous silica depending on the alloy. It is, on average, 100 times finer than portland cement, has 50 times the surface area, and is a highly reactive pozzolan (Thomas 1996, Neville 1996). The silica in silica fume reacts with Calcium Hydroxide (CH) to form C-S-H gel. The theoretical substitution rate needed to consume all the CH has been found to be approximately 10% (Neville 1996).

Workability of concrete containing silica fume will decrease because the high surface area requires more water to coat all of the particles, or a higher dosage of superplasticizer to compensate for the decreased concrete workability (Neville 1996). Usually a superplastcizer is used in mixtures containing silica fume to offset the decreased workability and disperse the particles after densification for shipping. Silica fume also improves early strength gain by providing nucleation sites for hydration

products. Silica fume will create a refined pore structure with smaller radii (Valenza and Scherer 2007).

Use of silica fume as a SCM has shown mixed results in salt scaling. Bleszynski et al. (2002) found the increase in silica fume reduces scaling. Sellevold, et al. (1991), and Jacobsen (1995) have, however, found that silica-fume concrete subjected to prolonged freeze/thaw cycles resulted in poor scaling performance. Silica fume acts as a filler and nucleation site until the pozzolanic reactions occurs (Valenza and Scherer 2007).

2.6.3 Blast Furnace Slag

Blast furnace slag is the non-metallic by-product from the production of pig iron in a blast furnace. It consists essentially of silicates and alumino-silicates of calcium and other constituents. For every 1,000 kg (2,204 lb) of pig iron produced, about 300 kg (661 lb) of slag is produced. Slag is produced from a liquid phase, which upon rapid cooling, forms pellets of solidified glass. This glass is then ground to a fineness similar to that of cement (Neville 1996). The maximum practical slag substitution to consume all CH has been determined to be 50%. Higher cement-replacement levels may require an alkali activator for practical use (Valenza and Scherer 2007, Neville 1996). Slag hydration will produce more C-S-H, which may result in a denser microstructure (Neville 1996).

Slag will improve workability of the concrete because of a better dispersion of the cementitious particles and the limited amount of water that slag will absorb during mixing. Slag often slows hydration time of the concrete because the glass has to be broken down by hydroxyl ions. When slag concrete is young (0-7 days), it has less strength than ordinary portland cement concrete (OPC); however, after 28 days, slag concrete may be stronger than OPC concrete (Neville 1996). Fine slag will delay and reduce bleeding of concrete. If the concrete is prematurely finished before the bleeding is completed, the surface layer may become weaker and exhibit poor salt-scaling resistance. (Bleszynski et al. 2002)

When carbonation occurs in blast furnace slag concrete, it results in a coarser microstructure, which makes the surface weaker and more susceptible to salt scaling

(Valenza and Scherer 2007). Concrete containing high volumes of slag has been shown to carbonate at a much higher rate than ordinary portland cement concrete because of formation of two polymorphs of calcium carbonate: aragonite and vaterite. As the slag concrete carbonates, it will decalcify the C-S-H, leaving a coarser microstructure (Ngala and Page 1997). Unlike ordinary portland cement concrete, carbonation in slag concrete reduces salt-scaling resistance (Litvan and Meyer 1986).

2.6.4 Ternary Blends

Ternary blends are a combination of portland cement with two SCMs (most commonly fly ash, silica fume, or slag). Often silica fume is used in low percentages with another SCM at a higher cement replacement dosage. This helps to overcome some of the side effects of the use of higher volumes of fly ash or slag such as lower early-strength gain or permeability. Ternary blends containing silica fume, fly ash, and blast furnace slag produce less permeable concrete than concrete containing only silica fume (Mindness et al. 2002).

2.7 Possible Mechanisms

Although the exact mechanism of salt scaling is not known, several theories have been proposed by different researchers. The following section reviews a few of these possible mechanisms.

2.7.1 Glue Spall

Glue spalling is a technique used to decorate glass. In decorative glass, an epoxy with inclusions is spread across a sandblasted glass surface. The epoxy is allowed to cure and the temperature of the glass is cooled. During cooling, stress from the thermal expansion mismatches that of the epoxy and inclusions cause the epoxy to crack. High tensile stresses then develop in the glass surface causing, the crack to propagate in the glass. Subsequently, when cracks in the glass connect, a thin piece of glass is removed. Some researchers believe that a similar process happens at the surface of concrete causing salt scaling (Valenza and Scherer 2006).

Cracks in a concrete surface can be formed by two different processes: 1. propagation of pre-existing surface flaws, or 2. penetration of the crack from the ice layer into the surface. Concrete can be exposed to traffic, wind, rain, and other surface-deteriorating processes leaving flaws on its surface. The second type of cracking is the basis for the glue spall theory. Three situations can occur when ice cracks on the concrete surface: 1. The crack can arrest at the interface; 2. The crack can bifurcate along the interface; or 3. It can penetrate the concrete. After the crack reaches a critical depth, it then runs parallel to the surface. Cracks run into each other leaving a small piece of cement paste detached from the surface (Valenza and Scherer 2006). The demonstration can be seen in Figure 2-10.

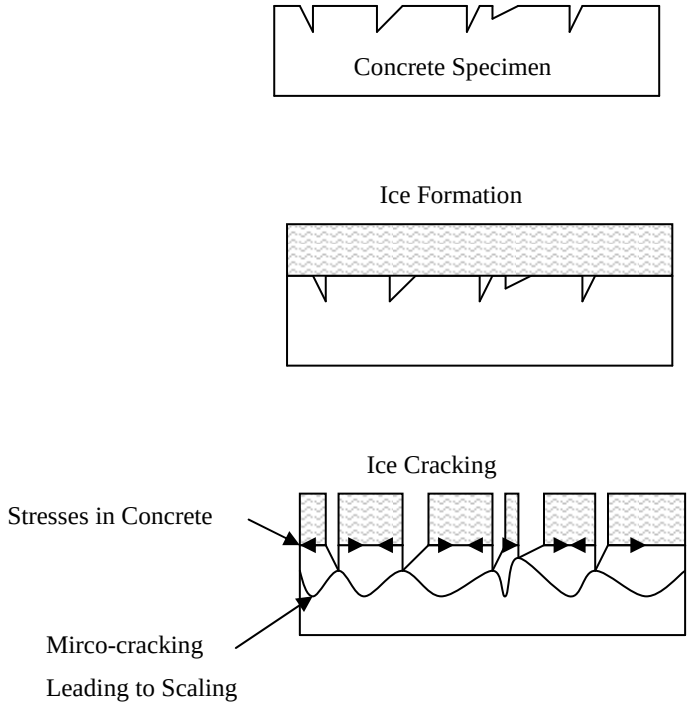

Figure 2-10 Glue Spalling (after Valenza and Scherer 2006)

The glue spall theory can explain the pessimum concentration effect discussed in section 2.4.5. When the saline solution starts to freeze, none of the salt enters the ice crystal lattice. Ice will nucleate and at first form only pure ice, while the salt is concentrated into small brine pockets inside the ice. These pockets weaken the ice.

Cracks then form and propagate across the surface of the concrete. If the saline concentration is too high, there will be a large number of brine pockets, which will cause the ice to be very weak, reducing the fracture energy that is applied to the concrete surface. This limits the damage that occurs to the concrete when exposed to solutions of high salt concentrations. When the concentration is too low, very few weak pockets are created in the ice, reducing cracking and spalling. The pessimum salt concentration in the solution that the concrete is exposed to is 3%, independent of the salt type (Valenza and Scherer 2006).

2.7.2 Differences in Pressures

Powers and Helmuth (1953) suggest that the presence of de-icer salts increases the difference between the vapor pressure over the supercooled water in capillary pores and that over the ice formed on all external faces of the paste. This can lead to osmotic pressures in various degrees of ice formation in different concrete layers. Ice formation can block the flow of water due to osmosis, which can create high stresses in the top concrete layers (Pigeon and Pleau 1995).

Browne and Cady (1975) suggest that variation in salt concentration, which produces gradient hydraulic pressures, causes salt scaling. Salt concentration on the surface is too high for ice to form; however, ice can form under the surface generating large hydraulic pressures that are strong enough to break flakes from the surface.

2.7.3 Layer Mechanism

Harnick and Rosli (1980) suggest a layer-by-layer freezing phenomenon leading to surface scaling. Three gradients work together in scaling. The first is the gradient of water content. The outer layer of concrete, where ice will form, has more water content then the inner layer. The second gradient is salt concentration. The outer layer of concrete will only contain a small amount of de-icer salt, making ice formation possible at temperatures close to the freezing point. However, in the layer underneath the surface, ice does not generally form because the salt concentration is too high. The third gradient is the thermal gradient. It takes a large amount of heat to melt the ice. This heat is

extracted from the concrete surface. Thus, the concrete cools rapidly, in turn causing a large thermal gradient. Ice formation on the surface creates stresses due to the varying expansion of the two layers and leads to scaling.

CHAPTER 3 - Durability Test Sites

Laboratory tests allow researchers to test material quality and test hypotheses under controlled conditions. They can isolate environmental and other exposures affecting concrete performance. Laboratory tests do not always, however, represent what happens in the field because the natural cycling exposure time, rate, and severity can be different. Application of salt will vary between the field and the laboratory. The field can have a varied application in just one slab, while the laboratory employs a more uniform application, usually harsher than the typical field application. As shown by Nokken et al. (2004), the curing temperature of 23 ^{o}C (73.5 ^{o}F) in the laboratory does not represent the average temperatures that concrete will experience in the field. They also found that the length of freezing cycles varied from 11-206 hours, compared to most ASTM test having freezing periods of 2-16 hours. Several durability test sites have been set up across the world to observe concrete in true environmental situations for different types of concrete distress. These can range from racks in the ocean to a small lot covered in concrete blocks and slabs. In this chapter, a few of these durability test sites and associated research will be discussed.

3.1 Treat Island Marine Exposure Station, Maine

Treat Island is located on the Bay of Fundy near Eastport, Maine. The location was established in 1936 by the United States Army Corps of Engineers. The facility has a series of racks that can hold specimens at mid-tide level, which are immersed twice daily by the rising of the tide. The tide can rise by as much as 6.7 meters (22 ft). The average ambient temperature during the coldest part of the winter is around -10 ^{o}C (14 ^{o}F). Depending on the severity of the winter, each specimen is subjected to between 100 to 160 freeze-thaw cycles per year. A series of other concrete specimens have been placed on a nearby beach to look at different concrete mixtures and the effects of ocean spray.

Approximately 22 active research projects are on going at Treat Island. Projects investigate a wide variety of properties of concrete. Current ongoing projects include

specimens on racks to monitor mass loss and volume change of mixtures. Durability of bonding new concrete to existing concrete has been researched at Treat Island. Master Builders (now the construction chemicals division of BASF) has sponsored scaling, corrosion-inhibitor, and concrete freeze-thaw resistance projects.

Each of the current projects at Treat Island examines different variables; however, most are focused on a specific material parameter and how it relates to salt water and freeze-thaw. A map of the specimens from the projects at Treat Island is provided in Figure 3-1, and a map of the specimens on the beach is shown in Figure 3-2.

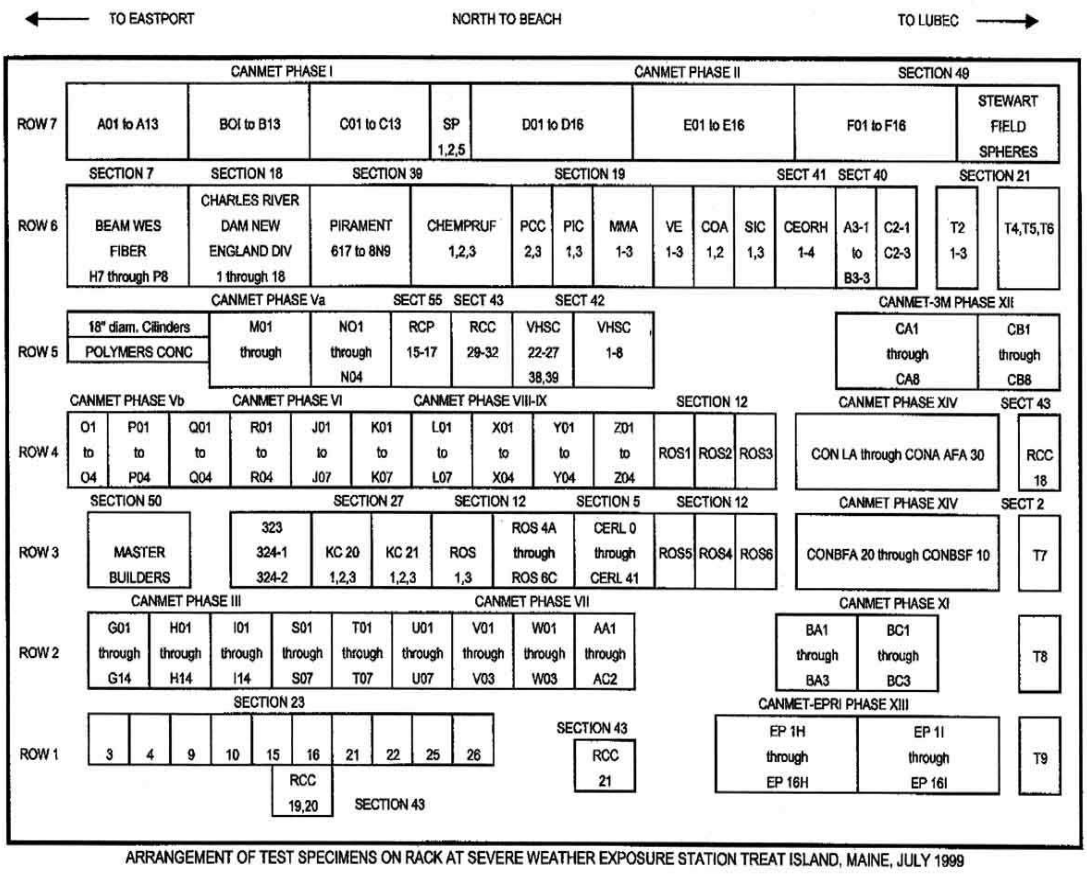

Figure 3-1 Map of Specimens on Racks at Treat Island (USACE 2010)

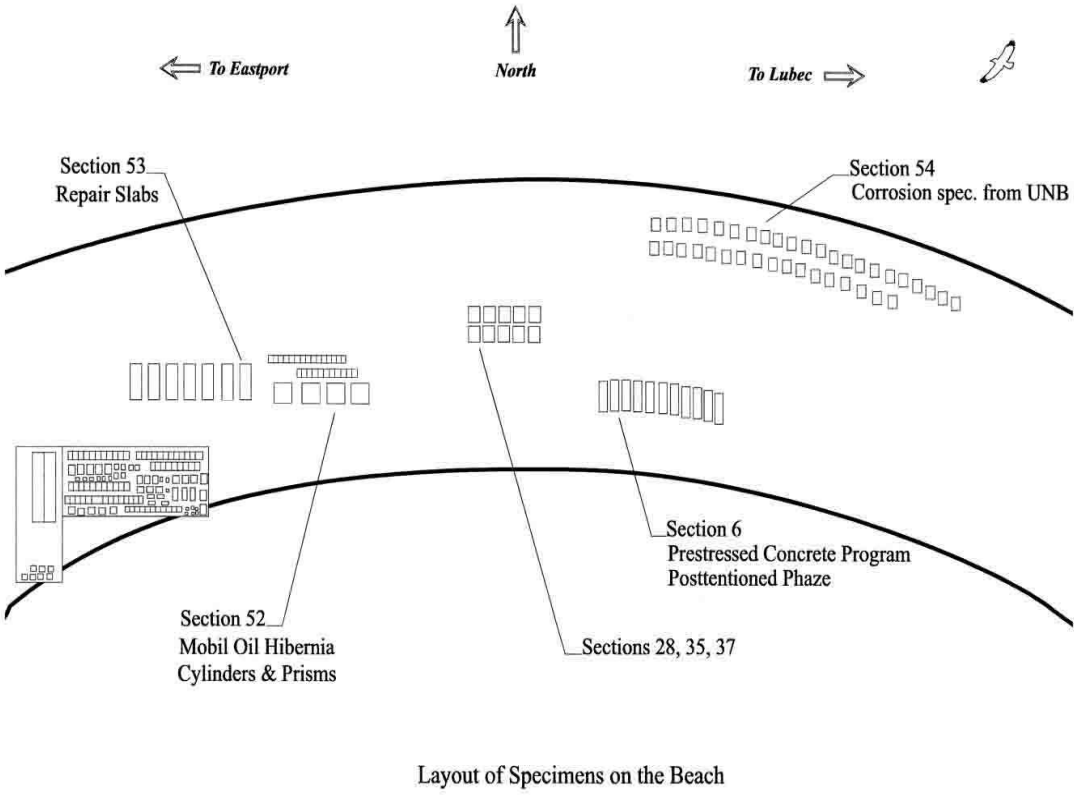

Figure 3-2 Map of Specimens on the Beach at Treat Island (USACE 2010)

3.2 CANMET, Ottawa, Canada

The Canada Centre for Mineral and Energy Technology (CANMET) is located in Ottawa, Canada. The site was established in 1991, primarily for validating accelerated ASR test methods and evaluating the effectiveness of various measures for preventing damage due to ASR. CANMET's mission is to develop an engineering database on the effectiveness of SCMs in controlling ASR. The site's objectives include comparing effectiveness of SCMs to reduce ASR expansion and cracking due to long-term field exposure, determining effects of exposure conditions such as the use of de-icing salt on ASR, and developing petrographic procedures to measure and quantify ASR damage. As of 1996, the site had samples of more than 125 concrete mixtures with 14 reactive aggregates from across the world. Specimens range from slabs 0.4 x 0.4 x 0.7 m (15 x 15x 28 in.) to 0.7 x 0.7 x 0.15 m (28 x 28 x 6 in.) prisms. The prism specimens are

arranged at different elevations. Some are set directly on the ground, while others sit on blocks off of the ground. The blocks have measuring points placed in them during batching. Periodically, expansion is measured (Fournier 1996). A picture of the CANMET is shown in Figure 3-3. CANMET has worked with the University of Texas-Austin in comparing results from the same mixtures.

Figure 3-3 CANMET Exposure Site (Benoit Fournier, personal communication, Nov. 24, 2009)

3.3 Concrete Durability Center, University of Texas-Austin

The University of Texas-Austin has developed a long-term exposure site, constructed in 2001 for comparison of ASR results with CANMET. The site is a 15.24 x 30.48 m (50 x 100 ft) section of land at the J.J. Pickle Research Campus of the University of Texas at Austin. The site is equipped with a weather station containing a data logger to monitor the weather along with temperature data from blocks cast with temperature sensors.

Funding for the site was provided by the Texas Department of Transportation (TxDOT), the Federal Highway Administration (FHWA), the International Center for Aggregate Research (ICAR), and the Electric Power Research Institute (EPRI). The site allows for long-term monitoring of progression of ASR and delayed ettringite formation (DEF) in concrete exposure blocks as shown in Figure 3-4. Concrete on this site contains

more than 35 aggregates from across North America and various preventative measures (supplementary cementing materials and chemical admixtures) to mitigate ASR.

In 2005, the site was expanded (with TxDOT support) to evaluate external sulfate attack (concrete specimens exposed to soils containing calcium sulfate, sodium sulfate, and magnesium sulfate). The sulfate exposure site can be seen in Figure 3-4.

The main goal of this outdoor exposure site testing is to ensure that accelerated laboratory testing most accurately predicts field performance. Data generated from this outdoor exposure site have already been instrumental in development of improved test methods and specifications at state, federal, and international levels (Thano Drimalas, personal communication, July 29, 2009).

Figure 3-4 UT Austin Exposure Site

3.4 BRE, United Kingdom

The Building Research Establishment (BRE) in the United Kingdom was built to monitor large concrete blocks stored on an outdoor exposure site. The BRE made concrete blocks ranging between the sizes of 350 mm (13.78 in.) to 900 mm (35.43 in.), and then stored them directly on the ground or ponded them in water or solutions as can be seen in Figure 3-5. The BRE has conducted research into ASR and other concrete durability using these blocks. DEMEC-type strain gauges and embedded reference points have been used to measure concrete expansion (Thomas et al. 2006).

Figure 3-5 BRE Exposure Site Blocks (Thomas et al. 2006)

3.5 Research Lots and Roads

Many researchers have taken advantage of new construction such as parking lots, sidewalks, roadways, and Jersey barriers to research salt scaling. New construction allows different mixes to be used in the same vicinity and be subjected to the same types of weathering. Researchers are able to observe how concrete reacts to normal use in natural weathering conditions. These field exposure sites allow for comparing laboratory test results versus natural exposure. The following section gives a few examples of what has been completed.

Marchand et al. (2005) of Laval University used construction of a new sidewalk in the city of Quebec, Canada, to test five different concrete mixes that incorporated SCMs. Some of the results from that study were discussed in Chapter 2. As of 2005, the concrete has been observed for 10 years with excellent behavior versus laboratory specimens that had a high failure rate. Both laboratory and field concrete specimens were made from the same concrete batches.

Bleszynski, et al. (2002) used replacement of a severely damaged service roadway at a cement plant in Picton, Ontario, Canada, to place seven different concrete mixtures and observe how the mixes performed versus laboratory specimens. As of 2002, the roadway had been observed for four years with all the concrete mixtures performing approximately the same.

CHAPTER 4 - Material Properties

This chapter discusses properties and testing of aggregates and materials used in concrete to place salt-scaling specimens and ASR durability blocks placed at the Kansas Outdoor Concrete Exposure site (KOCE).

4.1 Coarse Aggregate

The coarse aggregate, seen in Figure 4-1, used in all of the salt-scaling mixes, was a crushed limestone from a local Manhattan quarry shown in Figure 4-1. Siliceous river pea gravel from the Kansas River, shown in Figure 4-2, was used in the ASR blocks. Specific gravity and absorption were determined for three representative samples, according to ASTM C 127 (2007). The average of the three samples for each aggregate test is shown in Table 4-1 and Table 4-2 for the salt-scaling aggregate and ASR blocks, respectively.

Figure 4-1 Salt-Scaling Coarse Aggregate

Figure 4-2 ASR Coarse Aggregate

Table 4-1 Salt-Scaling, Coarse-Aggregate Properties

Saturated-Surface Dry (SSD) Specific Gravity	2.624
Oven-Dry Specific Gravity	2.554
Absorption (%)	2.8

Table 4-2 ASR Coarse-Aggregate Properties

Saturated-Surface Dry (SSD) Specific Gravity	2.57
Oven Dry Specific Gravity	2.488
Absorption (%)	3.3

The coarse-aggregate gradation was determined according to ASTM C 136 (2006). For a representative gradation, three five kg (11.02 lb) samples were sieved. The aggregates' particle-size distribution was determined from the average of the three samples shown in Figures 4-3 and 4-4, respectively. Nominal maximum size for the salt-scaling coarse aggregate was 19 mm (0.75 in), and 12.5 mm (0.5 in.) for the ASR coarse aggregate.

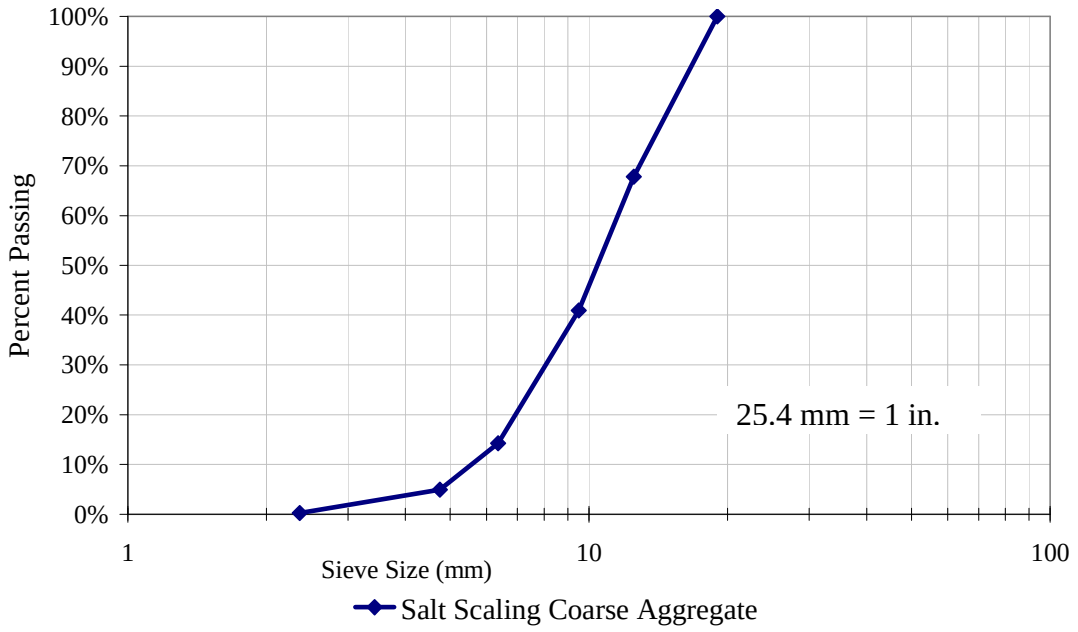

Figure 4-3 Salt-Scaling, Coarse-Aggregate Gradation

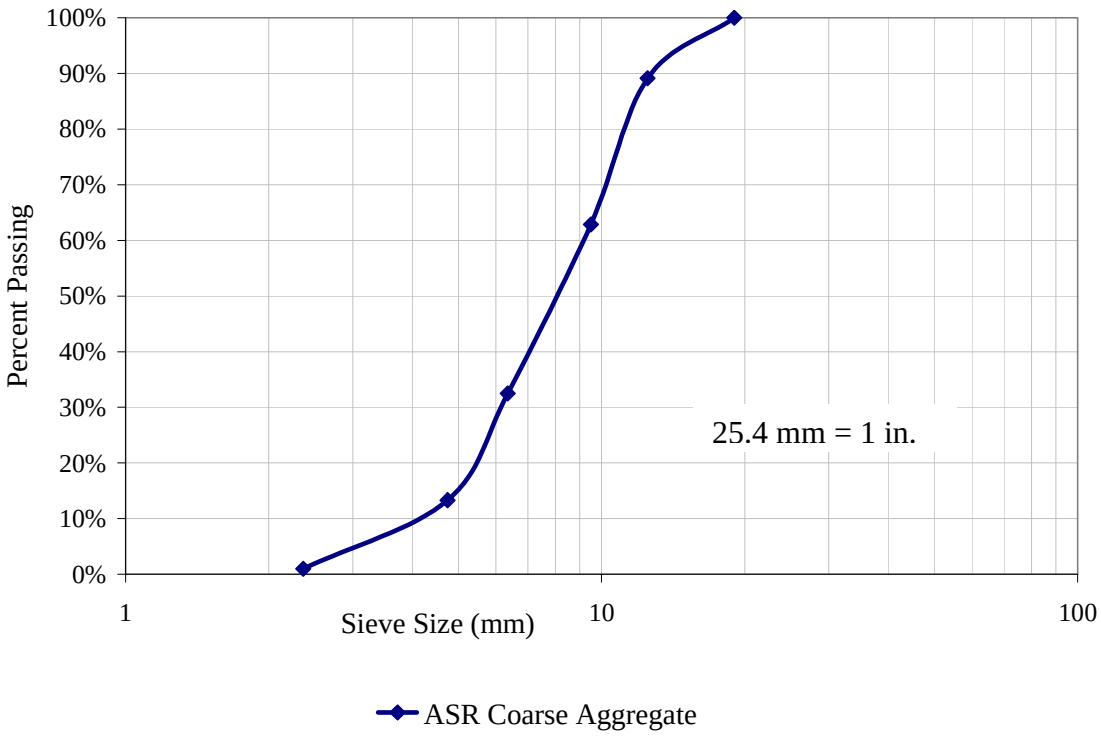

Figure 4-4 ASR Coarse-Aggregate Gradation

4.2 Fine Aggregate

The fine aggregate used for the salt-scaling test was concrete sand, a siliceous natural sand, from a local ready-mix plant as shown in Figure 4-5. The Kansas Department of Transportation (KDOT) identified a siliceous natural ASR reactive sand, shown in Figure 4-6, obtained in Junction City, Kansas.

ASTM C 128 (2007) was used to determine the specific gravity and absorption of three representative samples. Averages of the three samples for each fine-aggregate test are shown Table 4-3 and Table 4-4.

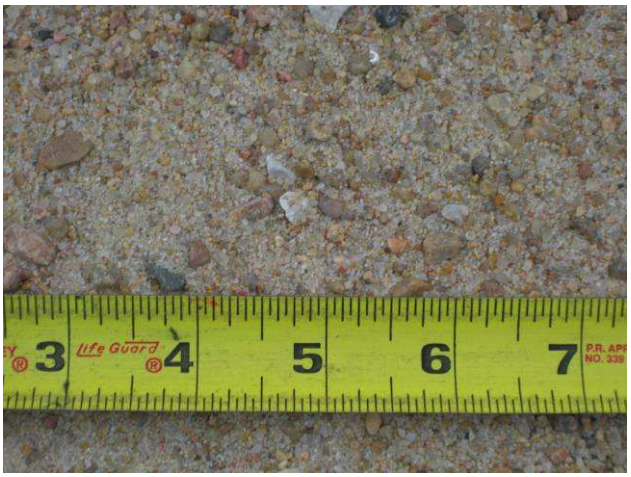

Figure 4-5 Salt-Scaling Fine Aggregate

Figure 4-6 ASR Fine Aggregate

Table 4-3 Salt-Scaling, Fine-Aggregate Properties

Saturated-Surface Dry (SSD) Specific Gravity	2.623
Oven-Dry Specific Gravity	2.605
Absorption (%)	0.7

Table 4-4 ASR Fine-Aggregate Properties

Saturated-Surface Dry (SSD) Specific Gravity	2.57
Oven-Dry Specific Gravity	2.488
Absorption (%)	0.5

Gradation was determined in the same fashion as for the coarse aggregate, following ASTM C 136 (2006). Average results of the three samples can be seen in Figure 4-7 and Figure 4-8. The fineness modulus (FM) was determined by adding the cumulative percentages retained on sieves of 4.75 mm (No. 4), 2.36 mm (No. 8), 1.18 mm (No. 16), 0.6 mm (No. 30), 0.3 mm (No. 50.), and 0.15 mm (No. 100) and then divided by 100. FM for the salt-scaling fine aggregate was 3.38. FM for the ASR fine aggregate was 3.63.

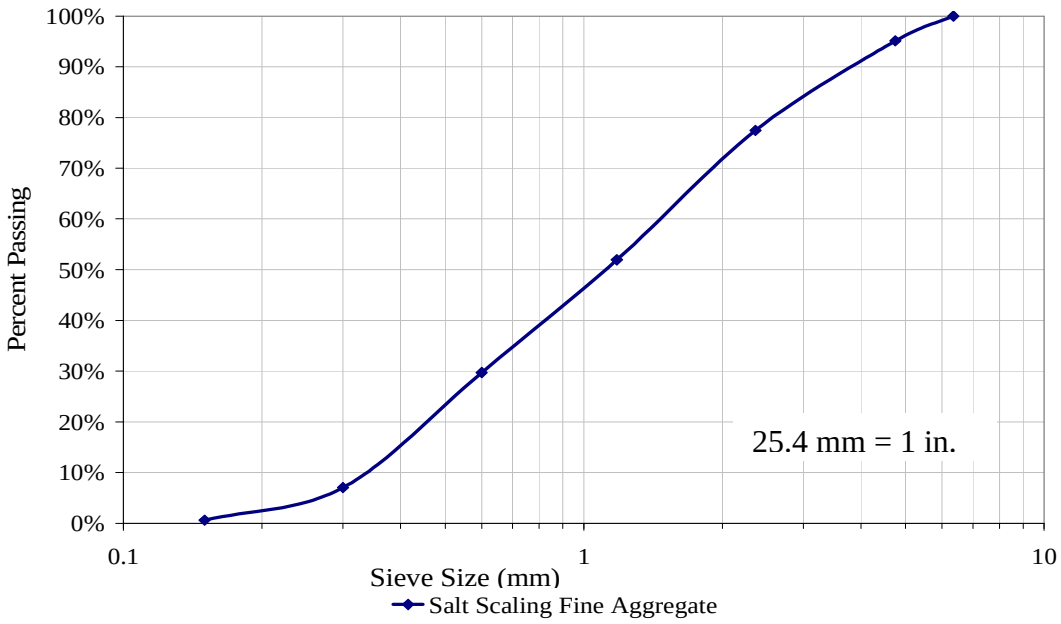

Figure 4-7 Salt-Scaling, Fine-Aggregate Gradation

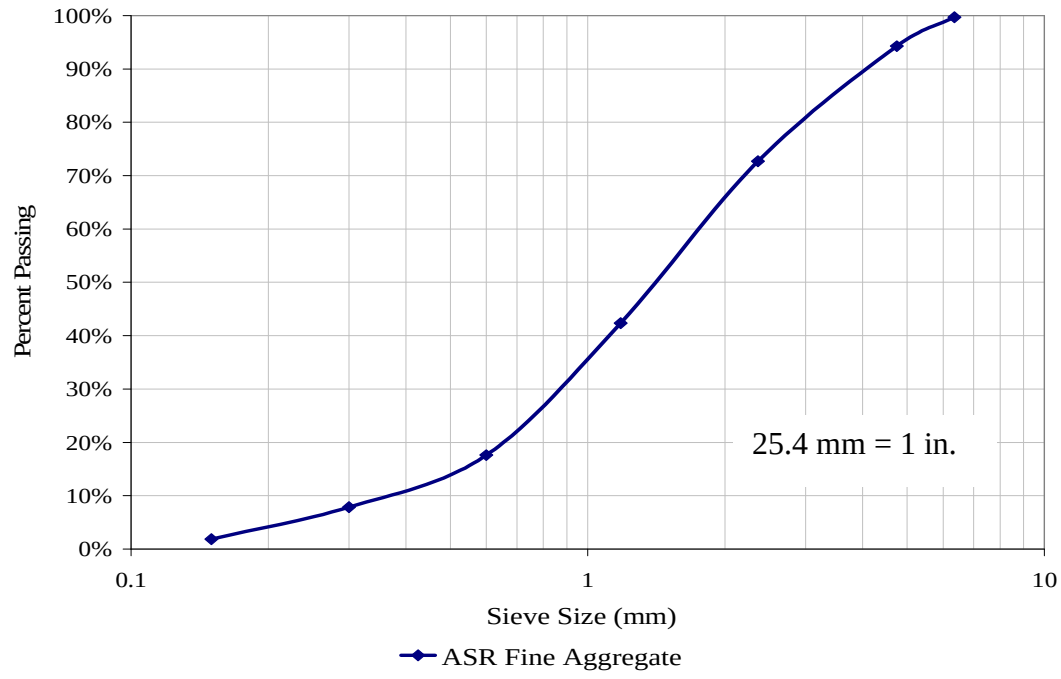

Figure 4-8 ASR Fine-Aggregate Gradation

4.3 Fly Ash

The fly ash used in this study was obtained from two different material suppliers. Nine different fly ashes were procured from across the United States: three Class F ashes and six Class C ashes. The fly ashes' chemical compositions were analyzed using x-ray fluorescence (XRF), with the results shown in Table 4-5. Samples of each fly ash were taken for future tests if needed.

Table 4-5 Fly Ash Properties

Fly Ash ID	**1**	**2**	**3**	**4**	**5**	**6**	**7**	**8**	**9**
Class	F	F	F	C	C	C	C	C	C
Specific Gravity	2.35	2.19	2.52	2.84	2.75	2.64	2.78	2.6	2.54
SiO_2 (%)	55.57	58.56	36.8	31.07	34.27	53.47	3.88	37.63	37.55
Al_2O_3 (%)	23.98	25.74	20.45	20.39	17.69	25.54	17.83	19.41	18.87
Fe_2o_3 (%)	4.18	5.49	5.41	8.24	5.99	4.33	5.54	7.05	5.91
Si+Al+Fe (%)	83.73	89.79	62.66	59.7	57.95	83.34	27.25	64.09	62.33
CaO (%)	8.06	4.53	24.94	26.03	26.87	9.29	27.98	23.32	23.74
MgO (%)	2.06	1.27	4.53	5.8	6.73	1.9	7.65	4.89	4.81
SO_3 (%)	0.5	0.39	1.35	1.54	2.12	0.63	2.86	1.47	2.37
Na_2O (%)	0.66	0.64	1.58	1.95	2.06	0.39	2.15	1.59	1.59
K_2O (%)	1.11	1.02	0.48	0.35	0.41	1.11	0.34	0.55	0.46

4.4 Cement

The cement was a Type I from The Monarch Cement Company. The cement oxide composition was measured by XRF with results shown in Table 4-6. Bogue calculations (ASTM C 150 2007) were used with the XRF results to compare theoretical values of C3S, C2S, C3A, and C4AF to the values found using the Rietveld method (Rietveld 1969).

Table 4-6 Cement Properties

SiO_2 (%)	21.34
Al_2O_3 (%)	4.74
Fe_2O_3 (%)	3.29
Si+Al+Fe (%)	29.37
CaO (%)	62.94
MgO (%)	1.69
SO_3 (%)	2.68
Na_2O (%)	0.14
K_2O (%)	0.53
C3S (%) (B)	49.85
C2S (%) (B)	23.57
C4AF (%) (B)	10.01
C3A (%) (B)	6.994
C3S (%) (R)	66.96
C2S (%) (R)	16.49
C4AF (%) (R)	9.29
C3A (%) (R)	2.92
Lime (%) (R)	0.12
Gypsum (%) (R)	2.31
Bassanite (%) (R)	1.68
Arcanite (K2SO4) (%) (R)	0.23
(B) - Bogue Calculation (R)- Rietveld Analysis	

4.5 Admixtures

The two admixtures used were a mid-range water reducer and an air entrainer. The mid-range water reducer was the Daracem 55 produced by W.R. Grace. The air entrainer was the Daravair 1000 produced by W.R. Grace.

CHAPTER 5 - Concrete Material Proportioning and Batching Procedure

This chapter discusses the procedure used for fresh and hardened concrete testing and final concrete mixture proportioning. In addition, the process for full batching for each type of specimen cast is given.

5.1 Absolute-Volume Method

For the mix designs, the absolute-volume method was used. Aggregate specific gravity and relative density were used to calculate the weight of each material required to produce 0.76 m^3 (1 yd^3) of concrete. ASTM C 672 (2003) standard calls for a target volume of 6% air, which was used in the design of all concrete mixtures. The volume of chemical admixtures was not included in the mixture design due to the small amounts required.

5.2 Trial Mixes

Trial mixtures for each batch were made to find the amount of air entrainer and mid-range water reducer needed to meet the required air content of 6±1% and slump of 75±15 mm (3±0.5 in). The trial mixes were mixed in a small Lancaster Counter Current Batch Mixer seen in Figure 5-1.

Figure 5-1 Lancaster Counter Current Batch Mixer

The procedure followed for laboratory batching is as follows:

1. Oven dry the sand. (Moisture variability was a concern because of the aggregate storage conditions available. The sand was oven dried before batching to reduce variability from moisture content.)
2. Batch the sand and rock the day before mixing, and store it in sealed buckets in the temperature-controlled mixing room until mixing.
3. Measure moisture conditions of the rock.
4. Adjust the weights for moisture condition.
5. Weigh out the correct amount of materials for batching (rock, sand, cement, fly ash, water, admixtures).
6. Wet the mixer pan and wipe with a towel to remove excess water.
7. Add the sand and rock into the pan and mix for one minute.
8. Add 1/4 to 1/3 of water into the pan.
9. Mix for 30 seconds.
10. Add the total amount of cement.
11. Add the total amount of fly ash.
12. Mix for 30 seconds.

13. Add the chemical admixtures.
14. Add the remaining water to pan.
15. Mix for 3 minutes.
16. Turn off the mixer for 2 minutes.
17. Mix for 2 minutes.
18. Check the concrete against slump and air requirements.

5.3 Finalized-Mix Design

After test batch results were complied, final mix designs were determined. Final mixture proportions are shown in Table 5-1.

Table 5-1 Theoretical Mixture Design

	kg/m^3					mL/m^3	
Mix	Cement	Fly Ash	Water	Rock	Sand	Air Entrainer	Mid-Range Water
Control	335.12	0.00	134.05	1099.23	736.27	43.60	1962.06
F1M	201.07	134.05	134.05	1075.46	721.93	218.01	926.53
F1V	189.65	126.43	126.43	1099.23	736.27	257.03	1028.13
F2M	201.07	134.05	134.05	1069.52	717.11	327.01	872.03
F2V	186.60	124.40	124.40	1099.23	736.27	303.48	859.86
F3M	201.07	134.05	134.05	1084.37	723.26	272.51	654.02
F3V	192.55	128.37	128.37	1099.23	736.27	313.16	782.91
F4M	201.07	134.05	134.05	1093.29	730.05	283.41	763.02
F4V	197.27	131.51	131.51	1099.23	736.27	278.05	855.53
F5M	201.07	134.05	134.05	1090.31	728.97	283.41	763.02
F5V	196.03	130.69	130.69	1099.23	730.33	286.94	797.04
F6M	201.07	134.05	134.05	1087.34	726.62	272.51	654.02
F6V	194.43	129.62	129.62	1099.23	736.27	316.21	737.83
1 kg/m^3 = 1.69 lb/yd ^{3} 1 mL/m^3 = 0.026 oz/yd^3							

5.4 Hardened-Concrete Testing

Hardened-concrete testing was conducted to find the strength of the concrete. After batching, three 100 x 200 mm (4 x 8 in.) cylinders of each mix were made to check compressive strength at 28 days according to ASTM C 39 (2005). Average maximum stress of the three cylinders was taken as the compressive strength for the batch

For the ASR blocks, three 150 x 300 mm (6 x 12 in.) cylinders were also made to measure the splitting-tensile strength according to ASTM C 496 (2004). Average maximum stress of three cylinders was used to calculate the splitting-tensile strength.

CHAPTER 6 - ASTM 672 Laboratory Testing

This chapter discusses specimen preparation, formwork, batching, casting, curing, and testing procedures used to perform the ASTM 672 salt-scaling testing.

6.1 Specimen Labeling

Six different fly ashes (F1-F6) were used in the laboratory testing. Two batches were cast for each fly ash. The first batch had a 40% substitution rate of fly ash for cement by mass. The designation used for these mixtures was the fly ash number followed by M, such as F1M. The second batch was a substitution by 40% mass of cement, but the total volume of paste was held constant to the volume of paste in the control. Therefore, the total mass of cement, fly ash, and water were lowered in order to keep the volume of paste constant. These mixtures were designated by the fly ash number followed by a V, such as F1V. For the test, nine specimens for each batch were made. Three were cured according to the standard procedure of covering with plastic for 24 hours. These were designated as "Air". Caution was taken to ensure that the plastic did not touch the specimens' surfaces. Six specimens were coated with a curing compound, which was designated with "CC." Three were used in laboratory testing and three were placed at the exposure site, as explained in Chapter 7.

6.2 Form Preparation

Standard five-gallon plastic buckets were cut into plastic rings, which were used both for the concrete specimen side forms and later for the dike walls. Minimum diameter to meet the 0.045 m^2 surface area was 23.93 cm (9.42 in.). The buckets tapered slightly, with a minimum diameter of 25.4 cm (10 in.) in the bucket bottom. Each bucket was cut into 88.9-mm (3.5 in.) sections using a wooden jig. Bottoms of the buckets were cut out and sanded smooth. Each form was cut on the side and duct taped back together to allow for easy removal after casting.

The day before batching, the forms were secured with silicone to a plastic-covered table shown in Figure 6-1. The silicone was used to stop leaking of water out

from the concrete during curing. The table accommodated 36 forms, which allowed for the casting of four batches on the same day. Before placement of concrete, Crete-Lease 880 – VOC Release Agent was applied to the forms.

Figure 6-1 Forms Secured to Table

6.3 Full-Batching Procedure for Laboratory Salt-Scaling Tests

The control mixture was batched by itself and was used to adjust the batching procedure, shown in Figure 6-2. On the second batch day, the F1M specimens were cast. On the third day F2M, F3M, F4M, and F5M were cast; followed by F6M, F1V, F2V, and F3V on the fourth day; and on the fifth batch day F4V, F5V, and F6V were cast.

The slump (ASTM C 143 2008) and fresh air content (ASTM C 231 2008) were measured for each concrete batch. Three 100 x 200 mm (4 x 8 in.) cylinders were made from each batch for compressive strength testing to be conducted at 28 days.

Figure 6-2 Adding Material to Lancaster Mixer

The concrete was then placed in the forms on the table in one lift. Each specimen was rodded 36 times with a 15.875-mm (5/8 in.)-diameter steel rod. The rod was used to strike off the top of the specimen leaving a smooth surface. The concrete was then allowed to bleed. After bleeding, the water absorbed back into the concrete. The concrete by that point was firm to the touch and was finished by "three sawing-motion passes of a wood strike-off board" (ASTM 672 2003). Then a 609.6-mm (24 in.) medium stiff brush, shown in Figure 6-3, was dragged across the concrete as specified, leaving a brushed surface as shown in Figure 6-4. One hundred seventeen salt-scaling specimens were cast in total.

Figure 6-3 Medium-Stiff Brush

Figure 6-4 Brushed-Concrete Surface

6.4 Curing

6.4.1 Plastic-Covered Curing

Immediately after the concrete was brushed, designated concrete specimens were covered with a polyethylene sheet as shown in Figure 6-5. The plastic sheet was not allowed to touch the surface of the concrete. Three concrete specimens for each mixture were cured for the first 24 hours using the polyethylene sheet, giving 39 specimens cured under plastic.

Figure 6-5 Plastic Covered Specimens

6.4.2 Curing Compound

A W.R. Meadows Sealtight 1610, a water-based concrete curing compound was applied to six concrete specimens for each batch. A hand sprayer was used to apply one coat of curing compound on each specimen. Great care was taken to try and ensure uniform coverage. Where there was overlap by the nozzle, however, the concrete received an extra amount of curing compound resulting in some streaking that can be seen in Figure 6-6. Curing compound was applied to 78 specimens in total.

Figure 6-6 Curing Compound Applied to Concrete Specimens

6.4.3 Moist Room

The forms were removed twenty-four hours after placing. Forms and specimens were labeled with fly ash type, type of curing, and specimen number for the mixture. Specimens were then placed in a moist room conforming, to ASTM C 511 (2006), until the age of 14 days.

6.4.4 Environmental Chamber

At the age of 14 days, the concrete specimens were transferred to the environmental chamber, which had a temperature of 23±2 ^{o}C (73.5±3.5 ^{o}F) and relative humidity between 45% and 55%. The specimens were kept in the chamber until the age of 28 days.

6.5 Freeze-Thaw Cycles

Specimen-top diameters were measured at three different locations. Three days before the specimens were to begin testing, the forms were taped back together and placed on the corresponding specimens. The forms were raised to form a dike above the finished surface of the concrete specimen and secured with silicone to form a watertight seal. Each specimen was subjected to 50 freeze-thaw cycles.

6.5.1 Calcium Chloride Solution

Excel 50 Calcium Chloride 94-97% Pellets from Scotwood Industries, Inc., were used for this test. Distilled water was mixed with the salt at a rate of 4 grams (0.14 oz.) of calcium chloride per 100 ml (3.38 fl. oz.) of water. At the age of 28 days, the solution was added to the top of the specimens to a depth of 6 mm (0.25 in).

6.5.2 Freezers

Two 0.42-m^3 (15 ft^3) and one 0.71-m^3 (25 ft^3) chest freezers were used as freezing chambers for this test. Ranco Electric Temperature Controllers, shown in Figure 6-7, were used to retrofit the freezers for digital temperature control. The controllers were set to -18 C (-0.4 ^{o}F) with a range of ± 1 ^{o}C (1.8 ^{o}F). This range was within the standard of -18±3 ^{o}C (-0.4±5.4 ^{o}F). The top of each freezer was insulated with Styrofoam to

conserve energy in the cooling of the freezers. Racks were built for each freezer to provide shelving to hold the specimens. Shelving allowed for approximately 50 mm (2 in.) of clearance for each level. Thermocouples were used to confirm a uniform temperature throughout the freezer. Two smaller freezers held 14 specimens each, while the larger freezer held 50 specimens. Frozen specimens can be seen in Figure 6-8.

The salt solutions were topped off to 6 mm (0.25 in.) above the concrete surface and then placed into the freezers. Specimen placement in the freezers was random to eliminate the variation of freezing time. Specimens were in the freezers for 16 to 18 hours, and were left in the freezer if an interruption in the testing occurred as specified by ASTM C 672 (2003).

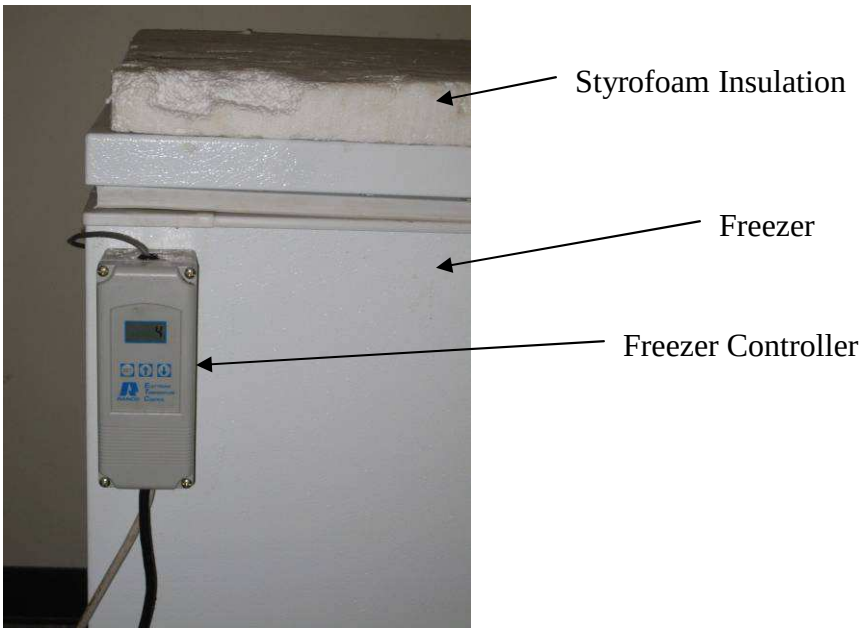

Figure 6-7 Freezer Control

Figure 6-8 Specimens in Freezers

6.5.3 Environmental Chamber

After 16 to 18 hours in the freezer, specimens were removed from the freezers and carted into the environmental chamber. They were placed on shelves for 6 to 8 hours. A dehumidifier was placed in the environmental chamber to reduce the humidity of the room to 50±5%. The cold specimens would sweat as they warmed up, causing humidity in the room to increase. The environmental chamber temperature was held at 23±2 ^{o}C. The environmental chamber temperature and relative humidity were monitored using a temperature and relative humidity probe. Specimens were checked for leaks in the dikes. If a leak was found, the specimen was dried off and the mass of the specimen was recorded. Silicone was added and/or removed to stop the leak. The mass was taken again and the difference recorded. After 6 to 8 hours in the environmental chamber, specimens were topped back off to a 6-mm depth of solution and put back into the freezers. Specimens sitting in the environmental chamber can be seen in Figure 6-9.

Figure 6-9 Specimens in Environmental Chamber

6.5.4 Measuring

After each five freeze-thaw cycles, the solution was drained and the specimens were rinsed off with tap water to remove any loose material. Cattle ear tags were made for each specimen as shown in Figure 6-10. The tag would indicate the fly ash (F1-F6) and type of substitution rate (M-mass or V-Volume), date cast, specimen number, and curing procedure (Air-plastic covered or CC-curing compound). Yellow tags were made for the specimens cured with plastic and white tags were made for the curing compound specimens. Tags were placed on corresponding specimens and a picture was taken of each. Each specimen was rated according to the ASTM 672 standard table shown in Table 2-2. Specimens were weighed on a scale with a capacity of 29.94 kg (66 lb) and an accuracy of 0.907 g (0.002 lb). Weighing of specimens comes from the MTO standard. Weights were taken as a more objective measurement.

Figure 6-10 Tags on Specimens

CHAPTER 7 - Exposure Site

7.1 Motivation for an Exposure Site

While laboratory testing gives some idea as to the changes that occur in concrete, as stated in Chapters 2 and 3, it may not be representative of true field exposure. An exposure site allows concrete to undergo natural weathering such as high summer heat and cold winter nights. The geography of Manhattan, Kansas is such that it is exposed to large changes in weather throughout the year, with many freezing and thawing cycles. Manhattan, on average, reaches a summer high of 33 ^{o}C (91 ^{o}F) in July and a winter low of -6 ^{o}C (21 ^{o}F) in January. Average annual precipitation for Manhattan is moderate at 97.14 cm (38.25 in.) (MSN Weather 2009). Precipitation comes in all forms such as rain, sleet, freezing rain, and snow. The wide variation of weather in Manhattan, makes it well suited for locating a concrete exposure site.

7.2 Equipment and Processes

A portion of underutilized land at Civil Infrastructure System Laboratory (CISL) was selected for the Kansas Outdoor Concrete Exposure (KOCE) site. CISL sits on a lot approximately 95 x 53 m (312 x 175 ft). An area of 21 x 53 m (69 x 174 ft) was designated as the new exposure site. After the area was surveyed, it was found to be approximately 0.6 m (2 ft) lower than the level of the rest of the lot. The proposed site design is shown in Figure 7-1, and the building and outdoor load frame is shown in Figure 7-2.

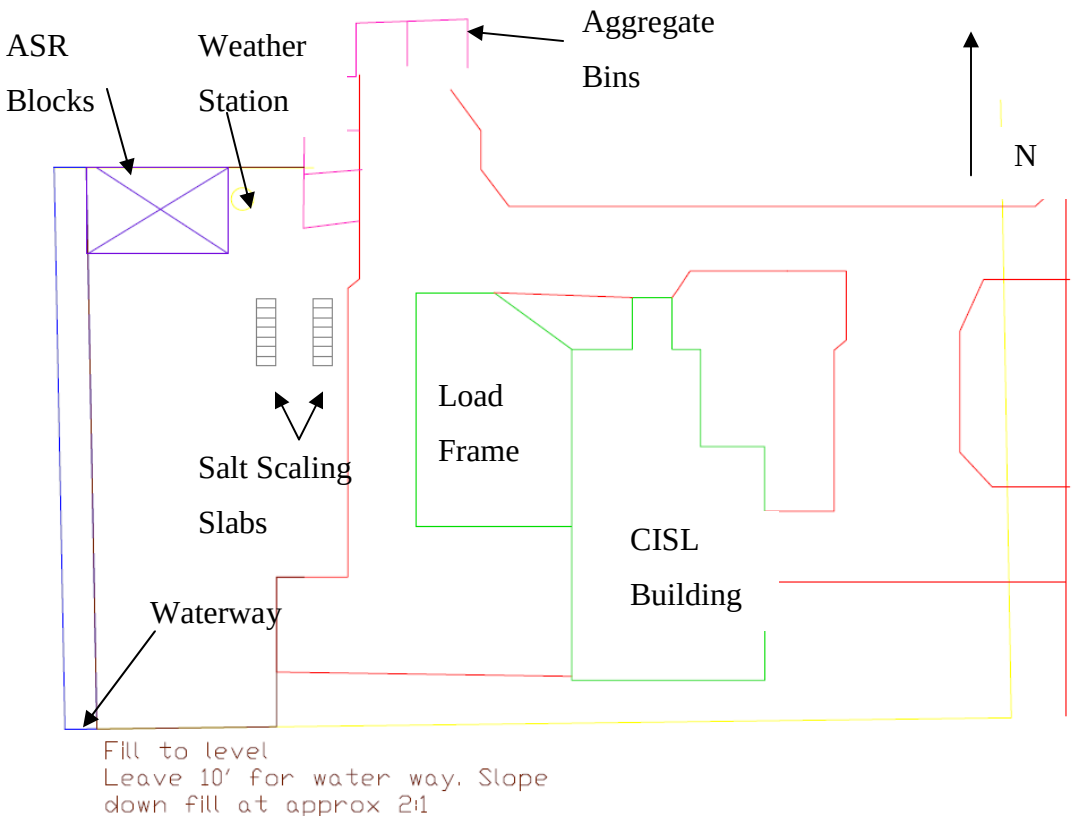

Figure 7-1 CISL Layout

Figure 7-2 CISL Building and Load Frame

7.2.1 Site Construction

The first step was to clear the KOCE site. To fill in the lower part of the site, shown in Figure 7-3, a local contractor was contacted, who agreed to supply excess fill from a local redevelopment near CISL. The contractor donated the fill and haul to CISL. The fill was stockpiled as shown in Figure 7-4. A skid steer was used to level the fill. A water level was built to assist leveling the ground. The water level, shown in Figure 7-5, could be operated by one person and was very accurate. There was not enough fill donated, however, to level the entire KOCE site. Fill leftover from CISL accelerated pavement testing research projects has been used to continue leveling of the area. To date, approximately three-fourths of the area has been leveled.

Figure 7-3 Picture of KOCE Site Before Construction, Showing Original Elevation

Figure 7-4 Local Contractor Delivering Fill

7.2.2 Slabs

As part of the salt-scaling testing, slabs were designed for outdoor exposure testing. The slabs were designed to be 1.8288 x 0.9144 x 0.1524 m (6 x 3 x 0.5 ft). Three sources of fly ash were secured for this test. Concrete mixtures for the salt-scaling slabs were as described later in section 7.2.2.2. Two sets of identical slabs were placed; one will receive salt treatment for years to come, while the second set will be left unsalted. A total of six fly ash slabs and one standard concrete mixture slab were placed per set.

7.2.2.1 Form Preparation

Two sets of slabs were placed at approximately 2.4 m (8 ft) apart to decrease the chance of salt being inadvertently applied to the second concrete slab set. The bottom of the base layer was set approximately 22.86 cm (8 in.) below the top soil-level elevation. Approximately 5.08 cm (2 in.) of AB3 was placed on the slab beds before setting the forms. The water level was used to check for uniform elevation.

Figure 7-5 Using Water Level to Check Elevation

For the forms, nominal size boards of 50.8 x 152.4 mm (2 x 6 in.) were used. These boards had an actual depth of 13.97 cm (5.5 in.). The tops of the boards were set to the elevations level with the top of the soil; crushed stone aggregate, AB3, was added and a plate vibrator, shown in Figure 7-6, was used to compact the base. Every other slab was formed up to size as shown in Figure 7-7. Before each slab was placed, wood forms were coated with Duogard Citrus Concrete Form Release Agent. After curing, the surrounding slabs acted as forms for two sides of the newer placements. Placement of each batch and date of placement can be seen in Figure 7-8.

Figure 7-6 Compacting AB3 Inside of Formwork

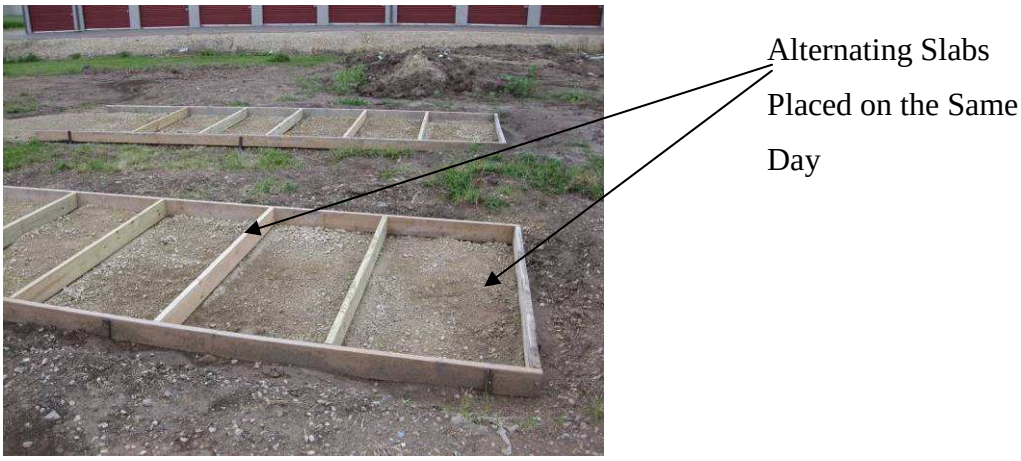

Figure 7-7 Individual Slabs Formed Up

Control 8/4/2009	F8M 8/5/2009	F7M 8/4/2009	F9M 8/5/2009	F7V 8/4/2009	F8V 8/5/2009	F9V 8/5/2009

N

Figure 7-8 Slab Diagram

7.2.2.2 Full-Batching Procedure for CISL Salt-Scaling Slabs

After test batching, final mixture designs were determined. The theoretical mixture design can be seen in Table 7-1.

Table 7-1 Theoretical Mixture Design for CISL Slabs

kg/m^3						mL/m^3	
Mix	**Cement**	**Fly Ash**	**Water**	**Rock**	**Sand**	**Air Entrainer**	**Mid-Range Water Reducer**
Outside Control	256.36	0.00	102.55	840.91	563.18	33.35	1500.97
F7M	153.82	102.55	102.55	834.09	558.64	58.37	583.71
F7V	150.28	100.19	100.18	840.91	563.18	65.17	570.28
F8M	153.82	102.55	102.55	831.82	554.09	50.03	542.02
F8V	148.27	98.85	98.85	840.91	563.18	64.30	562.65
F9M	153.82	102.55	102.55	829.55	554.09	41.69	583.71
F9V	147.55	98.36	98.36	840.91	563.18	63.99	559.91
1 kg/m^3 = 1.69 lb/yd ^{3} 1 mL/m^3 = 0.026 oz/yd^3							

Rock and sand were placed into barrels from the stockpiles the day before batching. The materials were weighed using a crane scale with a capacity of 907 kg (2,000lb) and an accuracy of 0.09 kg (0.2 lb). Three representative samples were taken of both the sand and rock. These were oven dried to obtain the moisture content of each material. The cement was weighed in a barrel in the same fashion. A pressurized air tank was filled with the water. After weighing out the water, an air compressor was connected to the tank and pressurized to 207 kPa (30 psi). The water tank is shown in Figure 7-9.

A portable 0.95-m^3 (1.25 yd^3) drum concrete mixer was used. Rock, sand, and cement were added to the hopper by lifting the barrels with a forklift and dumping them into the drum, as shown in Figure 7-10. Aggregates were added first, followed by the cementitious materials. The drum was pulled forward away from the hopper after being charged. The water valve was opened on the tank and pressurized water was discharged

into the drum while it was mixing. After 75% of the water had been added, the air entrainer and mid-range water reducer were added. The remaining water was used to rinse out the admixture containers and then added to the mixer.

Figure 7-9 Water Tank

Figure 7-10 Hopper and Mixer Setup for Mixing

Each concrete mixture was made in 0.71-m^3 (25 ft^3) batches. This allowed for 0.51 m^3 (18 ft^3) for the slabs, 0.06 m^3 (2 ft^3) for three laboratory-size specimens, 0.03

m^3 (1 ft^3) for testing slump and air content, 0.06 m^3 (2 ft^3) for compression cylinders, and 0.06 m^3 (2 ft^3) of extra concrete if needed. After adding the mixing water, the mixer was allowed to mix for 3 minutes, followed by 2 minutes of rest and finally 2 minutes of mixing. The concrete was tested for slump and fresh air content according to ASTM C 143 (2008) and ASTM C 231 (2008), respectively. Four 100 x 200-mm (4 x 8 in.) cylinders were made for each concrete batch.

A skid steer was used to transport the concrete from the mixer to the forms. A vibrator was used to consolidate the concrete in the forms. A screed board was used to level the concrete. The screed board was used for several passes to smooth the concrete surface. Three laboratory-size specimens were made out of the same batch. These specimens were made in the same fashion as the specimens made during the laboratory salt-scaling test. These small specimens will be used to investigate the effect of salt scaling due to the high amount of energy put into a small surface on the small specimens during finishing operations, compared to the larger slabs. The slab and small specimens after placement can be seen in Figure 7-11.

Figure 7-11 Slabs and Small Specimens

After bleeding had ceased in the slabs and small specimens, the concrete was brushed with the same broom used in the laboratory salt-scaling test. A sheet of plastic was placed over half of each slab. A single coat of curing compound was applied to half

of each slab not covered by the plastic, as can be seen in Figure 7-12. Curing compound was applied to the three small specimens as well. The plastic was removed after 24 hours. An iButton was placed in the center slab, F9M, 76.2 mm (3 in.) from the concrete surface. The temperature recorded by the iButton will be used to monitor the number of freezing and thawing cycles that the concrete actually experiences, not just the number of cycles estimated by the weather data.

Figure 7-12 Plastic-Covered Curing and Curing Compound Applied

Outside forms were removed 24 hours after the last slab was cast. The small specimens were set on the east side of the slabs designated for salt application at the same top elevation as the slabs. Pea gravel rock was placed around the small specimens in attempt to mange weeds in the future. Field-exposure specimens made during the laboratory salt-scaling testing were placed on the west side of the slab designated for salt application. A picture of the slabs and specimens can be seen in Figure 7-13.

Figure 7-13 Exposure Site Slabs and Specimens

The F7M slab concrete mix did not turn out as expected. It segregated during the mixing, giving a very poor and non-uniform slab. It is also expected to perform badly in salt scaling due to its poor quality concrete surface.

7.2.2.3 Application of Salt

The same calcium chloride salt used in the laboratory salt-scaling testing was and will continue to be applied for the next several years, by hand, at a rate of approximately 0.91 kg (2 lb) per application. The salt is being applied when the University's ground crews would normally apply deicer salt to sidewalks on campus; examples are snow and/or ice covering the slabs. Each application is recorded as shown in Table 7-2.

Table 7-2 Salt Application Table

#	Date	~ Amount	Performed by
1	11/16/2009	2 lb	Bortz
2	12/17/2009	3 lb	Testa
3	12/8/2009	3 lb	Testa
4	12/11/2009	2 lb	Bortz
5	12/14/2009	2 lb	Bortz
6	12/28/2009	2 lb	Bortz
7	12/30/2009	2 lb	Bortz
8	1/4/2010	2 lb	Testa
9	2/5/2010	2 lb	Bortz
10	2/8/2010	2 lb	Bortz

1 kg = 2.2 lb

7.2.3 ASR Blocks

As stated in Chapter 3, UT-Austin and CANMET have been monitoring concrete durability blocks for expansion caused by alkali-silica reactivity. Four concrete durability blocks were made at KSU to develop the procedure and infrastructure to begin to collect data for comparison with these two sites.

7.2.3.1 Durability Block Form Preparation

Pictures and measurement of forms used at UT-Austin and CANMET were obtained to ensure the concrete blocks were made to obtain comparable results. Plywood was cut to form a 0.4 x 0.4 x 0.7 m (15 x 15 x 28 in.) box. Two pieces of all-thread rod were placed on each end of the box to hold both form sides together during placement of concrete. The all-thread rods were loosened and removed during removal of the forms. Two complete forms were constructed. After completed construction of the forms, three coats of polyurethane were applied to each form to protect them during placement. Figure 7-14 shows the forms after construction.

UT-Austin and CANMET uses 508-mm (20 in.) and 152.4-mm (6 in.) DEMEC gauges to measure the changes in length. They place 9.5 x 76.2 mm (0.375 x 3 in.) stainless steel bolts with a center hole cast into the concrete to create the measuring points. In this study, a Whittemore gauge was used to measure the change in length of the blocks. This Whittemore gauge is only 203 mm (8 in.) in length. The blocks, however, are 0.7 m (28 in.) in length, so multiple points had to be imbedded in the blocks. Strips of metal were drilled with holes every 101.6 mm (4 in.). Stainless steel inserts, shown in Figure 7-15, were bolted using M3 x 0.05 x 12.7 mm (4-40 x 0.5 in.) flat-head cap screws to attach the strips of steel as shown in Figure 7-16. Duct tape was placed over the screw heads to keep concrete from covering them. Ends of the inserts were covered with silicone to ensure cleanliness of the threads during removal of screws. Strips of steel were bolted to the side of the forms as shown in Figure 7-17. Strips of woods were cut to hold the strips of steel at the top.

Figure 7-14 ASR Block Form

Figure 7-15 Stainless Steel Insert

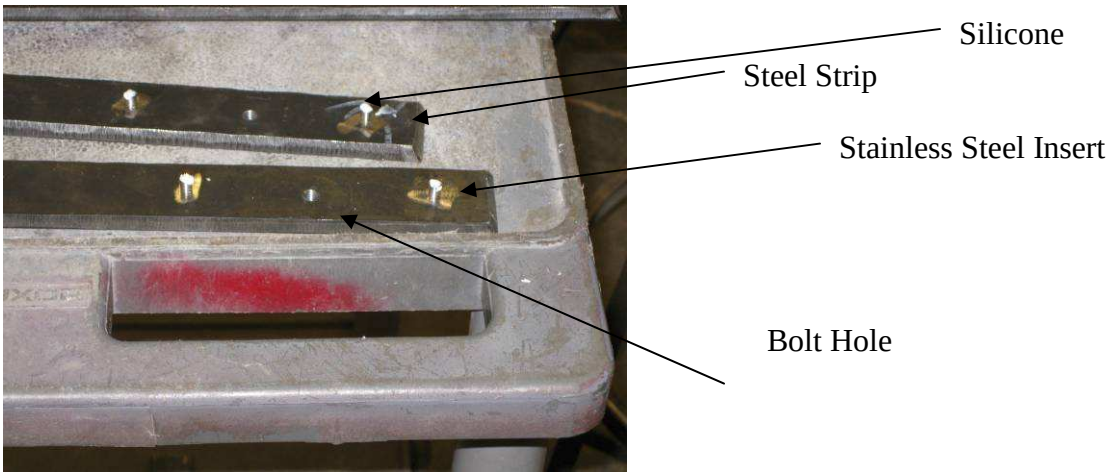

Figure 7-16 Inserts Bolted to Steel Strips

Figure 7-17 Steel Strips Bolted to the Forms

7.2.3.2 Full-Batching Procedure for CISL ASR Blocks

Four mixes were optimized during test batching using the same procedure as described in Chapter 5: 1.) a control mixture using the siliceous river pea gravel, 2.) a mix of 30% replacement of pea gravel with the limestone aggregate used in the salt scaling study, 3.) a mix of 25% cement replacement by mass of 5% Class F fly ash and 20% Class C fly ash, and 4.) a mix of 25% cement replacement by mass of 10% Class F fly ash and 15% Class C fly ash. The Class F fly ash used was fly ash 3, while the Class C was fly ash 8. The complete mixture design has been tabulated in Table 7-3.

Table 7-3 ASR Block Theoretical Mixture Design

	Mix	ASR Control	30% Limestone	5F-20C	10F-15C
kg/m^3	Cement	299.09	299.09	224.23	224.32
	Class F Fly Ash	0.00	0.00	14.95	29.91
	Class C Fly Ash	0.00	0.00	59.82	44.86
	Water	119.64	119.64	104.68	104.68
	Pea Gravel	772.73	540.91	795.45	794.09
	Limestone	0.00	231.82	0.00	0.00
	Sand	497.27	501.36	500.00	500.00
mL/m^3	Air Entrainer	127.32	127.32	292.84	331.04
1 kg/m^3 = 1.69 lb/yd ^{3} 1 mL/m^3 = 0.026 oz/yd^3					

Before placement of concrete in the forms, the wood was sprayed with Duogard Citrus Concrete Form Release Agent. Form release was applied to the steel strips using a rag saturated in product. Care was taken to avoid applying form release agent to the inserts used for measurement. Steel strips were then bolted to the form. Silicone was placed around the edges of the steel strips to make it easier to remove them after curing.

A Gilson Brothers Company 0.25-m^3 (9 ft^3) concrete mixer was used to mix the concrete for the ASR Blocks. The procedure for mixing was the same as stated in section 5.2.

After mixing, slump and air content were measured. The concrete was placed in the forms in two lifts. After each lift, a vibrator was used to consolidate the concrete. The top of the block was screeded off with a board. Wood strips holding the steel strips on the top surface were attached to the form 203 mm (8 in.) apart, as seen in Figure 7-18. A wood float was then used to finish the top surface. Four 100 x 200-mm (4 x 8 in.) cylinders and three 150 x 300-mm (6 x 12 in.) cylinders were made from each batch. A

thermocouple was placed in the 5F-20C block to monitor the temperature of the interior of the block as the block undergoes ASR expansion.

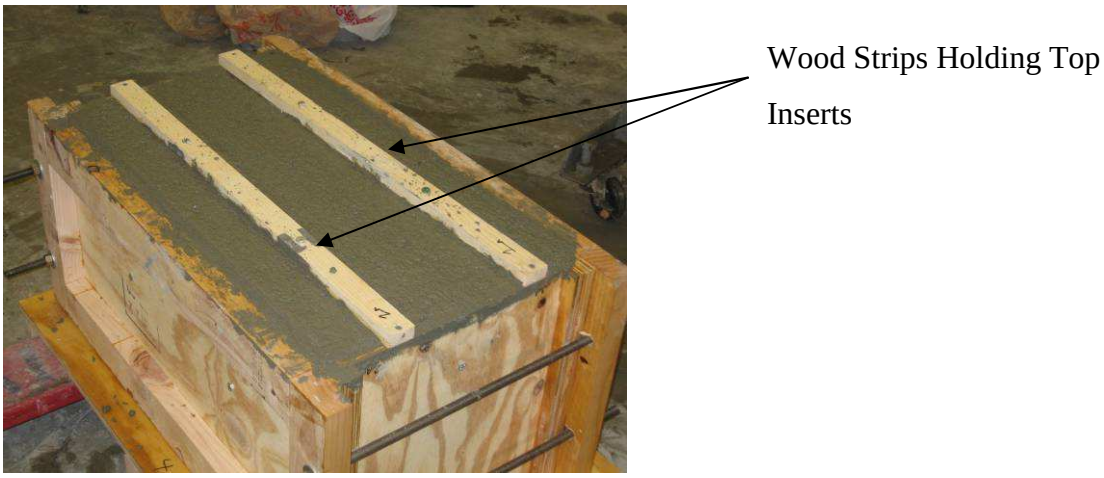

Figure 7-18 Concrete-Filled ASR Block Form

The blocks were allowed to bleed and after bleeding was complete, the blocks were covered with wet burlap. The burlap was soaked daily for seven days. The blocks were then removed from the forms. The steel strips were first unbolted from the wood forms. The all threads were loosened and the wood forms were removed. The duct tape was removed from the top of the steel strips revealing the heads of the screws holding the steel to the inserts. The screws were removed and the steel strips were gently removed from the concrete. The inserts were embedded in the concrete as shown in Figure 7-19.

Figure 7-19 Inserts Embedded in the Concrete

7.2.3.3 Procedure for Reading Whittemore Points

After the forms were removed, the distance between the points was measured using the Whitmore gauge shown in Figure 7-20. Initial readings were taken at room temperature of 22.2 ^{o}C (72 ^{o}F). All subsequent readings have to be taken at a temperature as close as possible to that to reduce temperature-induced strains. To reduce the effect of direct sunlight on the expansion of the concrete durability block, readings should also be taken on cloudy days or in low-light conditions (Figurski 2001). A wood block was used to ensure proper angle of the gauge. The holes were numbered left to right and the measurements were taken in the same direction each time. Errors can be introduced if the readings are taken with the gauge flipped in the opposite direction. The layout of points can be seen in Figure 7-21.

Figure 7-20 Whittemore Gauge

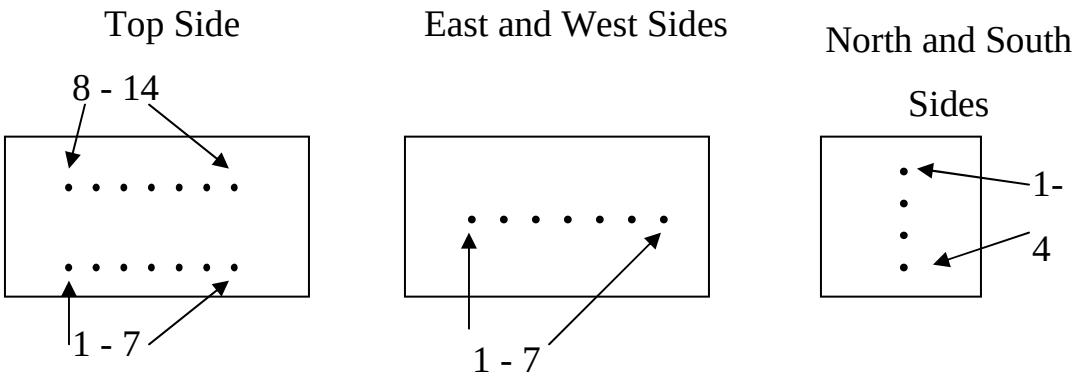

Figure 7-21 ASR Block-Point Layout

Each block was easily identified by yellow cattle tags epoxied to the block, as shown in Figure 7-22. Side A is the west wide; Side B is the east side; Side C and Side D are the north and south sides, respectively. The tags are fixed so they will not rotate.

Figure 7-22 Tag on Block

7.2.4 Weather Station

A Campbell Scientific weather station was installed at the exposure site to monitor the KOCE microclimate. All instruments are attached to a Campbell Scientific CR 800 datalogger, as shown in Figure 7-23. The data logger records hourly average temperature, wind speed and direction, solar energy, relative humidity, and amount of perception. The temperature of the 5F-20C block measured by the thermocouple is also recorded by the datalogger. A laptop is employed periodically to retrieve weather data recorded hourly on the data logger.

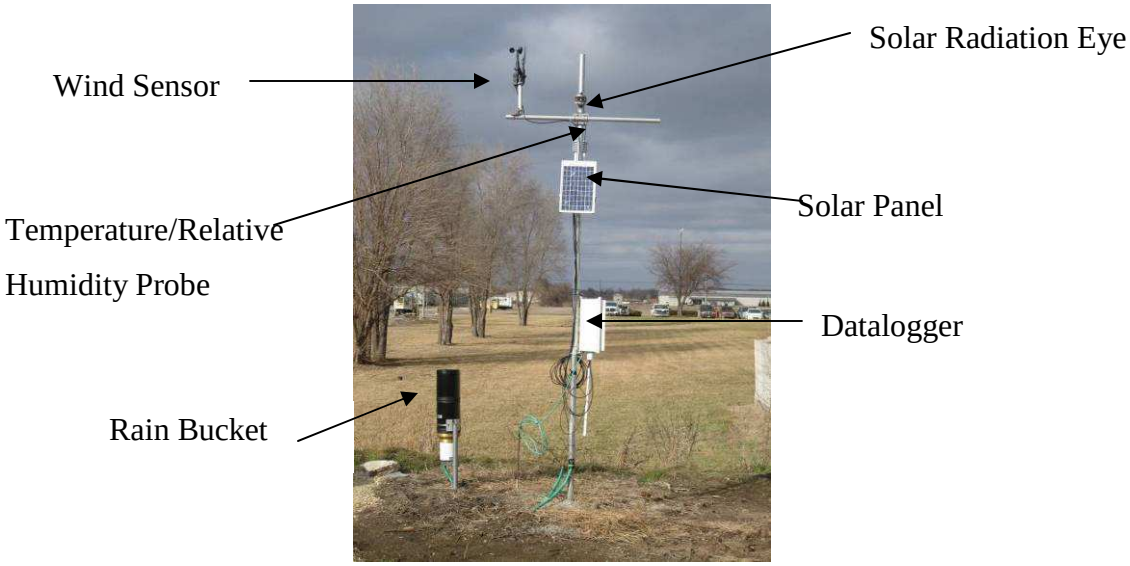

Figure 7-23 Weather Station

CHAPTER 8 - Results

This chapter reports results from fresh and hardened concrete properties testing, salt-scaling experiments, and early results from the ASR block expansion. Slump, air content, and compressive strength are given for each mix. For the salt-scaling laboratory test, weight loss and ratings of the specimens are reported. For the ASR block testing, splitting-tensile strength and Whittemore point-expansion readings are also reported.

8.1 Salt Scaling

The following section reports results from the salt-scaling experiments. The designation of "Air" stands for cured under plastic with an air gap between the plastic and the concrete surface, while "CC" stands for applied curing compound as discussed in section 6.1.

8.1.1 Fresh-Concrete Properties

Before placement of each mix, slump was measured as specified in ASTM C 143. The targeted range was 75±15 mm (3±0.5 in.). The test batches were crucial in ensuring that the full batches met the slump requirement. Table 8-1 shows the slump and fresh air content for all of the salt-scaling batches. Air content was measured at the same time as the slump. The air was measured following the process discussed in ASTM C 231. The required air was 5%-7%.

Table 8-1 Salt-Scaling Fresh Concrete Results

		Slump (mm)	Air (%)
Laboratory Batches	Control	64	6.75
	F1M	86	5
	F1V	64	5.75
	F2M	86	7
	F2V	70	5.75
	F3M	89	5.5
	F3V	64	5.75
	F4M	76	6.5
	F4V	86	5.25
	F5M	83	6.75
	F5V	70	6
	F6M	70	5.25
	F6V	83	6.25
CISL Slabs	Outside Control	64	5
	F7M	70	5.25
	F7V	83	5.75
	F8M	64	5.5
	F8V	64	5.75
	F9M	70	6.5
	F9V	86	6.75
25.4 mm = 1 in.			

8.1.2 Hardened-Concrete Properties

Compressive strength was determined at 28 days following the test, as specified in section 5.4.1, and was reported as the average strength of three cylinders. The mixtures were designed on a percent replacement of cement by fly ash, so no design consideration for strength was taken into account. Both F3 mixtures had low compressive strength, as seen in Figure 8-1, and the F7M mixture had a low compressive strength, as seen in Figure 8-2. This was expected, however, due to the poor quality of concrete produced as stated in section 7.2.2.2.

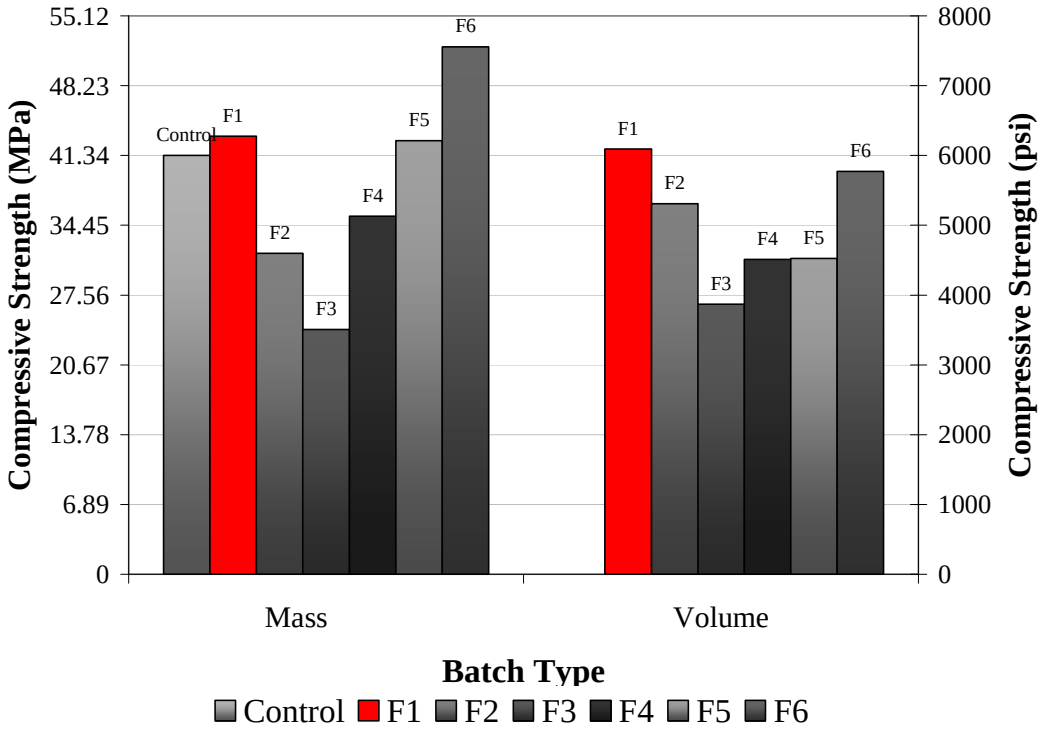

Figure 8-1 28-Day Compressive Strength Laboratory Mixtures

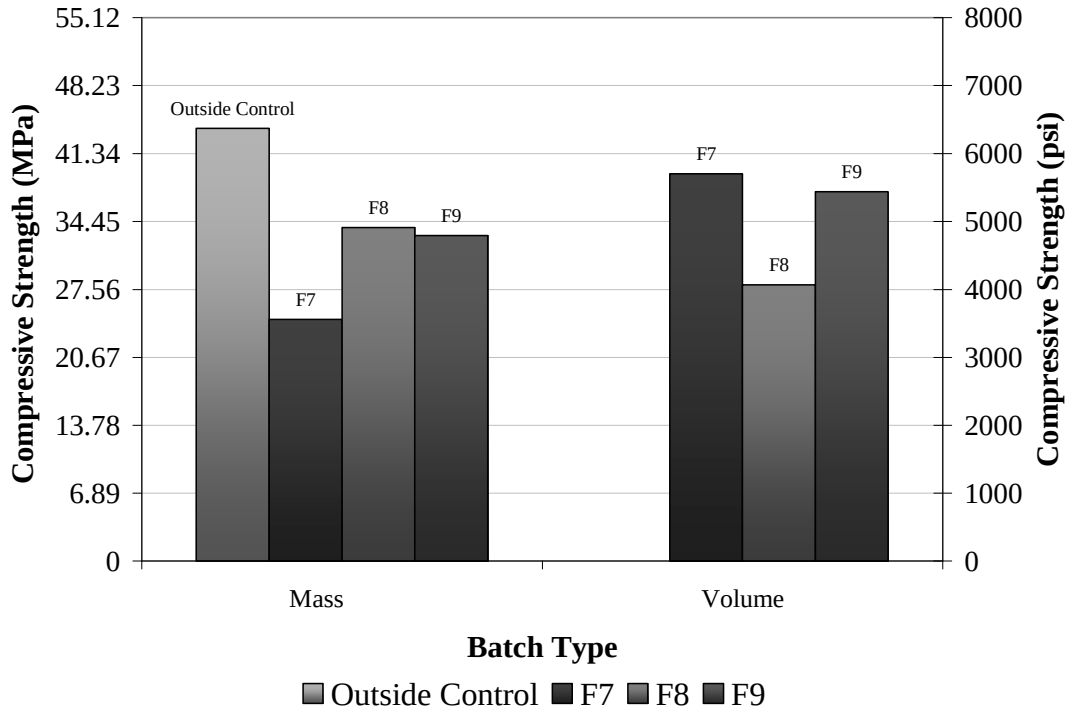

Figure 8-2 28-Day Compressive Strength of CISL Slabs

8.1.3 Weight Loss of Specimens and Ratings

Laboratory specimens were weighed and rated every five cycles as discussed in section 5.4.2. Results of the individual mixtures can be seen in Appendix A. Rating comparisons between type of fly ash substitution and curing methods can be seen in Figures 8-3 through 8-6.

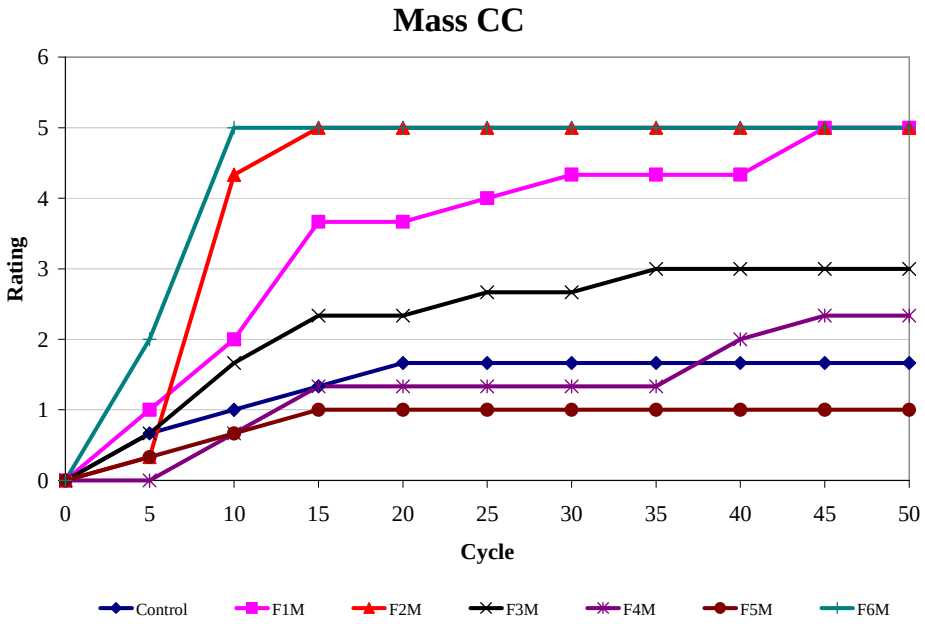

Figure 8-3 Mass Substitution with Curing Compound

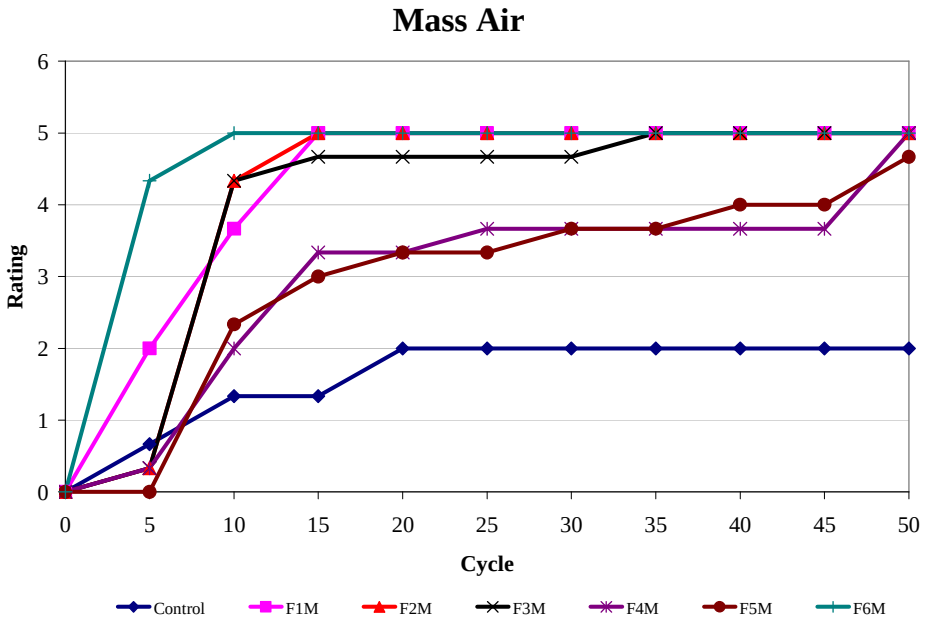

Figure 8-4 Mass Substitution with Air Curing

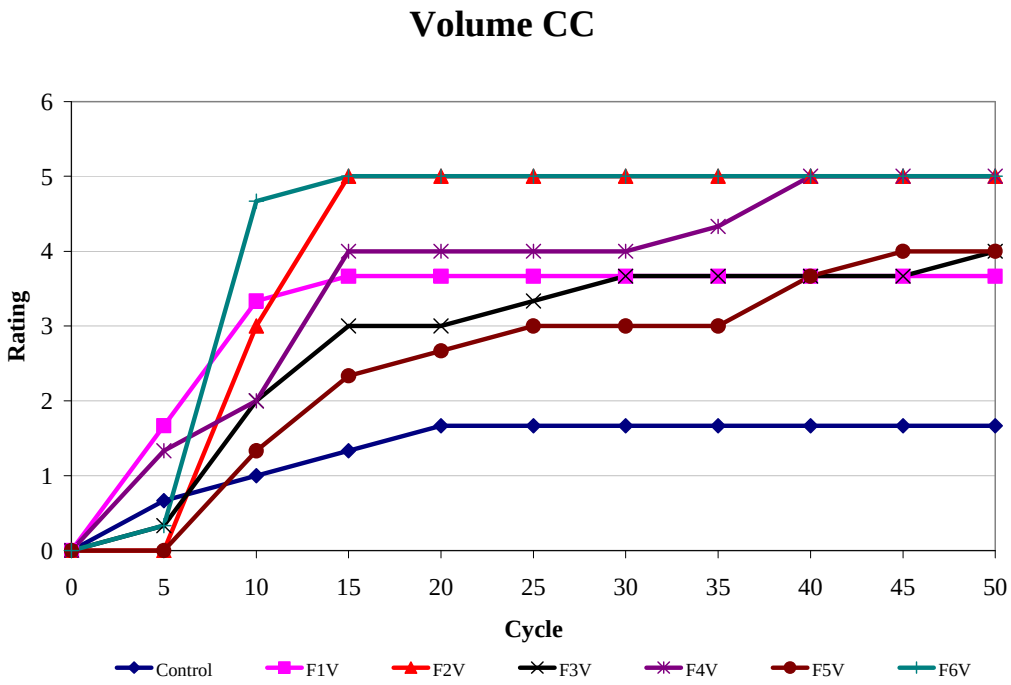

Figure 8-5 Volume Substitution with Curing Compound

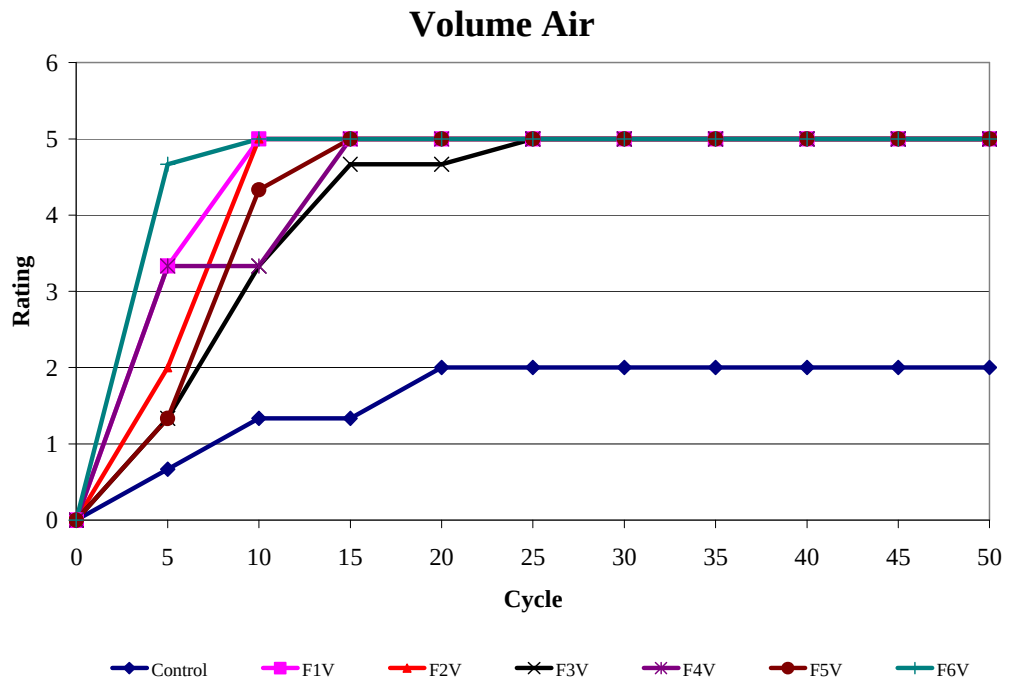

Figure 8-6 Volume Substitution with Air Curing

During the first freeze cycle for the F1V specimens, an electrical wire fell into the ponded salt water of the F1V CC #1 specimen. The wire left a turquoise-colored mark on the surface of the specimen. The CC #1 specimen outperformed the rest of its companion specimens as shown in Figures 8-7 and 8-8. These specimens have been saved to undergo more testing. The extent of shocking or any exact mechanisms involved is unknown. Future work should examine the potential of alternative curing methods with fly ash.

Cycle 0

Cycle 25

Cycle 50

Figure 8-7 F1V CC #1 Shocked Specimen

Cycle 0

Cycle 25

Cycle 50

Figure 8-8 F1V CC #2 Companion Specimen

As of early February 2010, salt has been applied to the concrete at the KOCE site on 10 separate occasions. No visual scaling has occurred on the slabs or small specimens.

8.2 Early Results ASR Blocks

This section reports the hardened concrete test and early Whittemore reading results. The blocks were left in the forms for seven days before deforming and taking initial length readings.

8.2.1 Fresh Concrete Properties

Like the salt-scaling test, the slump and air content of the batch were measured at the time of placement. The targeted slump was 75±15 mm (3±0.5 in.). The slump was taken following the procedure discussed in ASTM C 143. Slump and air content results are shown in

Table 8-2. All batches were within slump range. The air content for the ASR Blocks was determined following the process discussed in ASTM C 231 (2008). The target value was 5% to 7%. All batches were within range for air content.

Table 8-2 ASR Block Fresh Concrete Results

Block Number	Tag ID	Slump (mm)	Air Content (%)
1	CTL 1	88.9	5.75
2	30 Lime	76.2	5.25
3	5 F 20C	85.725	5.5
4	10 F 15 C	76.2	5.75
25.4 mm = 1 in.			

8.2.2 Compressive Strength

Compressive strength of the ASR block mixes was determined at 28 days following the test as specified in section 5.4.1. Results are shown in Figure 8-9.

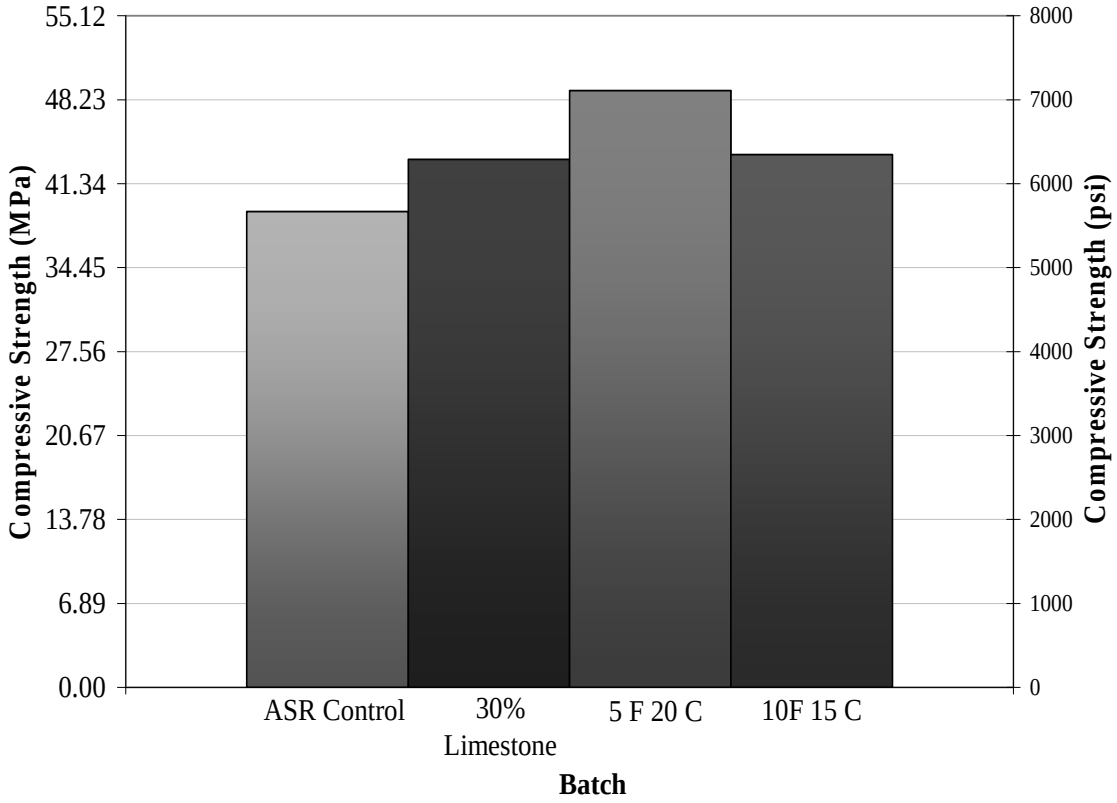

Figure 8-9 28-Day Compressive Strength of ASR Blocks

8.2.3 Split Tensile

Splitting-tensile strength was measured at 28 days following the procedure described in section 5.4.2. The test was completed for later research to compare the expansion to the tensile strength. Results are shown in Figure 8-10.

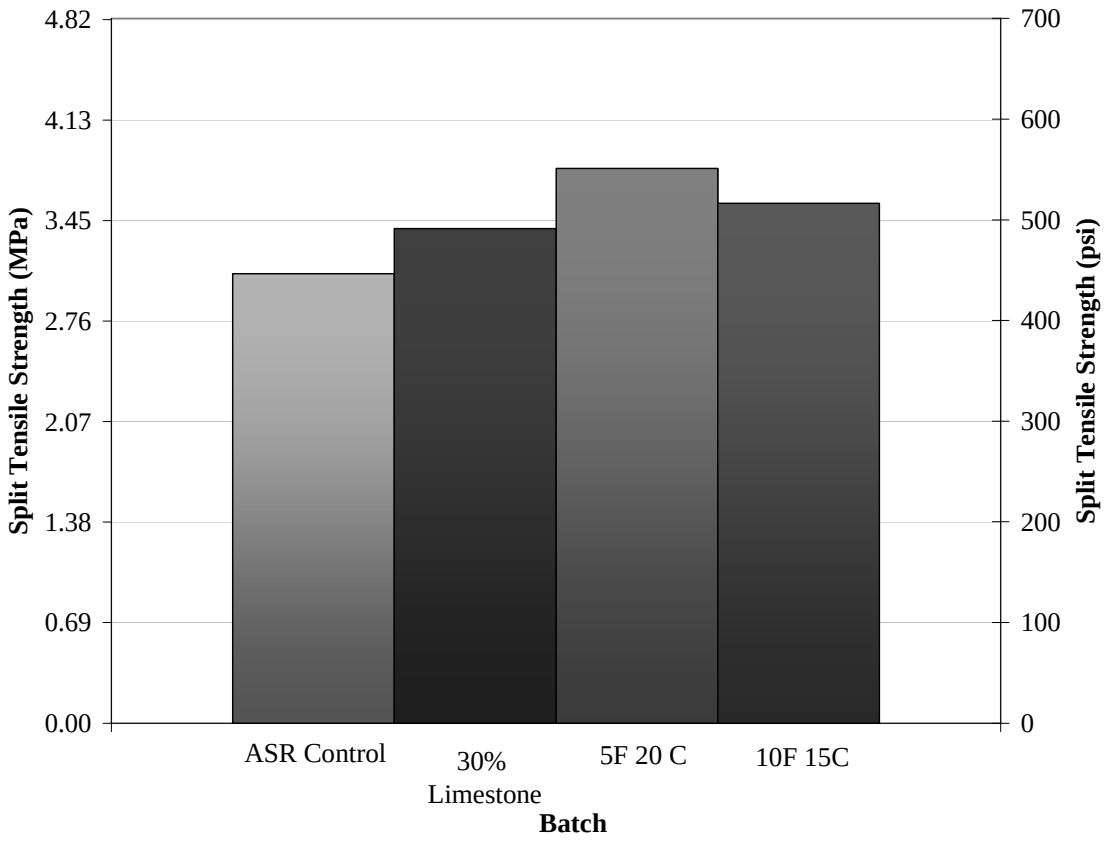

Figure 8-10 28-Day, Split-Tensile Strength ASR Blocks

8.2.4 Whittemore Readings

The length between the Whittemore points embedded in the concrete durability blocks are being measured using the procedure discussed in section 7.3.2.2, and will ideally be measured monthly. Currently, the Whittemore points have been read only twice: the initial reading and on October 1, 2009. No readings have been taken since October 1 because the air temperature has been below the required 22.2 ^{o}C (72 ^{o}F) to measure the length between Whittemore points. Figures 8-11 through 8-14 show the change of length between the two dates. Since there are only two data points for each measurement, length change is small and variable.

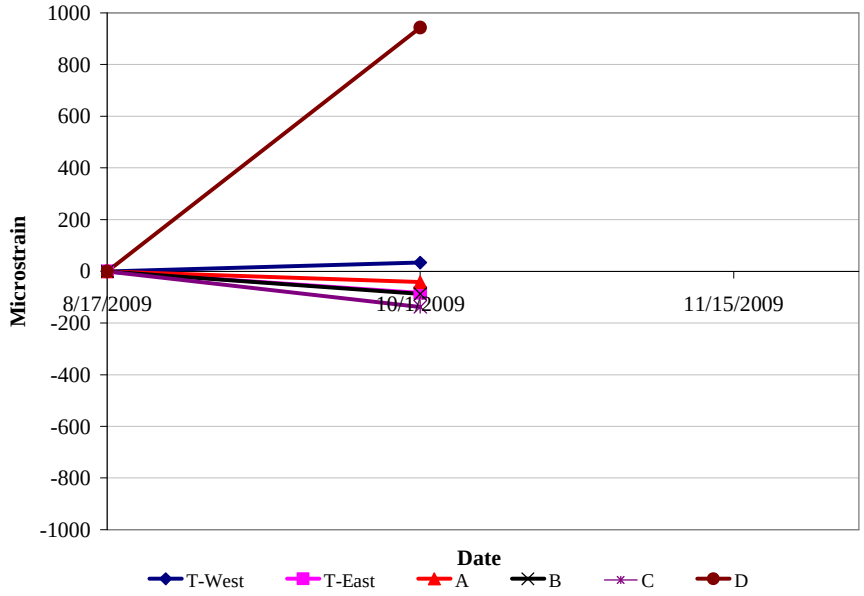

Figure 8-11 ASR Block Length Change (Control Mixture)

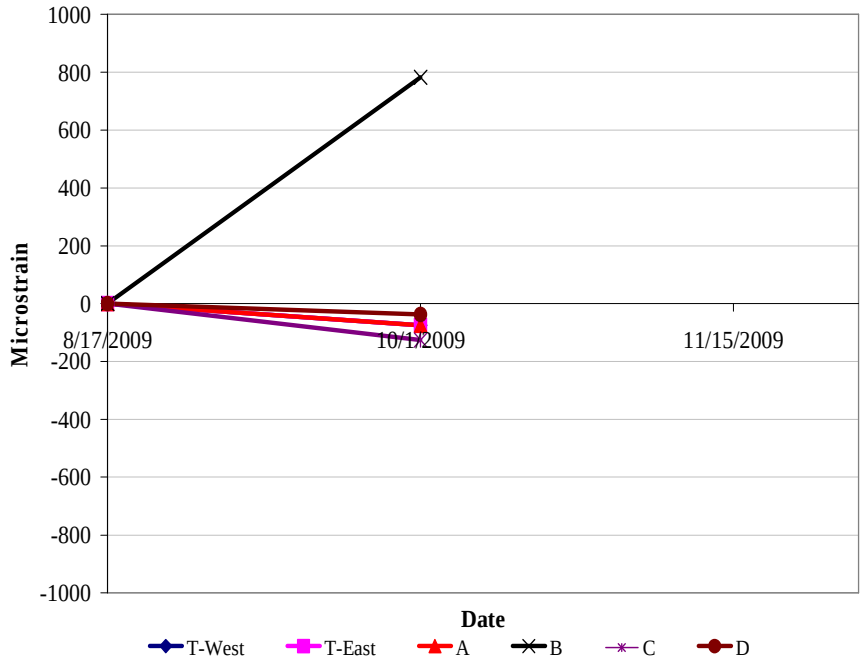

Figure 8-12 ASR Block Length Change (30% Limestone)

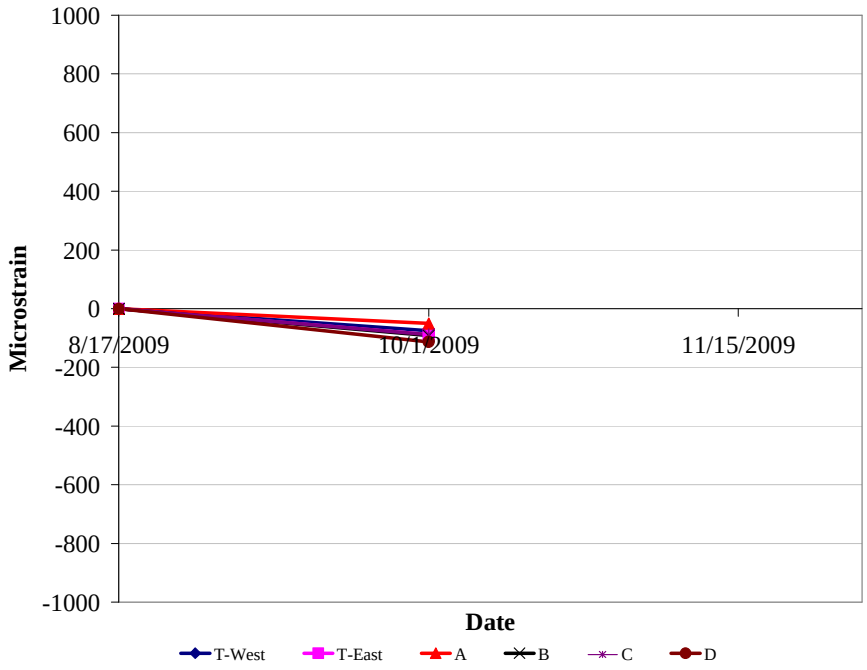

Figure 8-13 ASR Block Length Change (5F 20C)

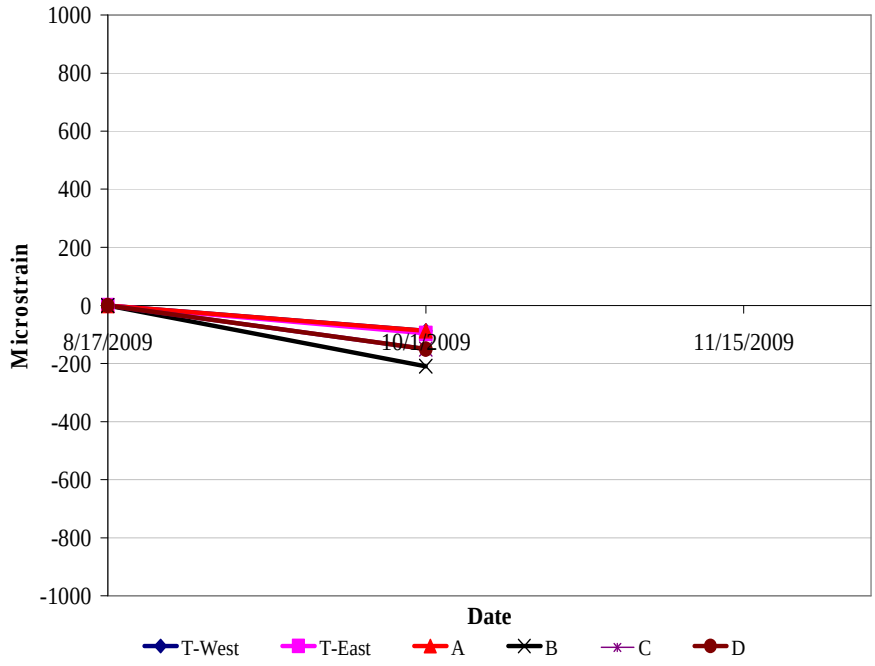

Figure 8-14 ASR Block Length Change (10F 15C)

8.3 Weather Data

Data charts for the weather station can be seen in Appendix B. The weather station has received a total of 246.8 mm (9.71 in.) of precipitation, with an average temperature of 5.4 ^{o}C (41.72 ^{o}F), an average relative humidity of 75.96%, and an average wind speed of 1.94 m/s (4.34 mph). The weather station has recorded the average air temperature, average relative humidity, average ASR block temperature, and total solar radiation every hour since installation. Data can be seen in Figures 8-15 through 8-19. The iButton placed in the slab records the temperature every hour as seen in Figure 8-20.

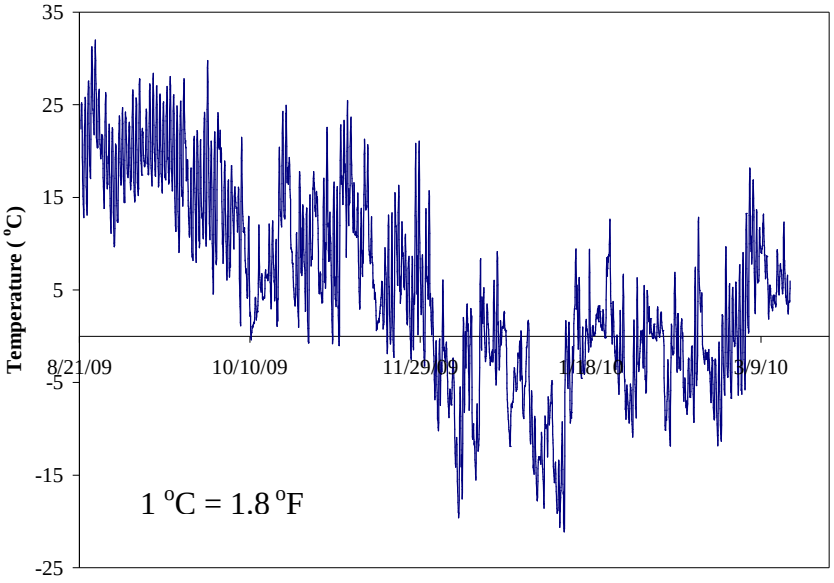

Figure 8-15 KOCE Air Temperature

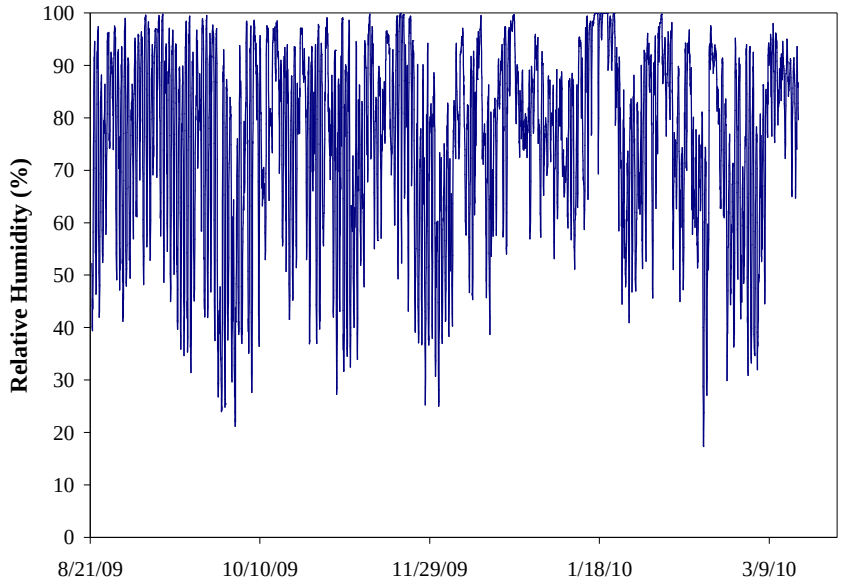

Figure 8-16 KOCE Relative Humidity

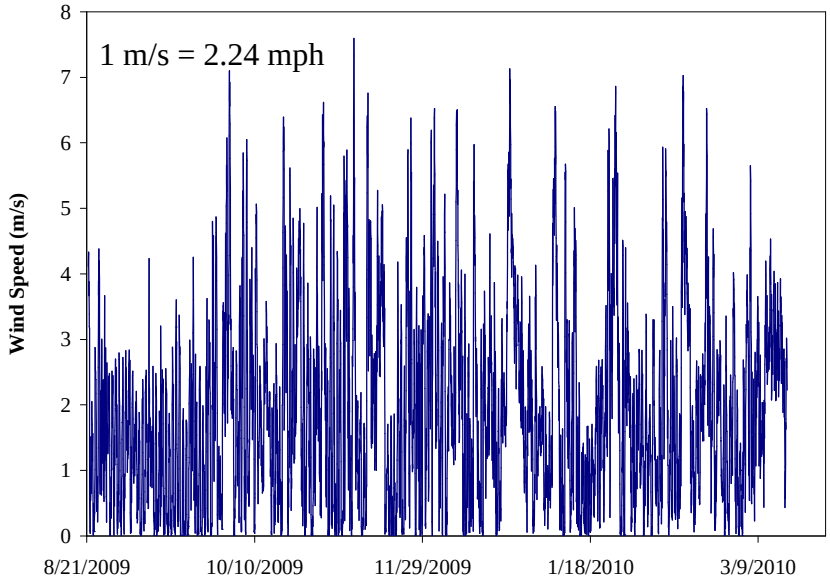

Figure 8-17 KOCE Wind Speed

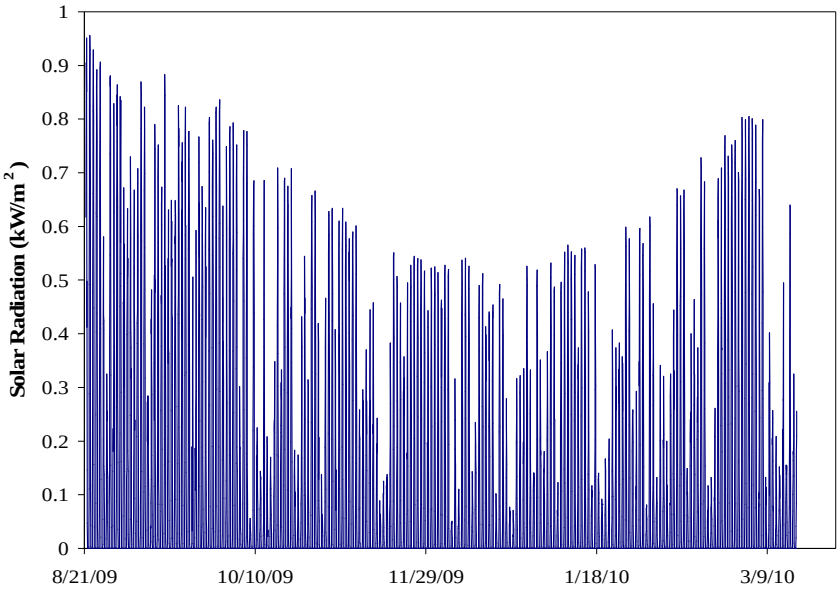

Figure 8-18 KOCE Solar Radiation

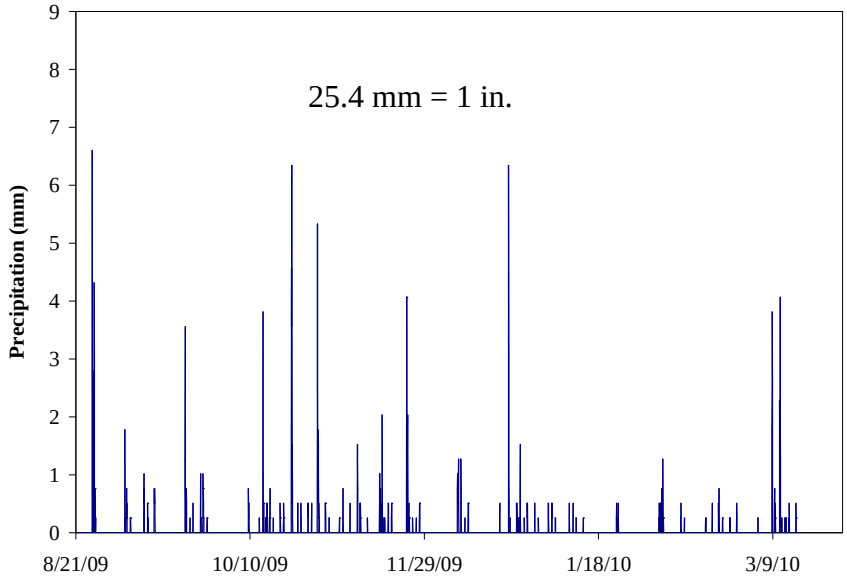

Figure 8-19 KOCE Precipitation

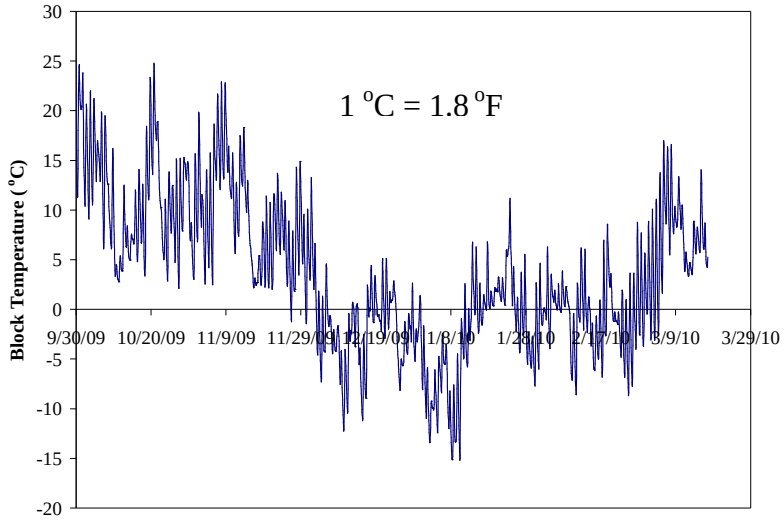

Figure 8-20 KOCE ASR Block Temperature

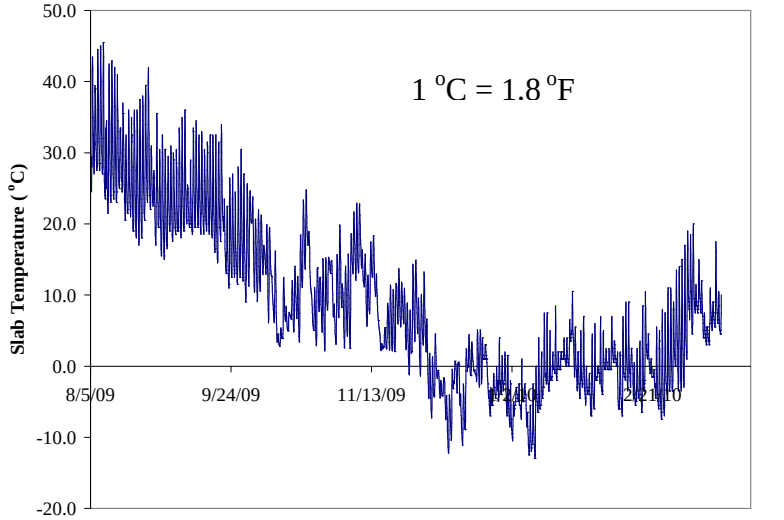

Figure 8-21 KOCE Slab Temperature

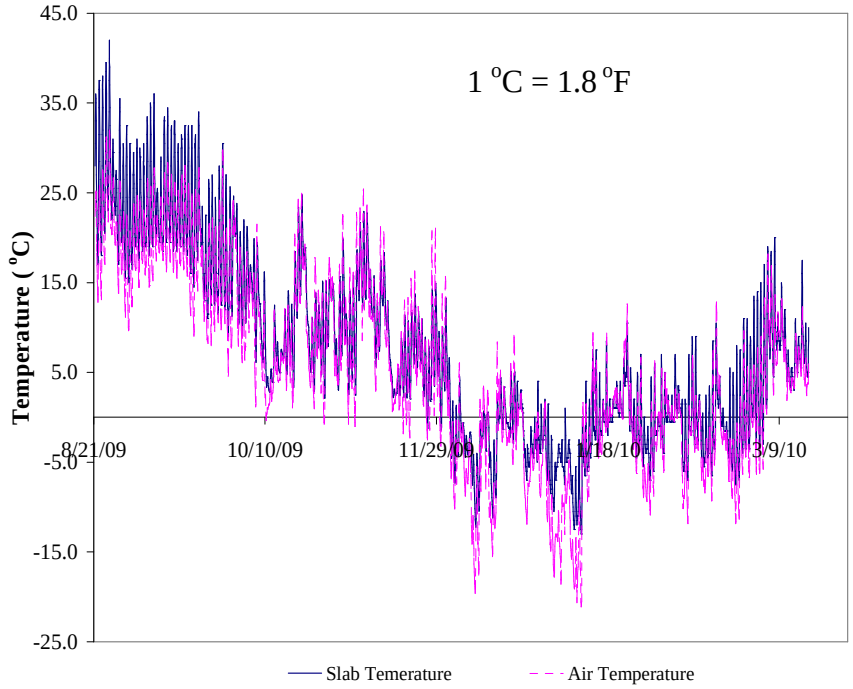

Figure 8-22 Air and Slab Temperature

The ambient air, ASR block, and slab undergo different amounts of freeze-thaw cycles. These differences are due to thermal mass of the concrete, salt concentration on top of the slab, sunlight warming the surfaces of the concrete, etc. The ASTM C 672 standard calls for a freezing cycle of -18 ± 3 oC (0 ± 5 °F). The air temperature only reached -15 °C (5 °F) on 12 separate days. The number of freeze-thaw cycles for each depends on what temperatures are considered to be a complete freeze-and-thaw cycle. In Table 8-3, a review of the number of complete freeze-thaw cycles, depending on the temperatures equated with a complete cycle. A 4% calcium chloride solution will have a freezing point of approximately -2 °C (28.4 °F) (The Engineering Toolbox 2010).

Table 8-3 Freeze-Thaw Cycles Depending on Temperatures

		Cycles		
Freeze (^{o}C)	**Thaw (^{o}C)**	**Air**	**Block**	**Slab**
<0	**>0**	61	50	60
-1	**2**	37	32	40
-2	**2**	30	25	33
-3	**2**	27	17	25
-4	**2**	21	13	16
-5	**2**	19	11	13
-10	**2**	7	2	2
-15	**2**	3	1	0

CHAPTER 9 - Discussion, Conclusions, and Recommendations

Results from Chapter 8, conclusions, and recommendations for future research and considerations will be discussed in this chapter.

9.1 Salt-Scaling Laboratory Discussion

9.1.1 Fresh and Hardened Concrete Testing Discussion

Test batches were crucial in order to meet ASTM C 672 standard specifications of a slump of 75±15 mm (3±0.5 in.) with the required air entrainment by adjusting the mid-range water-reducer dosage. Fly ash seemed to help with the workability and decreased the amount of mid-range water reducer needed to achieve the specified slump. All batches were within this range. These mixtures seem to be very dry for normal concrete that would be placed in a sidewalk or road. For the most part, the "M" (substitution by straight mass) mixes had a higher slump.

Air content for each batch fell in the specified range of 6±1%. The amount of AEA needed to achieve the required air content varied for each fly ash, possibly because of differences in the nature of the carbon present in each.

Compressive strength for each type of fly ash was similar, independent of the substitution method. F3 mixtures and the F7M batch had low compressive strength. The F7M batch was known to have batching problems and segregation, which could have affected the concrete strength.

9.1.2 ASTM C 672 Testing Discussion

The rating chart shown in Figure 2-5 was used to help guide the rating. Whole-number ratings were given for each rating. As seen in Figures 8-18 and 8-19, ratings for all fly ashes with substitution by volume of paste did not perform as well as the control, regardless of the curing method. Substitution by mass had more volume of paste, while substitution by volume of paste had the same volume of paste as the control. The paste could have been weaker than the control paste and thus could not withstand the stresses occurred during scaling. The best sets of specimens overall were those that had fly ash substitution by mass with curing compound applied. F2 and F6 fly ashes performed unsatisfactorily in salt scaling no matter the substitution

or curing method. The increase in paste content increased salt-scaling resistance. The curing compound also increased the salt-scaling resistance.

Mass change measurements of the specimens showed a mass gain early during the first few cycles, after which the concrete specimen mass began to decrease. This mass increase was from water absorption. Curing compound specimen results show they did not lose as much mass as the air-cured specimens, which corresponded to the visual ratings. Certain fly ash can be seen to perform poorly in salt scaling, as evidenced by the mass loss results of F6. All F6 specimens lost a greater amount of mass, even though the specimens absorbed water.

Compressive strength does not directly correlate with the salt-scaling durability. F6 had high compressive strength in both substitution methods; however, it performed very poorly in the salt scaling.

9.1.3 KOCE Site Concrete Discussion

Concrete at the KOCE had a longer curing period of up to 160 days for the small specimens, while the slabs had 103 days of curing before the first salt was applied. It has not shown any salt scaling to date. The scaling may take years to show if at all, because conditions are not as harsh as in ASTM C 672. Others have found similar results, as discussed in section 2.4.5.

9.2 ASR Block Discussion

A procedure has been developed using Whittemore points to measure expansion of concrete durability blocks under field exposure. It is recommended that steel forms be made for the concrete durability blocks when the current formwork set wears out. Steel forms will directly hold the inserts for the Whittemore points, eliminating problems with removing steel strips. The bottom of steel forms should hold the inserts for the top of the blocks. The blocks could then be flipped after curing in the forms. Continued monitoring of the concrete blocks will show effects of limestone sweetening and fly ash use on concrete ASR.

9.3 Conclusions

Experimental results found in this study can lead to the following conclusions:

1. The specific gravity of the fly ash and the subsequent change in volume of paste was not necessarily a predictor of salt-scaling durability.

2. Curing compound increases resistance to salt scaling.
3. Performance of concrete containing fly ash is heavily dependent on the type and source of fly ash used.
4. High compressive strength does not necessarily correlate with salt-scaling durability.
5. Concrete durability testing at the new KOCE site at CISL will yield valuable data for years to come regarding durability of concrete mixtures and structures.

9.4 Recommendations

1. Differences in fly ash properties need to be studied more in depth to understand which properties affect salt-scaling durability. Any possible change in the concrete microstructure at the surface of the concrete caused by high volumes of fly ash should also be studied.
2. Performance of the shocked specimen needs to be investigated further as a possible mitigation method.
3. Monitoring of the concrete slabs and durability blocks at KOCE should be continued for the next several years.
4. KSU should investigate opportunities to work with CANMET or UT-Austin to investigate ASR.

References

ACI 318-08 (2008). "Building Code Requirements for Structural Concrete and Commentary." *American Concrete Institute*, Farmington Hills, MI.

Afrani, I., and Rogers, C. (1994). "The Effects of Different Cementing Materials and Curing on Concrete Scaling." *Cement, Concrete, and Aggregate,* 16(2), 132-139.

ASTM C 39-05 (2005). "Standard Test Method for Compressive Strength of Cylindrical Concrete Specimens." *ASTM*, Philadelphia, PA.

ASTM C 125-07 (2007). "Standard Terminology Relating to Concrete and Concrete Aggregates." *ASTM*, Philadelphia, PA.

ASTM C 127-07 (2007). "Standard Test Method for Density, Relative Density (Specific Gravity), and Absorption of Coarse Aggregate." *ASTM*, Philadelphia, PA.

ASTM C 128-07a (2007). "Standard Test Method for Density, Relative Density (Specific Gravity), and Absorption of Fine Aggregate." *ASTM*, Philadelphia, PA.

ASTM C 136-06 (2006). "Standard Test Method for Sieve Analysis of Fine and Coarse Aggregates." *ASTM*, Philadelphia, PA.

ASTM C 143-08 (2008). "Standard Test Method for Slump of Hydraulic-Cement Concrete." *ASTM*, Philadelphia, PA.

ASTM C 150-07 (2007). "Standard Specification for Portland Cement." *ASTM*, Philadelphia, PA.

ASTM C 231-08b (2008). "Standard Test Method for Air content of Freshly Mixed Concrete by the Pressure Method." *ASTM*, Philadelphia, PA.

ASTM C 457-08a (2008). "Standard Test Method for Microscopical Determination of Parameters of the Air-Void System in Hardened Concrete." *ASTM*, Philadelphia, PA.

ASTM C 496-04 (2004). "Standard Test Method for Splitting-Tensile Strength of Cylindrical Concrete Specimens." *ASTM*, Philadelphia, PA.

ASTM C 511-06 (2006). "Standard Specification for Mixing Rooms, Moist Cabinets, Moist Rooms, and Water Storage Tanks Used in the Testing of Hydraulic Cements and Concretes." *ASTM*, Philadelphia, PA.

ASTM C 672-03 (2003). "Standard Test Method for Scaling resistance of Concrete Surfaces Exposed to Deicing Chemicals." *ASTM*, Philadelphia, PA.

Bilodeau, A., Sivasundaram, V., Painter, K., and Manlhotra, V. (1994). "Durability of Concrete Incorporating High Volumes of Fly Ash from Sources in the U.S." *ACI Materials Journal*, 91(1), 3-12.

Bleszynski, R., Hooten, R., Thomas, M., and Rogers, C. (2002). "Durability of Ternary Blend Concrete with Silica Fume and Blast Furnace Slag: Laboratory and Outdoor Exposure Site Studies." *ACI Materials Journal*, 99(5), 499-508.

Boyd, A., and Hooton, R. (2007). "Long-Term Performance of Concretes Containing Supplementary Cementing Materials." *Journal of Materials in Civil Engineering* 19(10) 820-825.

Browne, F.P., and Cady, P.D. (1975). "De-icer Scaling Mechanism in Concrete." "Durability of Concrete." *ACI Special Publication SP-47*, American Concrete Institute, Detroit, MI., 119.

Engineering Toolbox, The (2010). "Calcium Chloride-Water." http://www.engineeringtoolbox.com/calcium-chloride-water-d_1186.html, (April 2010).

FHWA (2006). "Integrated Materials and Construction Practices for Concrete Pavements." *Report No. FHWA HIF -07-004.*

Figurski, D. (2001). "Laboratory and Field Investigations of Alkali-Silica Reaction in Portland Cement Concrete." Master's Thesis, University of Texas at Austin, Austin, TX.

Fournier, B., and Malhotra, V.M. (1996). "Reducing Expansion Due to Alkali-Silica Reactivity." *Concrete International*, 18(3), 55-59.

Harnick, A.B., and Rosli, A. (1980). "Improving the Durability of Concrete to Freezing and De-icing Salts." *Durability of Building Materials and Components, Special Publication STP 691*, American Society for Testing and Materials, Philadelphia, pp 464-473.

Helmuth, R. (1987). "Fly Ash in Cement and Concrete." *PCA*, Skokie, IL, 203.

Jacobsen S. (1995). "Scaling and Cracking in Unsealed Freeze/Thaw Testing of Portland Cement and Silica Fume Concretes." Master's Thesis, Norwegian Institute of Technology, Trondheim, Norway.

Jozwiak-Niedzwiedzka, D. (2004) "How To Prevent Scaling of Concretes in Out-Door Structures." *US-Poland Workshop on Diagnostics of Concrete Materials and Structures for InFrastructure Facilities*, Warsaw, 55-62.

Juilland, P., Gallucci, E., Scrivener, K., and Flatt, R. (2008). "Early Hydration of Cementitious Materials." *Cement and Concrete Science Meeting*.

Kreijer P.C. (1984). "The Skin of Concrete Composition and Properties." *Materials and Structures*, 17(100), 75-283.

Litvan, G.G, and Meyer, A. (1986). "Carbonation of Granulated Blast Furnace Slag Cement Concrete During Twenty Years of Field Exposure." *Fly ash, Silica Fume, Slag and Natural Pozzolans in Concrete* Proceedings of the Second International Conference, Madrid, Spain, 1445-1462.

Marchand, J., Pleau, R., and Gagne, R. (1995). "Deterioration of Concrete due to Freezing and Thawing." *Materials Science of Concrete*, American Ceramic Society, 283-354.

Marchand, J., Maltais, Y., Machabee, Y., Talbot, C., and Pigeon, M. (1997). "Effects of Fly Ash on Microstructure and De-icer Salt-Scaling Resistance of Concrete." *Proceedings of the International RILEM Workshop on Resistance of Concrete to Freezing and Thawing with or Without De-icing Chemicals*, University of Essen, 11-20.

Marchand, J., Pigeon, M., Bager, D., and Talbot, C. (1999). "Influence of Chloride Solution Concentration on De-icer Salt-Scaling Deterioration of Concrete." *ACI Materials Journal*, 96(4), 429-436.

Marchand, J., Machabee, Y., and Jolin M. (2005). "De-icer Salt-Scaling Resistance of Supplementary Cementing Material Concrete: Laboratory Results Against Field Performance." *Cement Combinations for Durable Concrete Proceedings of the International Conference*, 579-590.

Mindness, S. Young, J., and Darwin, D. (2002). "Concrete." *Prentice Hall*, 2nd Ed, New Jersey, 644.

MSN Weather
http://weather.msn.com/monthly_averages.aspx?wealocations=wc:USKS0358&q=Manhattan%2c+KS+forecast:averagesm, (Dec. 29, 2009).

MTO LS-412 (1989). "Scaling Resistance of Concrete Surfaces Exposed to De-icing Chemicals." *Ministry of Transportation*, Ontario.

Neville, A.M. (1996). "Properties of Concrete." 4th edition Wiley, Hoboken, New Jersey, 844.

Ngala, V.T., and Page, C.L. (1997). "Effects of Carbonation on Pore Structure and Diffusional Properties of Hydrated Cement Paste." *Cement and Concrete Research.* 27(7), 995-1007.

Nokken, M., Hooton, R., and Rogers, C. (2004). " Measured Internal Temperature in Concrete Exposed to Outdoor Cyclic Freezing." *Cement, Concrete, and Aggregate*, 26(1), 26-31.

Pigeon, M., and Pleau, R. (1995), "Durability of Concrete in Cold Climates," *Taylor and Francis*, London, 244.

Powers, T.C., and Helmuth, R.A. (1953). "Theory of Volume Changes in Hardened Portland Cement Pastes During Freezing." *Proceedings of the Highway Research Board*, 32, 285-297.

Powers, T.C. (1954). "Void Spacing as a Basis for producing Air-Entrained Concrete." *Journal of American Concrete Institute*, 25(9), 741-760.

Rietveld, H. (1969). "A Profile Refinement Method for Nuclear and Magnetic Structures." *Journal of Applied Crystallography*, (2), 65-71.

Roberts, L., and Taylor, P. (2007). "Understanding Cement-SCM-Admixture Interaction Issues." *Concrete International*, 29(1), 33-41.

Schindler, A., and Folliard, K. (2006). "Heat of Hydration Models for Cementitious Materials." *ACI Materials Journal*, 102(1), 24-33.

Sellevold, E., and Farstadm T. (1991). "Frost/Salt Testing of Concrete "Effect of Test Parameters and Concrete Moisture History." *Nordic Concrete Research*, 10, 121-138.

Setzer, M., and Auberg, A. (1995). "Freeze-thaw and De-icing Salt Resistance of Concrete Testing by the CDF Method, CDF Resistance Limit, and Evaluation of Precision." *Materials and Structures*, 28, 16-31.

Setzer, M., Fagerlund, G., and Janssen, D. (1996). "CDF TEST— Test Method for the Freeze-Thaw Resistance of Concrete –Tests with Sodium Chloride Solution." *TC 117*, July 1996.

Setzer, M. (1997). "TC 117-FDC: Freeze-Thaw and De-icing Resistance of Concrete" *Materials and Structures*, Supplement March 1997, 3-6.

Siddique, Z., Hossain, M., and Parcells Jr., W. (2007). "Effect of Curing on Roughness Development of Concrete Pavements." *Journal of Materials in Civil Engineering*, 19(7), 575-582.

Siebel, E. (1989). "Air-Void Characteristics and Freezing-and-Thawing Resistance of Superplasticized Air-Entrained Concrete with High Workability." *ACI Special Publication, SP-119*, 297-319.

SS 43 72 44 (1992). "Concrete Testing—Hardened Concrete-Frost Resistance" *Stanardierings-kommissionen i Sverige.*

Sommer, H. (1979). "The Precision of the Microscopical Determination of the Air-Void System in Hardened Concrete." *Cement, Concrete, and Aggregates*, 1(2), 49-55.

Thomas, M., (1996). "The Use of Silica Fume to Control Expansion Due to Alkali-Aggregate Reactivity in Concrete." *University of Toronto, for Lafarge Canada Inc*, 74.

Thomas, M., Fournier, B., Folliard, K., Ideker, J., and Shehata, M. (2006). "Test Methods for Evaluating Preventive Measures for Controlling Expansion Due to Alkali-Silica Reaction in Concrete." *Research Report ICAR 302-1 International Center for Aggregates Research.*

U.S. Army Corps of Engineers (2010). "Concrete Technology." http://www.cement.org/tech/images/treat_Fig2.jpg, March, 2010.

Valenza II, J., and Scherer G. (2005). "Mechanism of Salt Scaling." *Materials and Structures*, 38(4), 479-488.

Valenza II, J., and Scherer G. (2006). "Mechanism for Salt Scaling." *Journal of the American Ceramic Society*, 89(4), 1161-1179.

Valenza II, J., and Scherer G. (2007). "A Review of Salt Scaling: I. Phenomenology." *Cement and Concrete Research*, (37), 1007-1021.

Appendix A - Salt-Scaling Results by Mixture

Figures in this appendix show average weight loss and ratings of the three identical specimens. The first figure for each mixture represents the amount of mass loss in kg/m^2. The conversion factor from kg/m^2 to lb/ft^2 is 0.205. A negative mass loss represents a gain in mass. The mass gain is attributed to the specimens absorbing water. The second figure for each batch visual rating is based on the ASTM 672 standard. All lines are the average of three specimens.

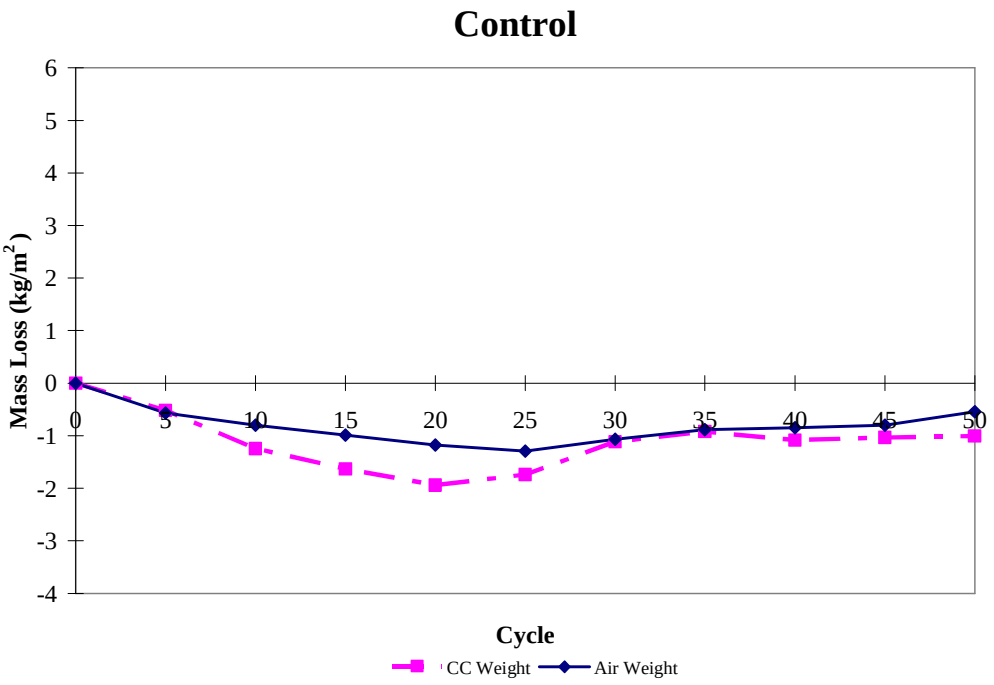

Figure A-1 Control Batch Mass Change Results

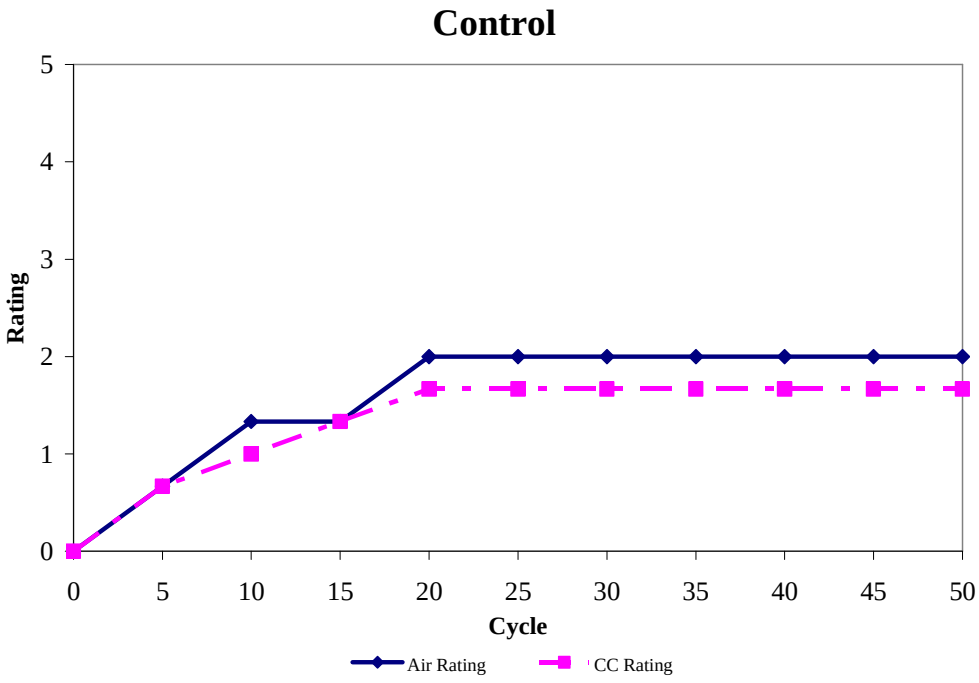

Figure A-2 Control Rating Results

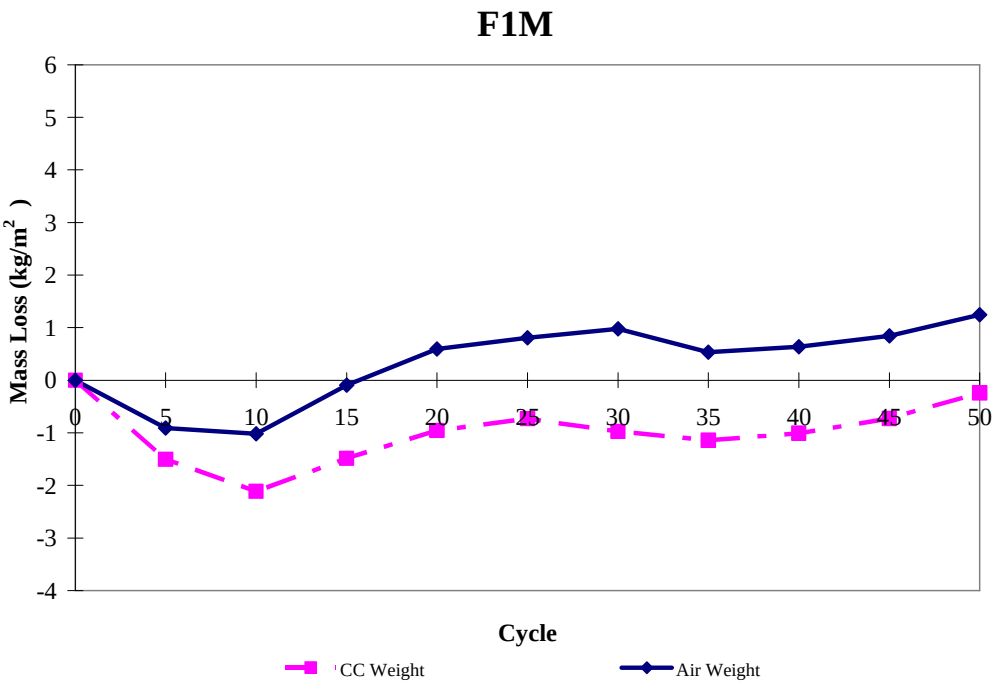

Figure A-3 F1M Mass Change Results

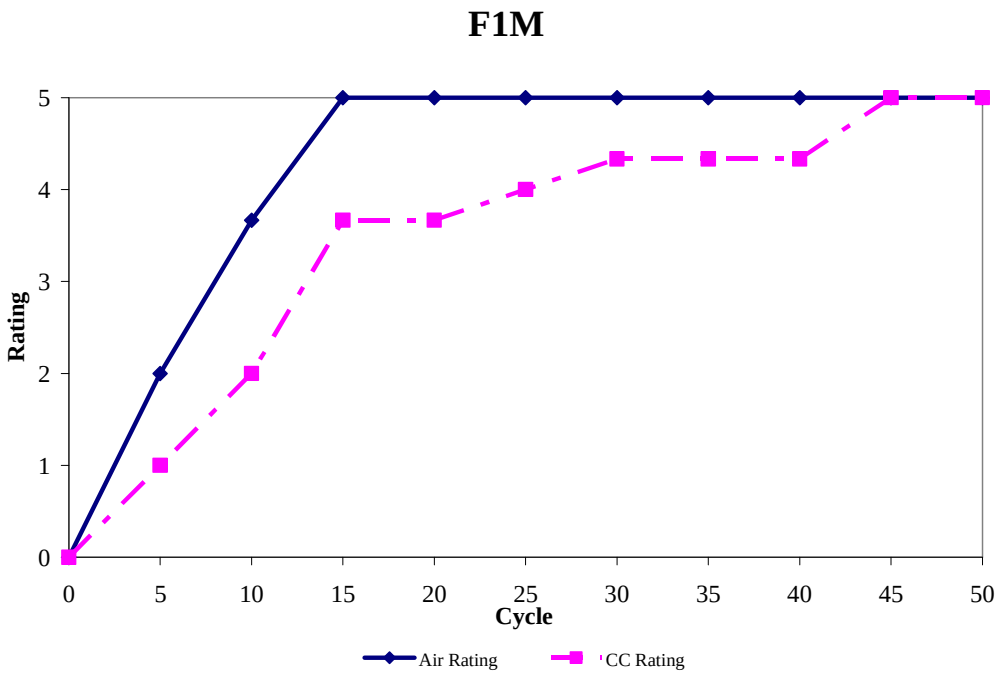

Figure A-4 F1M Rating Results

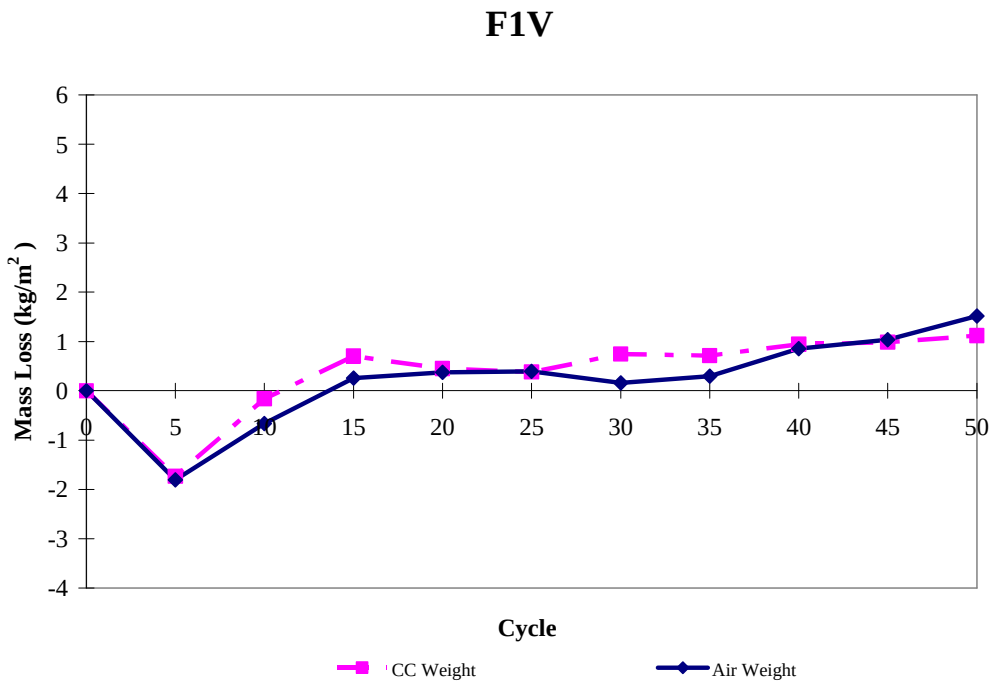

Figure A-5 F1V Mass Change Results

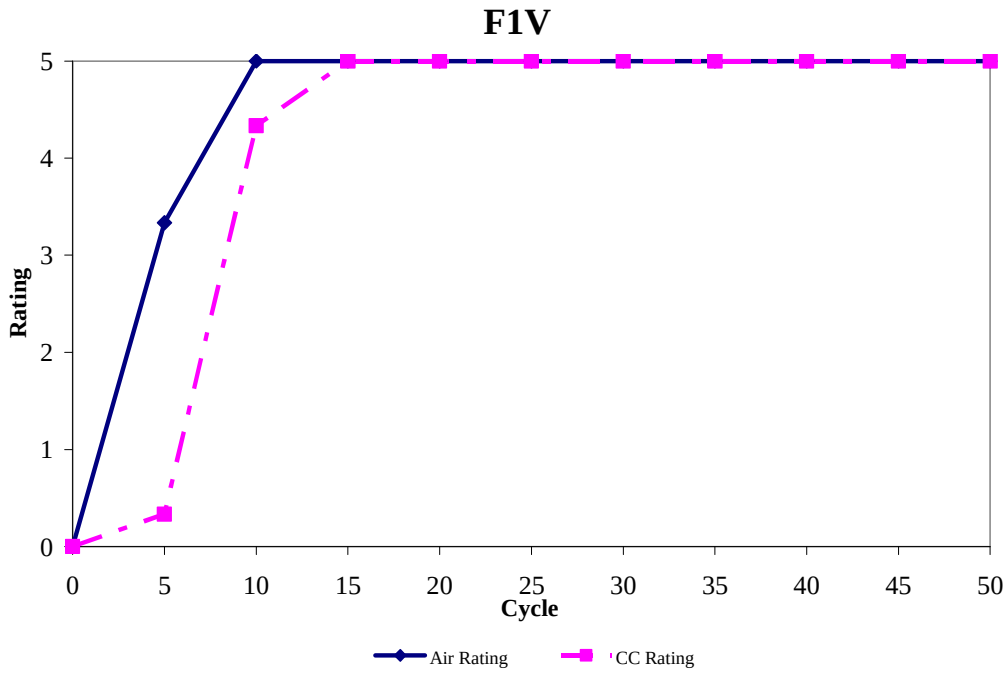

Figure A-6 F1V Rating Results

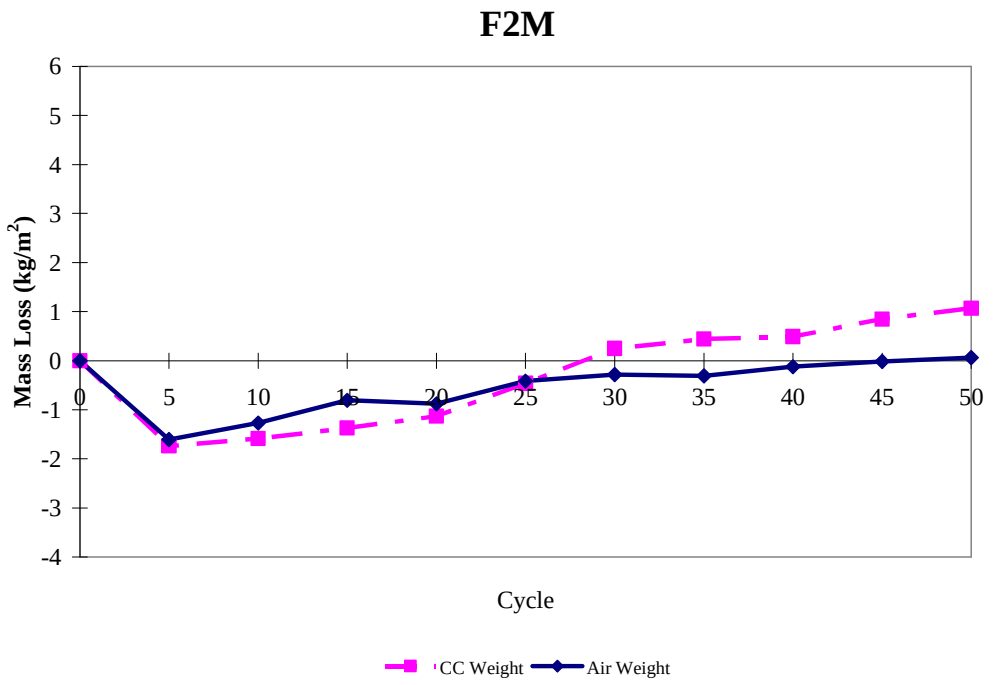

Figure A-7 F2M Mass Change Results

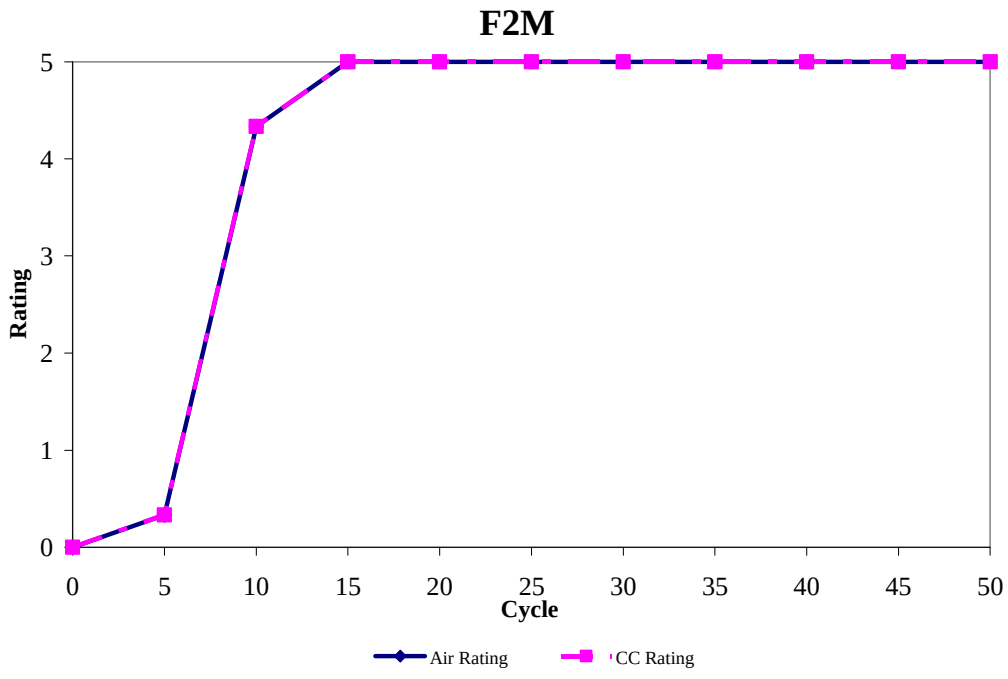

Figure A-8 F2M Rating Results

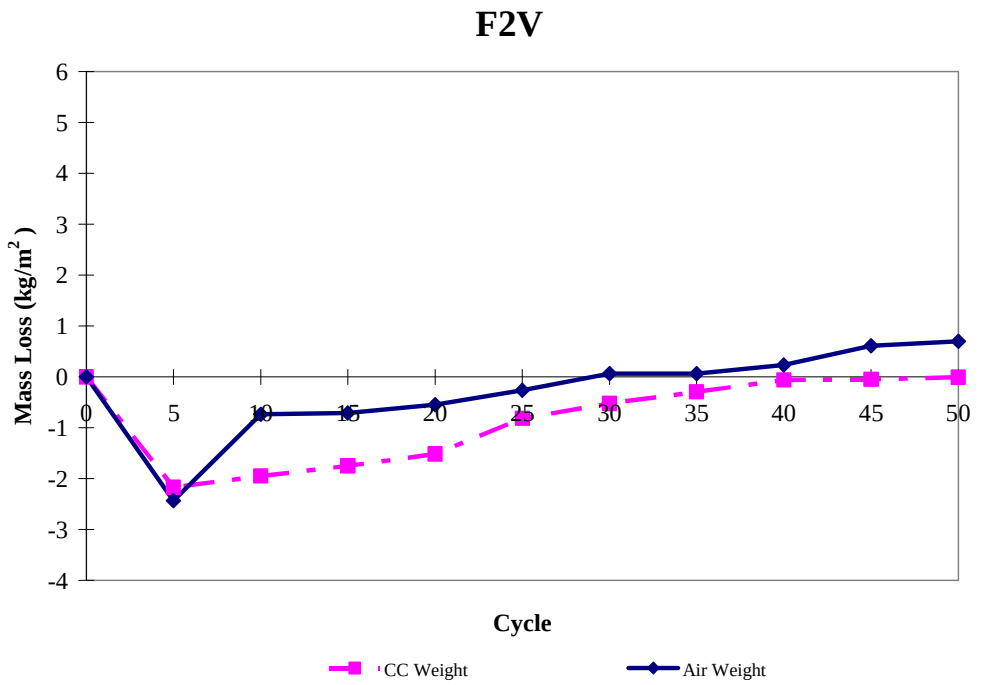

Figure A-9 F2V Mass Change Results

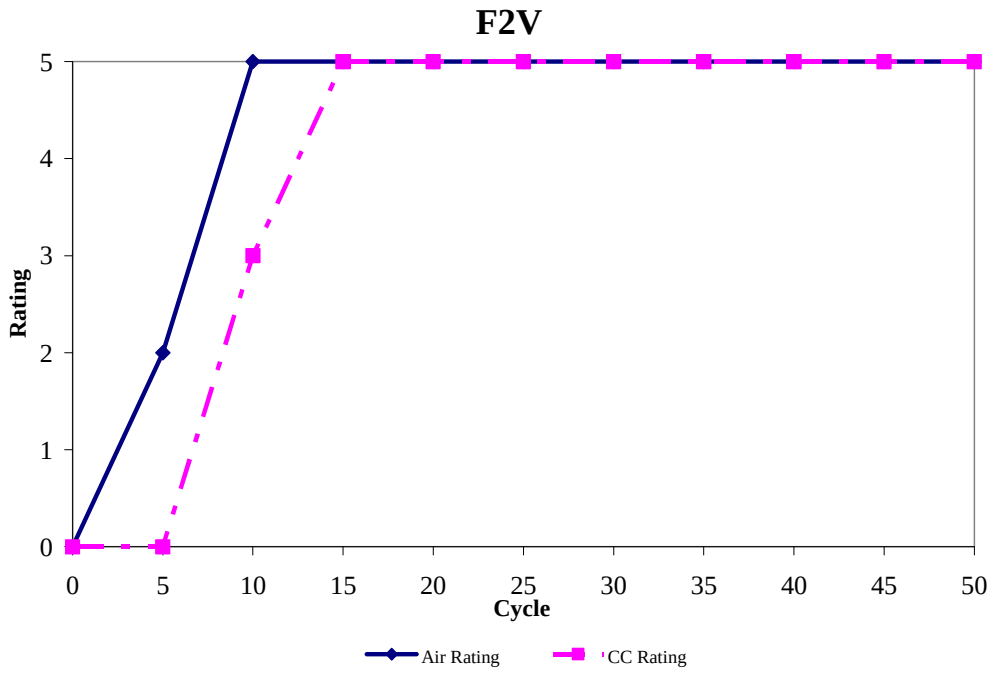

Figure A-10 F2V Rating Results

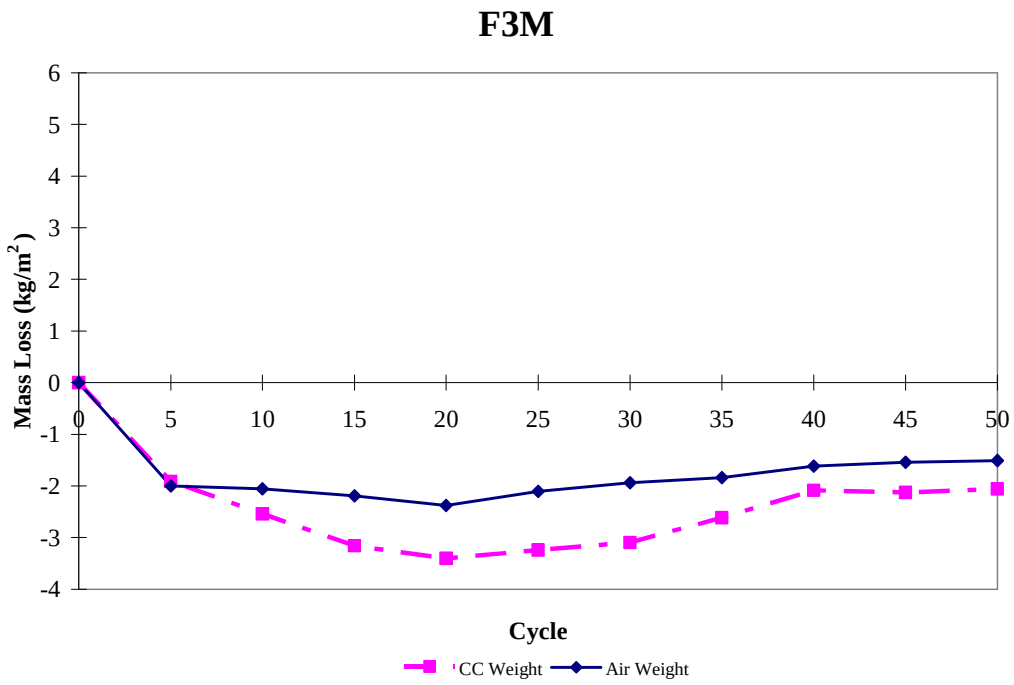

Figure A-11 F3M Mass Change Results

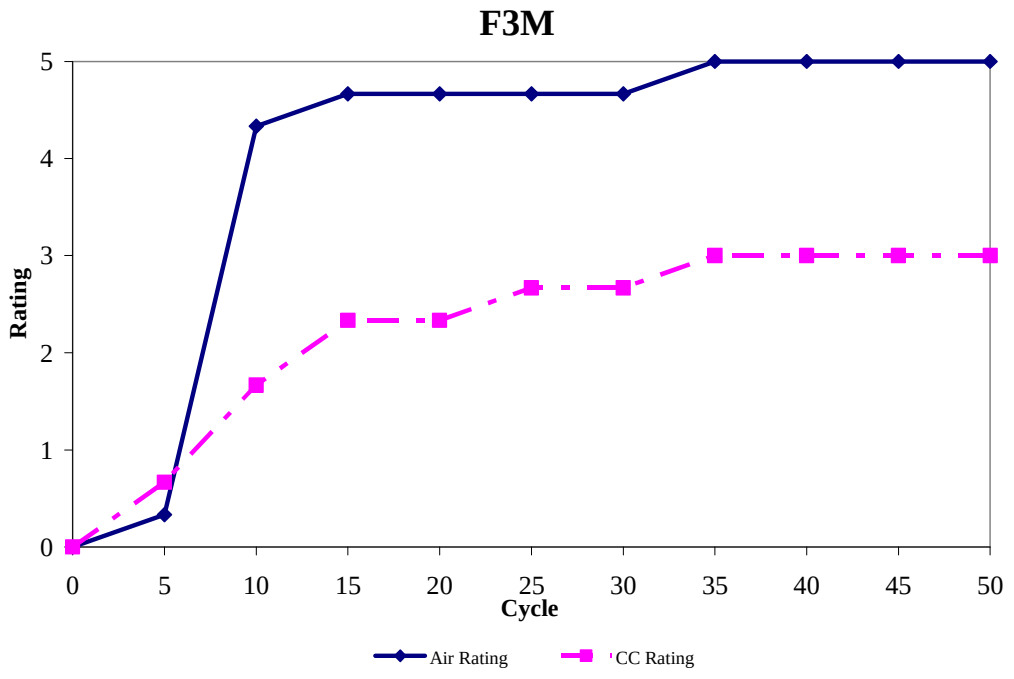

Figure A-12 F3M Rating Results

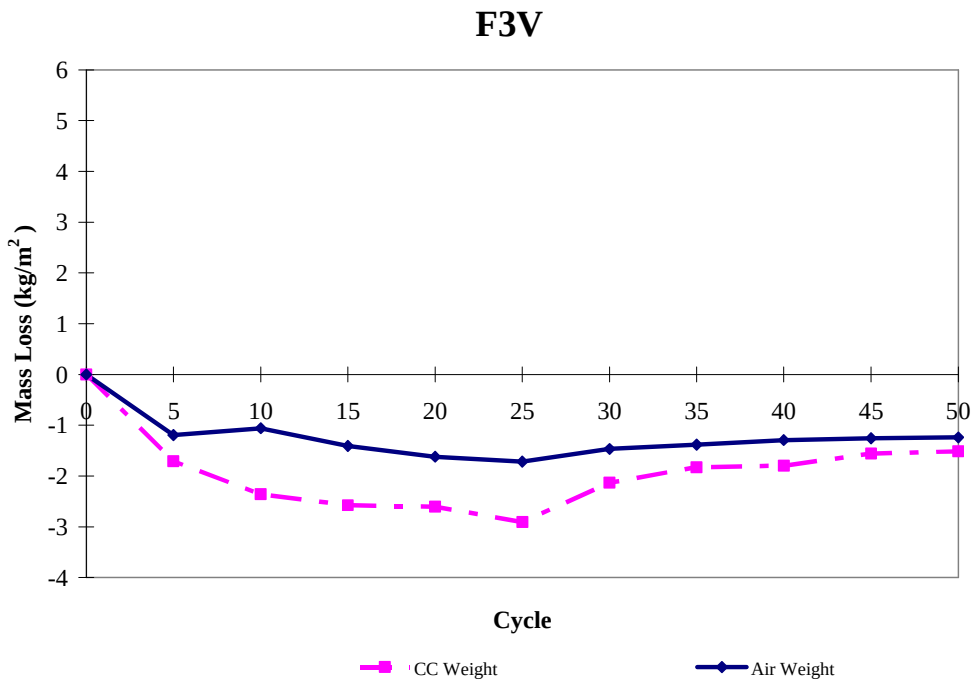

Figure A-13 F3V Mass Change Results

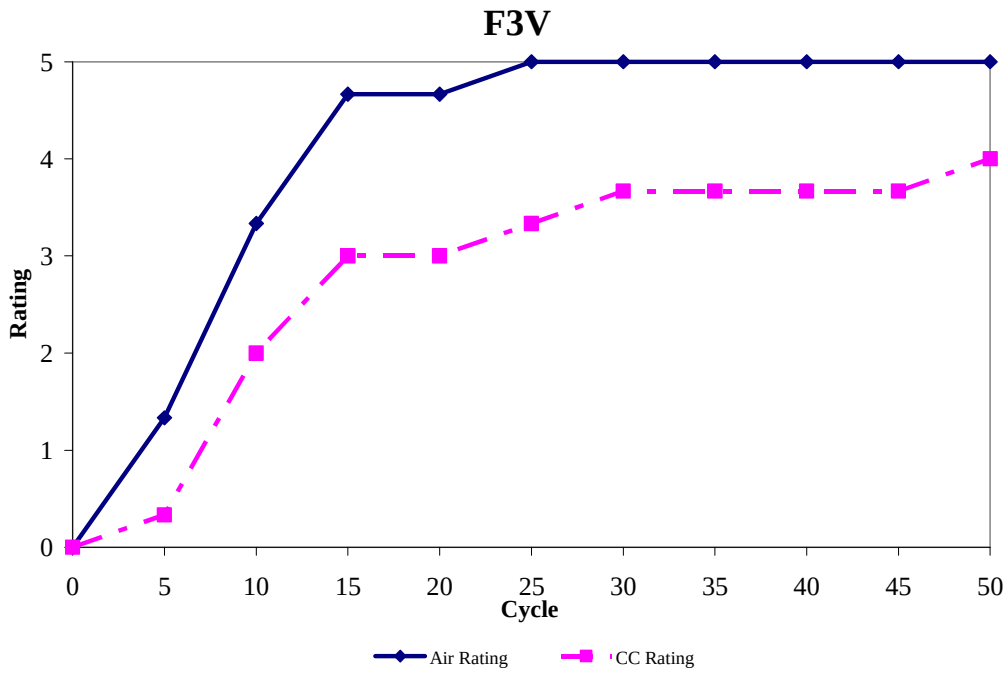

Figure A-14 F3V Rating Results

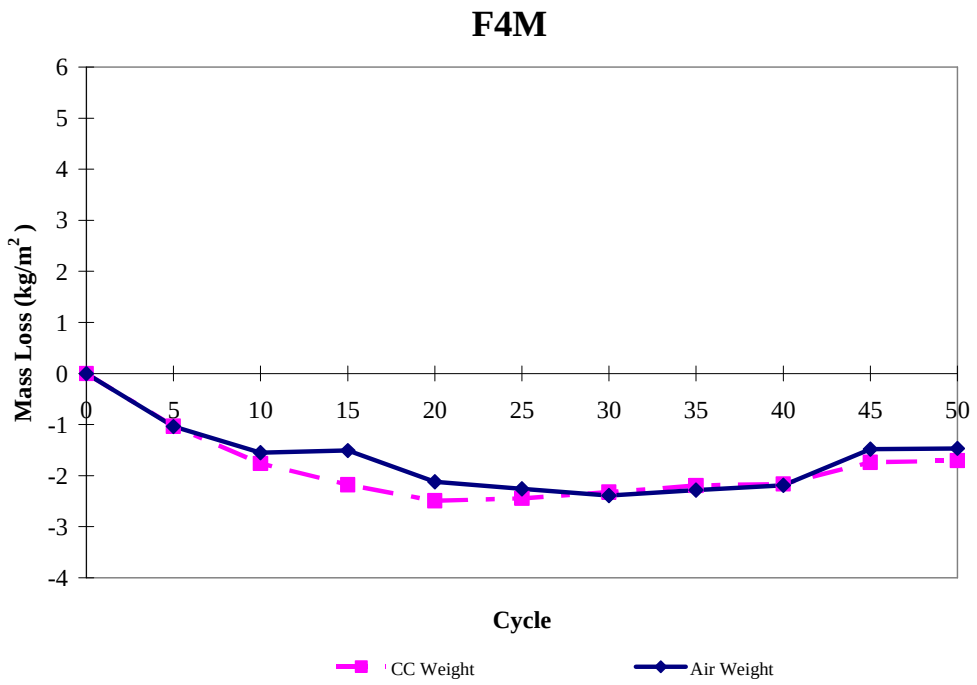

Figure A-15 F4M Mass Change Results

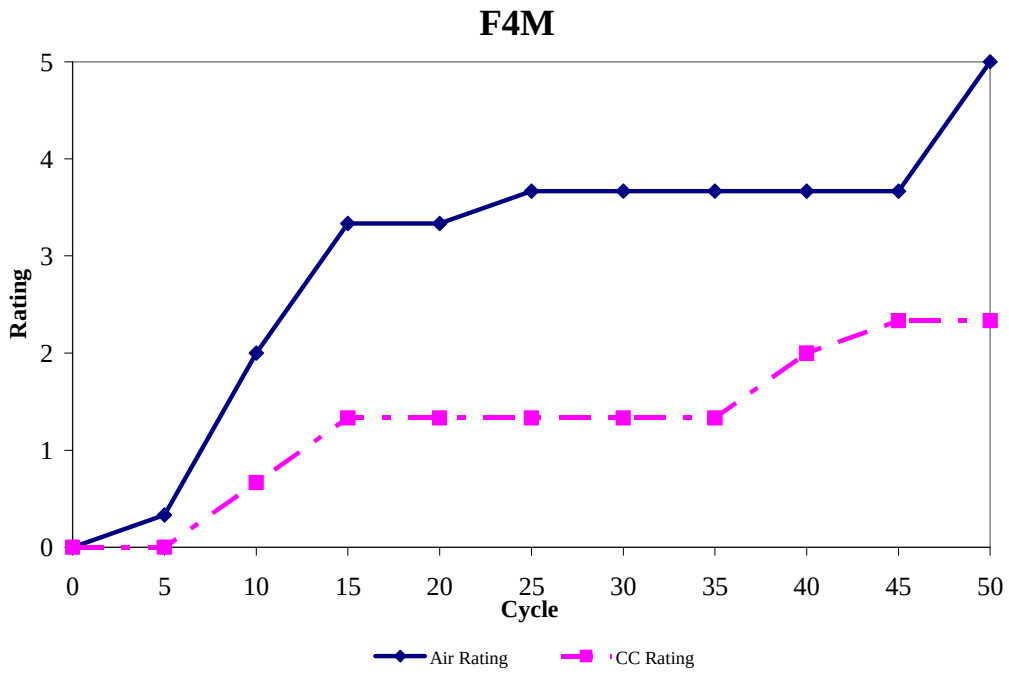

Figure A-16 F4M Rating Results

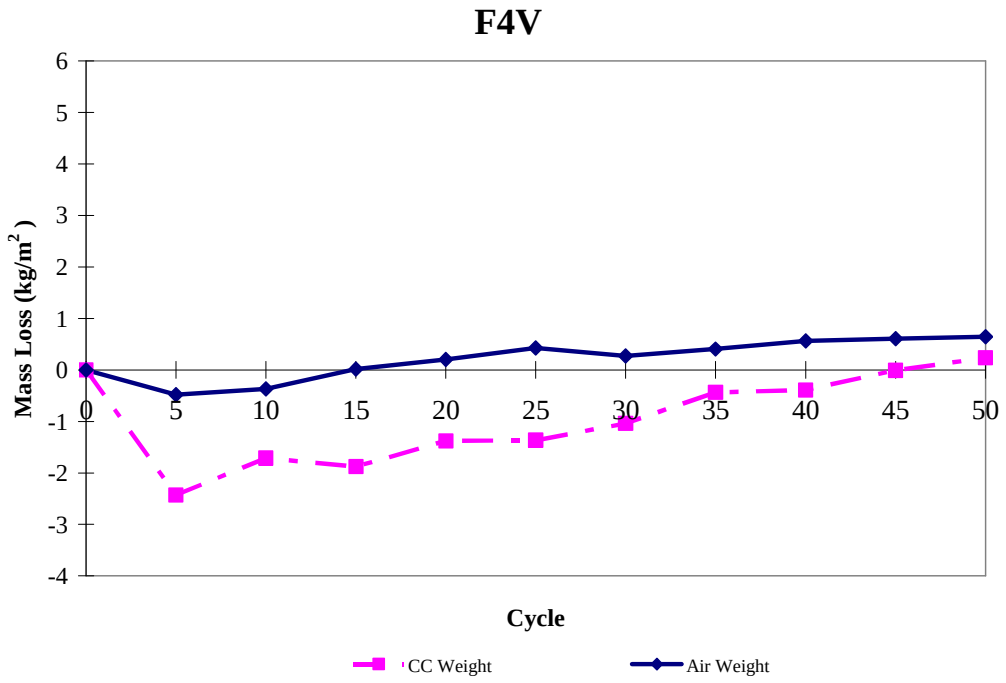

Figure A-17 F4V Mass Change Results

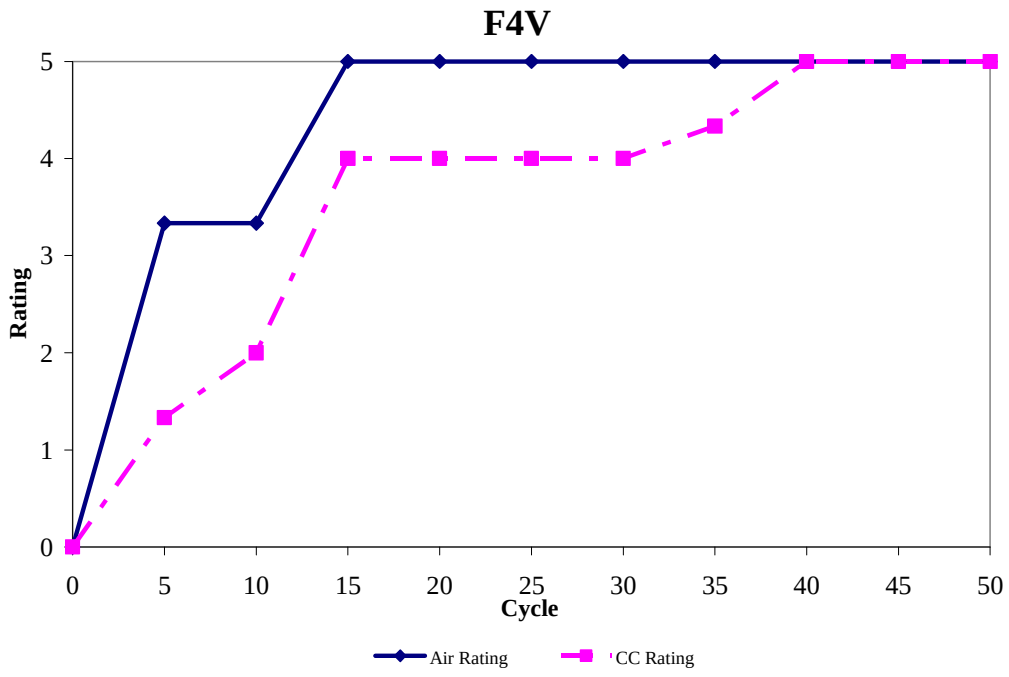

Figure A-18 F4V Rating Results

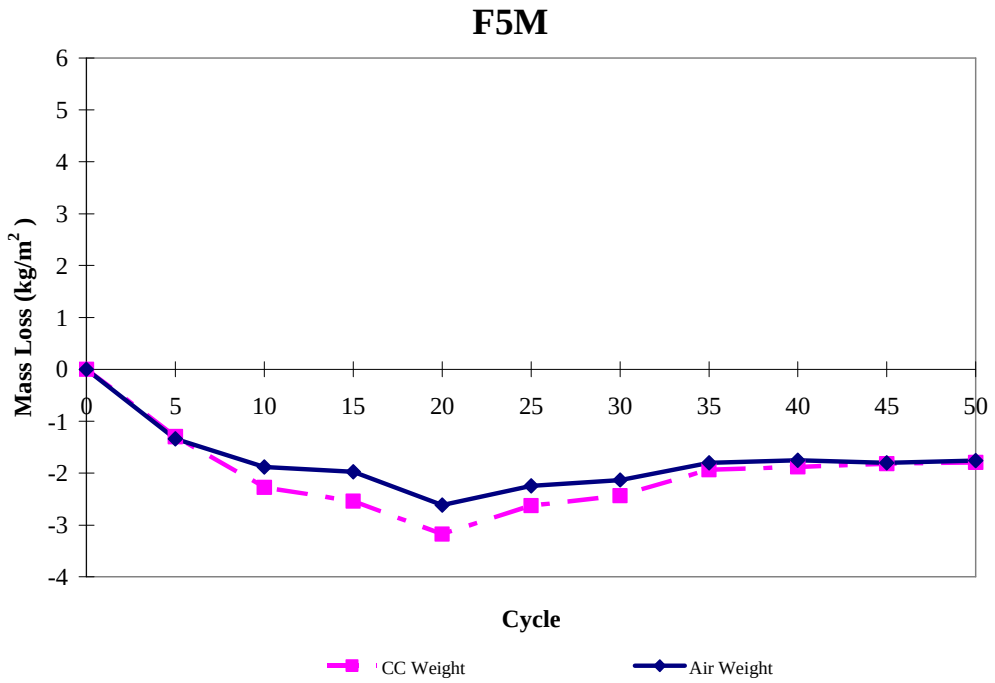

Figure A-19 F5M Mass Change Results

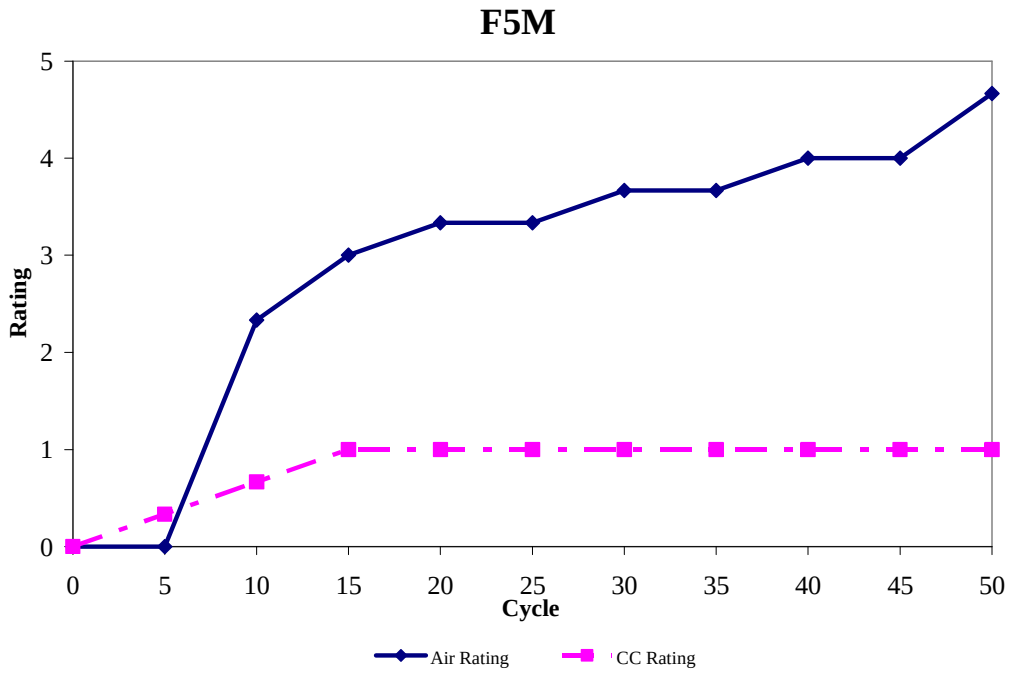

Figure A-20 F5M Rating Results

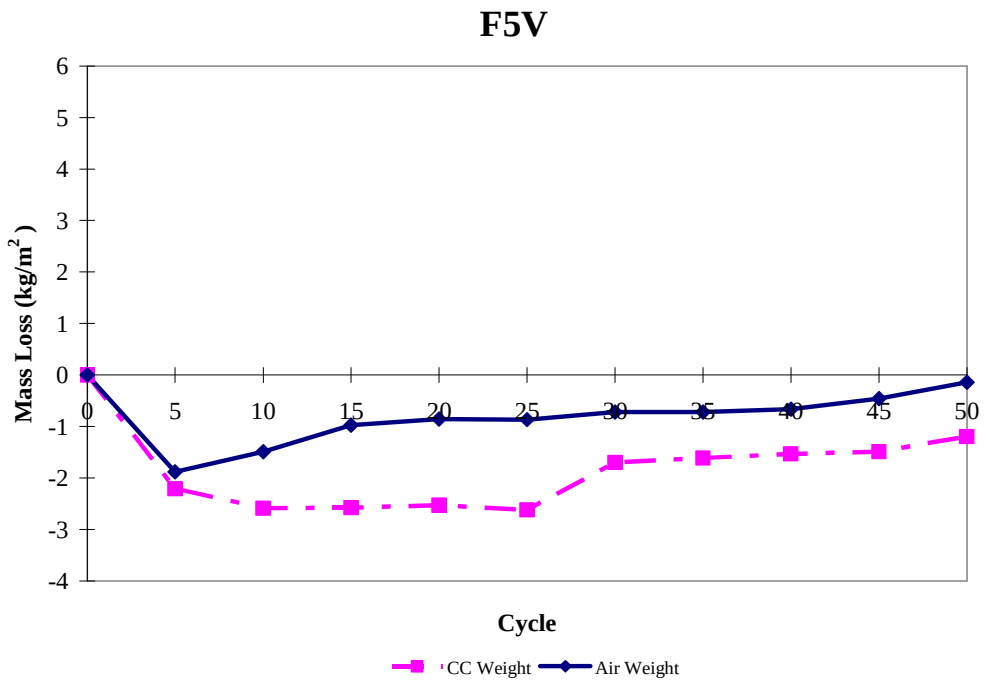

Figure A-21 F5V Mass Change Results

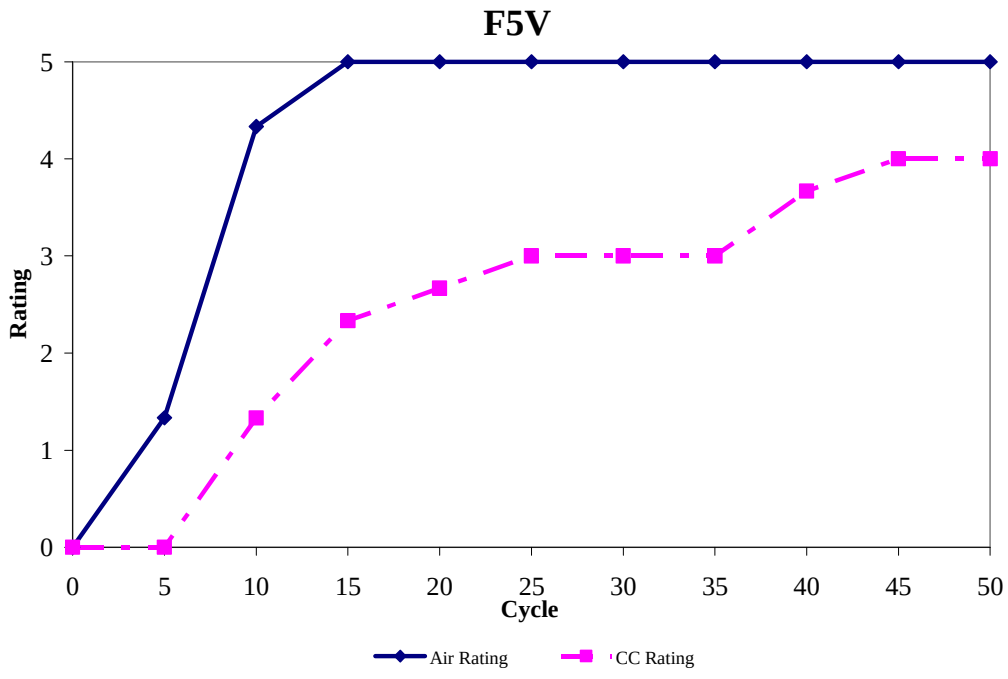

Figure A-22 F5V Rating Results

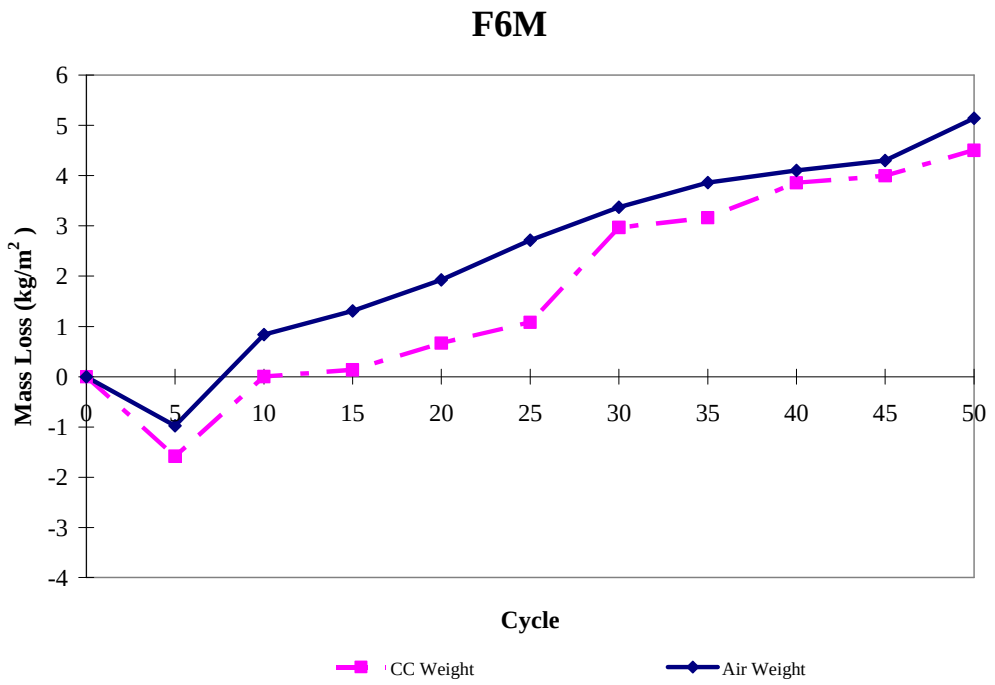

Figure A-23 F6M Mass Change Results

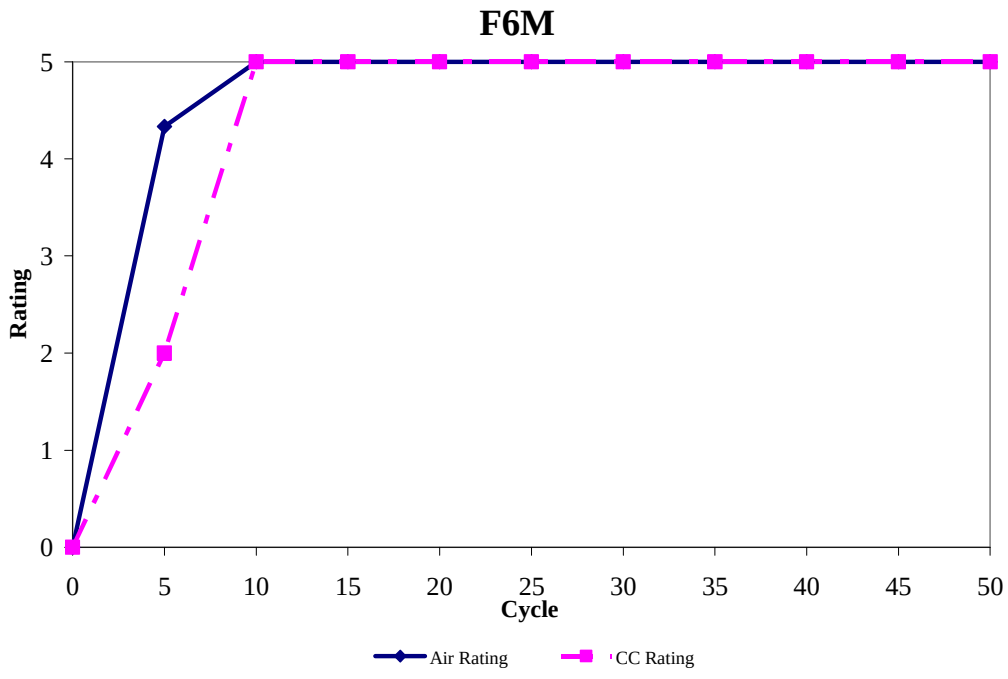

Figure A-24 Rating Results

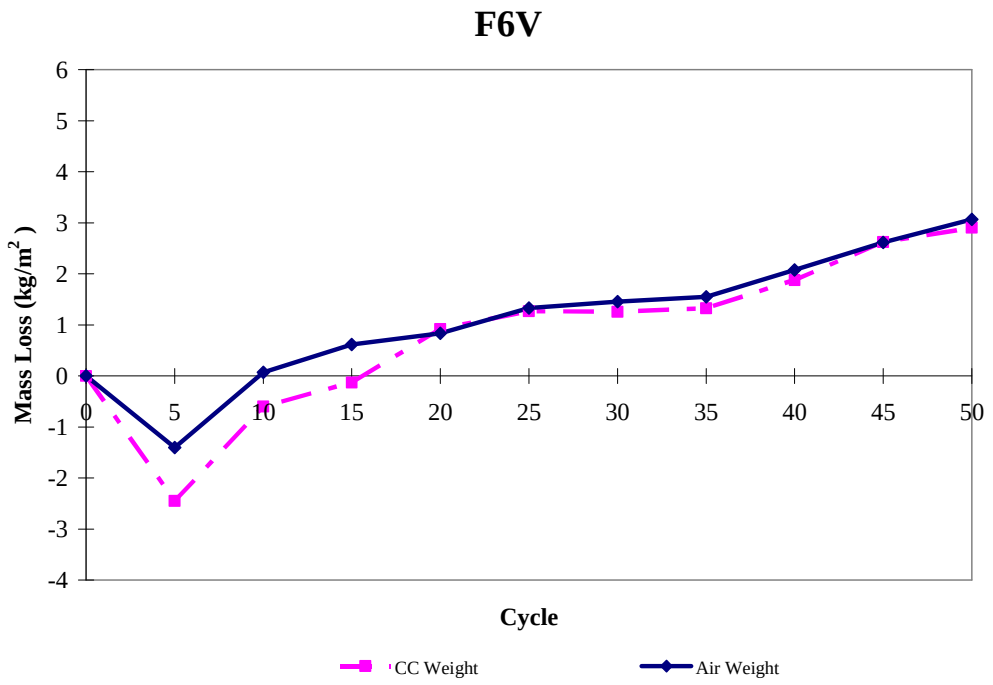

Figure A-25 F6V Mass Change Results

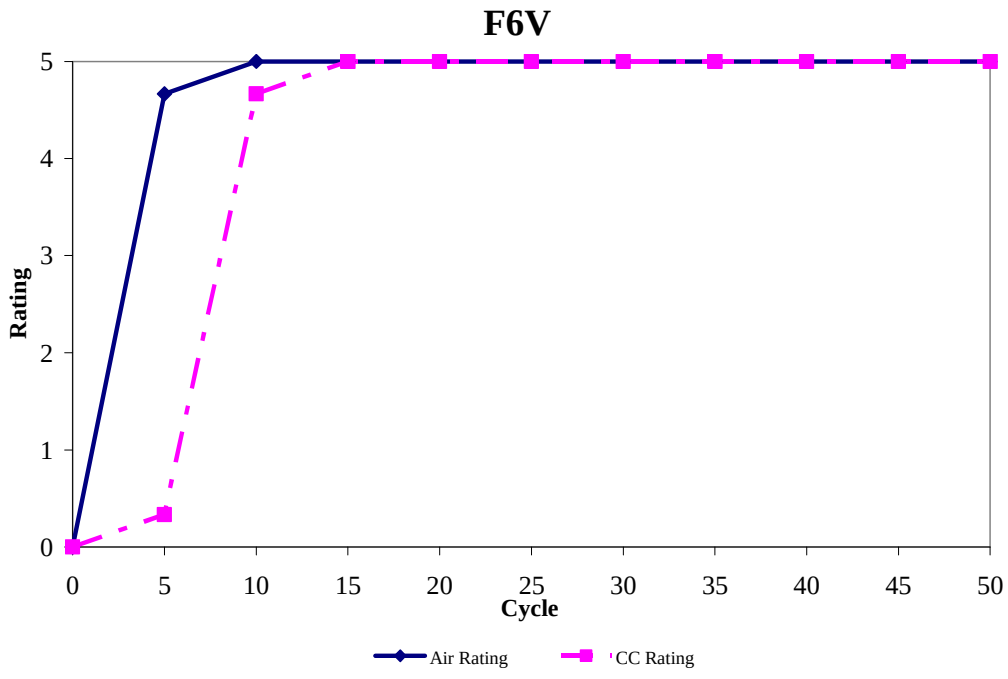

Figure A-26 F6V Rating Results